Alma Mater Studiorum · Università di Bologna

Scuola di Scienze
Dipartimento di Fisica e Astronomia
Corso di Laurea Magistrale in Fisica

On the Dynamics and Stability of Rotating Higher Dimensional Black Holes

Relatore:
Prof. Roberto Balbinot

Correlatore:
Assistant Prof. Jácome Armas

Presentata da:
Enrico Parisini

Anno Accademico 2017/2018

Abstract

We study the stability of fast-spinning $D = 5$ black rings making use of the blackfold formalism. We also construct a new effective theory involving blackfolds with transverse momenta, able to describe rotating higher dimensional black holes with a set of finite angular momenta. The blackfold approach is a perturbative formalism that allows to capture the behaviour of higher dimensional black holes with high angular momenta. We use it to discuss the dynamic instabilities of boosted black strings, obtaining the expressions for longitudinal and elastic quasinormal modes up to $O(r_0^2)$. A longitudinal Gregory-Laflamme instability is found, as expected. We also study the instabilities of black rings, and we compute the quasinormal frequencies for high mode numbers $m = kR$ and up to $O(r_0)$. They agree with the corresponding large-D frequencies, and they signal the presence of a Gregory-Laflamme instability. Finally, we construct a new effective theory describing blackfolds with transverse angular momenta, considering explicitly Kerr black strings, doubly-spinning Myers-Perry black strings and black ring strings. We use these results to build six-dimensional solutions with $S^2 \times \mathbb{T}^2$ horizon topology, and *black ring p-balls* with even p, endowed with horizon geometry $S^2 \times S^1 \times \mathbb{B}^p$. The range of validity of our calculation includes relatively low reduced transverse momenta $j \gtrsim 0.1$, considerably improving the original blackfold description of a large class of configurations. Finally, as an example, we analyse the leading order stability of black ring p-branes and of $D = 5$ Myers-Perry black branes. In both cases, any accessible configuration turns out to be unstable.

Sommario

In questa tesi studiamo la stabilità di $D = 5$ black rings utilizzando l'approccio blackfold. Compiamo anche la costruzione sistematica di una nuova teoria effettiva basata su blackfolds con momenti trasversi, in modo tale da poter descrivere buchi neri rotanti in dimensioni più alte con solo alcuni momenti angolari in regime di ultra-rotazione. Introduciamo inizialmente la teoria dei buchi neri in dimensioni più alte, analizzando nello specifico le soluzioni di Myers-Perry e i black rings. Presentiamo poi l'approccio blackfold, un formalismo perturbativo che permette di descrivere il comportamento di buchi neri in dimensione più alta con alti momenti angolari. Lo impieghiamo quindi per discutere le instabilità della dinamica di black strings con boost non nullo, per cui otteniamo la forma esplicita dei modi quasinormali longitudinali ed elastici trascurando correzioni di ordine $O(r_0^2)$ con validità per ogni dimensione trasversa $n = D-4$. Si rileva la presenza di una instabilità longitudinale di Gregory-Laflamme, come da aspettative. Introducendo un contributo di curvatura estrinseca, analizziamo la stabilità dei black rings, di cui calcoliamo le frequenze quasinormali per alti modi $m = kR$ e trascurando termini di ordine $O(r_0)$. I risultati sono in perfetto accordo con quelli corrispondenti provenienti dall'approssimazione di alta dimensione D, e riscontriamo la presenza di una instabilità di Gregory-Laflamme. Il secondo raggiungimento di questa tesi è la costruzione di una nuova teoria effettiva in grado di descrivere blackfolds con momenti angolari trasversi. Valutiamo il tensore energia-impulso effettivo secondo la prescrizione quasilocale di Brown-York e otteniamo le equazioni estrinseche dei blackfold per black strings costruite a partire da Kerr, da Myers-Perry con due rotazioni e da black rings, commentando in particolare generalizzazioni a un numero più alto di momenti angolari trasversi e di dimensioni extra. Usiamo quindi questi risultati per generare nuove soluzioni approssimate in sei dimensioni con topologia $S^2 \times \mathbb{T}^2$, oltre che *black ring p-balls* con p pari, con orizzonte di geometria spaziale $S^2 \times S^1 \times \mathbb{B}^p$. L'analisi dei diagrammi di fase mostra che i risultati trovati sono validi fino a momenti angolari ridotti relativamente bassi $j \gtrsim 0.1$, segnalando un miglioramento significativo rispetto all'approccio blackfold originale. Studiamo infine la stabilità di due classi rappresentative di black branes che è possibile usare come punti di partenza di questa nuova teoria effettive, cioè black ring black branes e $D = 5$ Myers-Perry black branes. In entrambi i casi, si riscontra una instabilità di Gregory-Laflamme per ogni configurazione accessibile.

Contents

Introduction

Several properties are well-established for stationary asymptotically flat black holes in four dimensions. For instance, they must be endowed with spherical horizon topology, they are all uniquely determined by their mass, electric charge and angular momentum, and they also satisfy the so-called *Laws of Black Hole Mechanics*. Moreover, their most striking feature seems to reside in the possibility of attributing them a thermodynamic nature.

One may then ask oneself if these are essential aspects of black holes, or if they are simply four dimensional accidents. By performing a dimensional reduction of General Relativity, we see that gravity in lower dimensions has a rather different behaviour from the one that it exhibits in $D = 4$: for example, in $D = 3$ there is no asymptotically flat vacuum black hole solution to Einstein's Field Equations at all. This simple observation hints at the possibility that black holes in higher dimensions may actually behave very differently. Indeed, it turns out that not all the properties above are universal, since non-spherical horizons are allowed and uniqueness can be continuously broken in higher dimensions, as we will see in Chapter 2. However, the Laws of Black Hole Mechanics are dimension-independent, and in turn this suggests that black holes must be thought of as thermodynamic objects and that there must be a sound underlying black hole Statistical Mechanics.

Besides the interest in understanding how gravity itself behaves in general, there is also the possibility that higher dimensional black holes may describe actual physical configurations, if large extra-dimensions exist. Thus, it is reasonable to inspect the stability under perturbations of these higher dimensional solutions, in order to learn if they are long-lasting and if we should expect to see their effects on the observable universe. The idea is to perturb stationary solutions and to study the phase transitions that can occur between them. If instabilities are presents, lumpy or pinched horizon configurations can arise, and actually from numerical analyses [1] naked singularities are seen to show up in these cases. On the other hand, black holes in $D = 4$ are believed to be stable under perturbations. Considering the stability of higher dimensional black holes becomes then a new interesting way to study the validity of the Cosmic Censorship Conjecture, which requires no naked singularity to arise from the evolution of regular physical initial configurations.

A particularly useful perturbative formalism to deal with higher dimensional black holes is the *blackfold approach*. It describes solutions with a well-separated hierarchy of length scales along different directions over the horizon. Its starting point is the observation that, in some specific limit of high angular momenta, the entire set of known neutral rotating black holes geometries in higher dimensions behave locally as *black p-branes*. The geometry of these objects can be understood as the product between the $D \geq 4$ generalization to Schwarzschild black holes and a certain number p of flat directions. We define the *worldvolume* of the black brane as constituted by the product of the flat extra-directions with the timelike direction of the Schsarzschild sector, while the *transverse space* is formed by the remaining spatial directions. In view of this, the blackfold approach takes black branes as leading order configurations to describe locally ultra-spinning rotating black holes. Then, at the leading order, the hierarchy of length scales mentioned above consists of the horizon radius r_0 of the transverse space, and of the extrinsic curvature radius R characterizing worldvolume deformations, with $r_0/R \ll 1$.

As a consequence, this separation of length scales allows to split the gravitational degrees of freedom into short wavelength and long wavelength ones. The latter are described by a background spacetime into which the worldvolume is embedded, while the former are gathered into an effective theory describing a fluid living on the worldvolume. This effective fluid is a perfect one at leading order in r_0/R, while, for example, it gets viscous contributions at first order. The intrinsic and extrinsic dynamics of the effective fluid within the background spacetime are encoded into the *blackfold equations*, which follow in turn from Einstein's Equations, and they account for the behaviour of the black hole itself in the high angular momenta limit.

Conversely, one can use the blackfold formalism to generate new solutions with high angular momenta. In this regime, the stability analysis of black holes becomes easier as well, since it translates into the study of longitudinal and elastic perturbations acting on the effective fluid. It is well-known that neutral black branes are unstable, due to the so-called Gregory-Laflamme instability, a long wavelength instability involving oscillatory perturbations along the worldvolume directions. Given that blackfolds are locally wrapped black p-branes, we expect also ultra-spinning black holes to suffer from such an instability. As we will see in Section 4.1, this is actually the case.

The aim of this thesis is twofold. After reviewing different aspects of higher-dimensional black holes and of the blackfold approach in the first three chapters, in Chapter 4 we make use of the blackfold approach to analyse the dynamic instability of black rings. They constitute a particular class of $D = 5$ exact solutions with horizon topology $S^2 \times S^1$, where the sphere S^2 is characterized by a length scale r_0 while the circle S^1 has associated length scale R. Numerical studies [2, 3] support the presence of several dynamic instabilities for this class of solutions. Thin rings with $r_0 \lesssim R$ suffer from a longitudinal instability similar to the one found by Gregory and Laflamme for flat black branes. On the other hand, fat black rings with $r_0 \gtrsim R$ appear to be unstable under elastic perturbations.

Even though it was the first family of black holes with a non-spherical horizon topology to be discovered, a complete theoretical picture of their dynamics is still lacking, as analytic treatments are difficult to perform using the exact solution. It has been possible to capture the behaviour of black rings only partially, for example by expanding the theory in a large number of dimensions D, as performed in [4, 5]. In [6], it was also shown that the blackfold approach is able to describe very accurately the stationary sector of black rings. Furthermore, numerical data is not statistically significant for very thin rings with $r_0 \lesssim 0.1\,R$, and this fact makes it even more interesting to study this issue from the blackfold point of view.

The second aim of this thesis is to build a new effective theory based on the blackfold formalism and to describe higher dimensional solutions with non-zero angular momenta along transverse directions. Once analysed the foundations of this effective theory in Chapter 5, we will make use of it in Chapter 6 to inspect new classes of solutions in $D \geq 6$ built from black ring blackfolds. Finally, as representative examples, we will study the leading order stability of black ring blackfolds and 5D Myers-Perry blackfolds, and make a comparison with the stability of Schwarzschild blackfolds.

Chapter 1

An Introduction to General Relativity

In this chapter, we present several well known solutions and results concerning 4-dimensional black holes. We will restrict ourselves to proving or obtaining only the aspects that are relevant to the work carried out in this thesis.

1.1 Einstein Field Equations

The Einstein Field Equations (EFE)

$$R_{\mu\nu} - \frac{1}{2} g_{\mu\nu} R = 8\pi T_{\mu\nu} \tag{1.1}$$

relate the D-dimensional spacetime geometry described by a metric tensor $g_{\mu\nu}$ to the energy distribution determined by the stress-energy tensor $T_{\mu\nu}$. They can be obtained in several ways, either following Einstein's path of searching for a relativistic generalization to Newtonian gravitation, or from a variational principle, performing a variation of the classical Hilbert-Einstein action

$$I_{HE} \;=\; \int d^4x \sqrt{-g} \left[\frac{R}{16\pi G} + \mathcal{L}_M \right], \tag{1.2}$$

where $\mathcal{L}_M$ is the Lagrangian density of the matter content of the spacetime. From this action integral, one recovers eq. (1.1), with the stress-energy tensor defined as

$$T_{\mu\nu} = -\frac{2}{\sqrt{-g}} \frac{\delta(\sqrt{-g}\mathcal{L}_M)}{\delta g^{\mu\nu}}. \tag{1.3}$$

Let us now analyse the meaning of finding a solution to these equations. Recalling the symmetry of $g_{\mu\nu}$, eq. (1.1) corresponds to $\frac{1}{2}D(D+1)$ second order PDEs with the $\frac{1}{2}D(D+1)$ independent components of $g_{\mu\nu}$ as variables. Then one could think that a

metric tensor is uniquely determined by a specific stress-energy tensor $T_{\mu\nu}$ and a well-posed set of boundary conditions. On the contrary, the metric components are expressed in terms of the chosen set of coordinates, but of course we expect the solution to EFE to be chart-independent. This explains why we must think of the solution to EFE as an equivalence class of D-dimensional metric tensors $g_{\mu\nu}$ related by diffeomorphisms.

Indeed, we can trace the source of these additional D degrees of freedom within the known contracted Bianchi identities

$$\nabla_\nu G^{\mu\nu} = \nabla_\nu \left(R^{\mu\nu} - \frac{1}{2} R g^{\mu\nu} \right) = 0, \tag{1.4}$$

corresponding to D differential equations among the $\frac{1}{2}D(D+1)$ field equations. As a consequence, we are left with only $\frac{1}{2}D(D+1) - D$ independent equations of motion fixing the metric components.

Equation (1.4) can be also considered as a dynamical one. From (1.1), it implies

$$\nabla_\mu T^{\mu\nu} = 0, \tag{1.5}$$

which is a set of D equations dictating the evolution of the matter content of our spacetime according to its curvature (encoded in the connection, which enters the covariant derivative). Equation (1.5) includes the conservation of the energy stress tensor as well, and in case of flat spacetime in Cartesian coordinates the familiar conservation law $\partial_\alpha T^{\alpha\beta} = 0$ is recovered.

Finally, we notice that EFE reduce to $R_{\mu\nu} = 0$ in regions where a vacuum condition holds, namely $T_{\mu\nu} = 0$. We will only have the chance to appreciate a part of the great variety of physical situations that are described by this single set of equations.

1.2 Schwarzschild solution

A particularly important $D = 4$ vacuum solution is the Schwarzschild metric

$$ds^2 = -\left(1 - \frac{r_0}{r}\right) dt^2 + \left(1 - \frac{r_0}{r}\right)^{-1} dr^2 + r^2 \left(\sin^2\theta \, d\varphi^2 + d\theta^2\right). \tag{1.6}$$

The coordinate t refers to the proper time of a static observer at spatial infinity, while the angular coordinates $0 \leq \phi < 2\pi$ and $0 \leq \theta \leq \pi$ parametrize the sphere S^2 obtained as spacelike surfaces at $t, r = const.$ The radial coordinate r is chosen according to the areal gauge, in such a way that a sphere determined by a certain r has surface $4\pi r^2$.

It is important to point out the asymptotic flatness of this solution, since we recover the Minkowski metric in spherical coordinates in the limit $r \to \infty$. Besides being spherically symmetric, this solution has also an isometry defined by the Killing vector ∂_t.

The metric components are independent of the coordinate t, in such a way that we can state that (1.6) is static for $r > r_0$. In the region $r < r_0$ the coordinate t becomes spacelike while r becomes timelike, so that r and t switch their role. As a consequence, we see easily that the metric cannot be static for an observer inside the horizon, since its components do depend on r.

In particular, as proven by Birkhoff's theorem, it can be shown that the Schwarzschild metric is the unique $D = 4$ asymptotically flat vacuum solution to EFE describing the gravitational field outside a static and spherical symmetric source of mass m. Taking the weak field limit, we can compare the local acceleration measured by a static observer at spatial infinity with the Newtonian one, and in this way it is possible to fix $r_0 = 2Gm$.

Let us now inspect the concept of horizon [7]. We consider first a null hypersurface $\mathcal{N}$, that is a 3-surface whose normal vector has a null norm anywhere on it but non-vanishing components. Then $\mathcal{N}$ is said to be a *Killing horizon* if there exists a Killing vector field ξ^α with a neighbourhood of $\mathcal{N}$ as domain, such that ξ^α must be orthogonal to $\mathcal{N}$. Since ξ^α has constant null norm on $\mathcal{N}$, the gradient of $\xi^\alpha \xi_a$ is orthogonal to $\mathcal{N}$ as well, and hence it will be proportional to ξ^α. Thus, for some scalar function κ over $\mathcal{N}$, it holds true that

$$\nabla_\alpha (\xi^\beta \xi_\beta)\big|_{\mathcal{N}} = -2\kappa \xi_\alpha, \tag{1.7}$$

where we label κ as the *surface gravity* associated to the Killing horizon $\mathcal{N}$. Making use of the definition of a Killing vector, we can also rewrite (1.7) as

$$\xi^\beta \nabla_\beta \xi^\alpha \big|_{\mathcal{N}} = \kappa \xi^\alpha. \tag{1.8}$$

It is interesting to recall that the affine parametrization of a geodesic trajectory is unique (neglecting possible translations). If we describe a geodesic arbitrarily parametrized and with V as tangent vector, it is well known that the geodesic equation

$$\nabla_V V = 0 \tag{1.9}$$

does not hold any more. Instead, we have in general

$$\nabla_V V \propto V. \tag{1.10}$$

From this point of view, equation (1.8) suggests that κ essentially measures to what extent the integral curve of ξ^α cannot be affinely parametrized. In connection with this, it can be shown that the surface gravity corresponds to the force per unit mass required at infinity to maintain a static observer near the horizon [8].

Returning to the Schwarzschild solution, we observe that the Killing vector ∂_t is null at $r = r_0$, and hence we recognize the 3-surface $r = r_0$ to be a Killing horizon, with generator ∂_t. From the definitions given above, it is also easy to compute its surface gravity, which results in

$$\kappa = \frac{1}{4Gm}, \tag{1.11}$$

clearly implying that the bigger is a black hole, the lower is its surface gravity.

However, we still have to analyse the regularity of this spacetime near $r = r_0$. A first hint comes from the Kretschmann scalar $R_{\mu\nu\rho\sigma}R^{\mu\nu\rho\sigma}$, which is finite at $r = r_0$. It is also possible to find an analytical extension of the solution (1.6), showing that the singularity on the horizon is just related to Schwarzschild coordinates.

If we restrict ourselves to the vicinity of $r = r_0$, by setting $r - 2Gm \simeq \frac{\xi^2}{8m}$, the metric reads

$$ds^2 \simeq -\frac{\xi^2}{16m^2}dt^2 + d\xi^2 + 4m^2 d\Omega^2_{(2)}. \tag{1.12}$$

Putting aside the S^2 sector, we observe that the first two terms in the r.h.s are similar to a 2-dimensional flat metric $d\rho^2 + \rho^2 d\phi^2$ in polar coordinates, once we identify $\xi \to \rho$ and $\frac{t}{4m} \to i\phi$. We have not solved the singularity in $r = r_0$ yet, since it has simply been translated into the well known polar coordinates' singularity at $\rho = 0$. If we move to Cartesian coordinates, by defining[1]

$$X = \rho\cos(\phi) = \xi\cosh\frac{t}{4m} \tag{1.13}$$

$$T = \rho\sin(\phi) = \xi\sinh\frac{t}{4m}, \tag{1.14}$$

the metric near the horizon takes the form

$$ds^2 \simeq -dT^2 + dX^2 + 4m^2 d\Omega^2_{(2)}. \tag{1.15}$$

It means that the Schwarzschild metric can be smoothly deformed into the product of $\mathbb{R}^{1+1} \times S^2$ in that region, and we can safely state that the spacetime is regular at $r = r_0$, which is the Killing horizon of this solution. Two other very common sets of coordinates regular at the horizon are the ones by Eddington and Finkelstein. Considering the outgoing chart, we define the Regge-Wheeler tortoise radial coordinate

$$r^* = r + 2Gm\ln\left|\frac{r}{2Gm} - 1\right| \tag{1.16}$$

and the null coordinate $v = t + r^*$, related to outgoing null geodesics. Consequently, the Schwarzschild metric reads

$$ds^2 = -\left(1 - \frac{2Gm}{r}\right)dv^2 + 2dvdr + r^2 d\Omega_2^2, \tag{1.17}$$

which again is regular at $r = r_0$.

We now turn to the study of the other singularity of the metric, namely the one occurring at $r = 0$. Here the Kretschmann scalar diverges, hence we are in the presence

[1] In fact, in this way we are considering the expansion of Kruskal coordinates near the horizon.

of an actual curvature singularity. It is important to notice that r is a timelike coordinate in this region, and $r = const$ identifies spacelike surfaces. We conclude that $r = 0$ is a spacelike singularity, and must be thought of as at an instant in time and not at a point in space, according to an infalling observer. We have already mentioned that r and t switch roles for $r < r_0$, with r becoming a timelike coordinate and t becoming a spacelike coordinate. From a physical point of view, it means that an observer cannot be static here, and must have lower and lower values of r as time goes by. Then nothing can prevent him from getting to the origin $r = 0$, where tidal forces diverge.

From the analysis of radial null trajectories, it is also easy to show that an observer placed in r_O measures the frequency of a signal emitted at r_E as

$$\nu_O = \sqrt{\frac{g_{tt}(r_E)}{g_{tt}(r_O)}}\,\nu_E, \tag{1.18}$$

which has limit

$$\nu_O = \sqrt{g_{tt}(r_E)}\nu_E \tag{1.19}$$

for an observer placed at spatial infinity. In particular, if the signal is emitted at $r_E = r_0$, $g_{tt}(r_E)$ vanishes and the observer at infinity will never receive it. Therefore, this Killing horizon is also a surface of infinite redshift.

1.3 Kerr solution

We say that a black hole is *stationary* if its metric admits a Killing vector field which is timelike at spatial infinity. It was shown by Carter and Hawking that the most general neutral stationary black hole solution with an axial symmetry is described by the Kerr metric. In the so-called Boyer-Lindquist coordinates [9, 10, 11], it reads

$$\begin{aligned} ds^2 = &-\frac{\Delta - a^2\sin^2\theta}{\rho^2}dt^2 - \frac{2a\sin^2\theta\,(r^2+a^2-\Delta)}{\rho^2}dtd\phi + \\ &+\frac{\rho^2}{\Delta}dr^2 + \rho^2 d\theta^2 + \left(r^2 + a^2 + \frac{\mu r}{\rho^2}a^2\sin^2\theta\right)\sin^2\theta d\phi^2, \end{aligned} \tag{1.20}$$

where we have defined

$$\rho^2 = r^2 + a^2\cos^2\theta, \qquad \Delta = r^2 + a^2 - \mu r. \tag{1.21}$$

Its components do not depend on the coordinate ϕ, which is compatible with the requirement of axial symmetry. We notice that it is not static according to an observer at infinity, due to the presence of the mixing term $g_{t\phi}$. The parameters of this solutions are μ and a, which describe the mass and the angular momentum density of this class of solutions. Actually, one finds that the spacetime is asymptotically flat; furthermore,

considering up to $O(1/r)$ contributions, one sees that μ coincides with twice the ADM mass, while the ADM angular momentum has the form $J = \frac{1}{2}a\mu$.

In the limit $a \to 0$, we recover the Schwarzschild solution and thus staticity at spatial infinity. Instead, if we take $\mu \to 0$, we obtain the flat metric in ellipsoidal coordinates:

$$ds^2 = -dt^2 + \frac{\rho^2}{r^2 + a^2} dr^2 + \rho^2 d\theta^2 + (r^2 + a^2) \sin^2 \theta d\phi^2, \tag{1.22}$$

with

$$\begin{aligned} x =& \sqrt{r^2 + a^2} \sin\theta \sin\phi, \\ y =& \sqrt{r^2 + a^2} \sin\theta \cos\phi, \\ z =& r \cos\theta. \end{aligned} \tag{1.23}$$

The Kerr metric (1.20) is apparently singular at $\Delta = 0$ and $\rho^2 = 0$. In the latter case, one can show that the Kretschmann invariant diverges and thus it points out to a curvature singularity. We also notice that $\rho^2 = 0$ holds only if $r = 0$ and $\theta = \frac{\pi}{2}$. In view of (1.23), then this singularity corresponds to a circular ring on the equatorial plane $\theta = \frac{\pi}{2}$, with radius a. Of course, this feature is linked to the presence of an angular momentum, and we see that the ring degenerates into the known Schwarzschild point-like singularity if $a \to 0$. Nonetheless, in case of rotation, it is important to stress that the spacetime is regular in the region in the center of the ring.

While $\rho^2 = 0$ turns out to describe a curvature singularity, for $\Delta = 0$ the Kretschmann scalar does not diverge and hence we expect that it is possible to find other sets of coordinates in such a way that the new metric is manifestly regular here. Kerr coordinates are a suitable set, and in principle they are a generalization of Eddington-Finkelstein coordinates for Schwarzschild.

We observe that the condition $\Delta = 0$ dictating the singularity of g_{rr} in (1.20) is satisfied when the radial coordinate gets the values

$$r_\pm = \frac{\mu}{2} \pm \sqrt{\frac{\mu^2}{4} - a^2}. \tag{1.24}$$

It is easy to see that the surfaces described by $r = r_+$ and $r = r_-$ are null surfaces, and we will label them *outer* and *inner horizon* respectively. Of course, the presence of $r_\pm$ divides the spacetime into three regions:

- $r > r_+$, which is is the exterior of the black hole, where r is a spacelike coordinate;
- $r_- < r < r_+$, where r is the timelike coordinate, and hence both ingoing and outgoing observers must fall towards the inner horizon;
- $r < r_-$, and here r is again spacelike. This is the region in which the physical singularity $\rho^2 = 0$ resides.

It is noteworthy that r_+ and r_- coincide if $\mu = 2a$, and in this case we have a single degenerate horizon. This condition is called *extremality*, and we notice that for $a > \frac{\mu}{2}$ there is no horizon at all. A physical observer could move from the singularity to infinity and then we say that a *naked singularity* is present when the *Kerr bound* $a \leq \frac{\mu}{2}$ is not satisfied.

A rather peculiar feature of the Kerr metric is that even observers with zero angular momentum have a non-vanishing angular velocity. This *frame dragging effect* is easily understood to be due to the spin of the black hole itself. The co-rotation angular velocity for such an observer placed in (r, θ) is

$$\Omega = \frac{\mu a r}{(r^2 + a^2)^2 - a^2 \sin^2\theta \Delta} \tag{1.25}$$

and it has always the same sign as the black hole angular momentum.

As it can be easily inspected, the Kerr metric (1.20) in these coordinates admits two Killing vectors, namely ∂_t and ∂_ϕ. Their specific combination

$$\mathbf{k} = \partial_t + \Omega_H \partial_\phi \tag{1.26}$$

can be shown to generate the outer horizon $r = r_+$, which is then also a Killing horizon, with

$$\Omega_H = \frac{a}{r_+^2 + a^2}. \tag{1.27}$$

In particular, we observe that $\Omega(r_+) = \Omega_H$, a fact that can be interpreted by saying that, due to frame dragging, a zero angular momentum observer at $r = r_+$ has the same angular velocity as the (outer horizon of the) black hole.

When more than one parameter enter a class of solutions, it can be interesting to study its phase space in order to compare its properties in different regimes. We proceed by defining some dimensionless quantities with reference to a unique common scale, and we conveniently choose it to be the total mass of the solution. We consider the reduced angular momentum

$$j = \frac{J}{GM^2} = \frac{2a}{\mu}, \tag{1.28}$$

and the reduced horizon area

$$a_H = \frac{\mathcal{A}_H}{8\pi G M^2} = 1 + \sqrt{1 - \frac{4a^2}{\mu^2}} = 1 + \sqrt{1 - j^2}, \tag{1.29}$$

where the outer horizon area can be easily computed from the spatial sections of the metric at $r = r_+$ and it results

$$\mathcal{A}_H = 2\pi\mu \left(\mu + \sqrt{\mu^2 - 4a^2}\right). \tag{1.30}$$

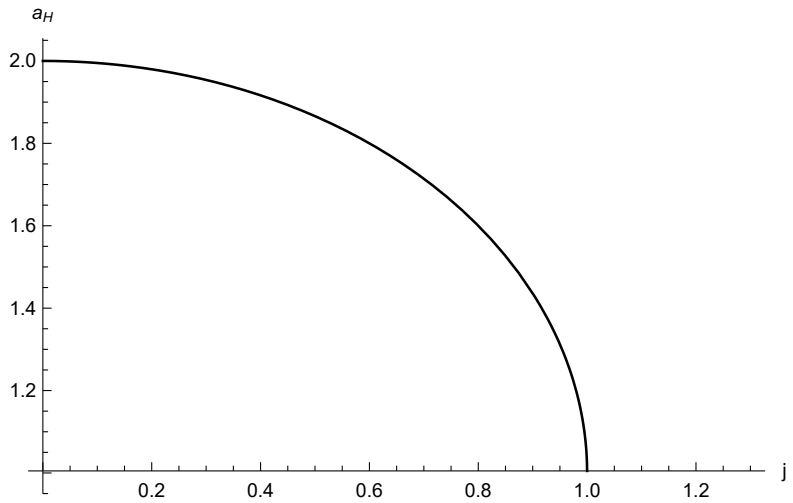

Figure 1.1: We show here the phase diagram for Kerr black holes. In the Schwarzschild limit $j \to 0$ the reduced area is maximal, while it decreases up to vanish approaching extremality $j = 1$, where the Kerr bound is saturated and the horizon disappears.

In Figure 1.1 the behaviour of the reduced area in terms of j is plotted. We approach extremality in the limit $a \to \frac{\mu}{2}$, that is when $j \to 1$, and there a vanishing reduced horizon area agrees with the disappearance of the horizon itself discussed above.

In Section 1.2 we saw that a convenient way of finding the horizon of a static solution is to simply look at the points where $g_{tt} = 0$, since we had a timelike Killing vector ∂_t which is orthogonal to spatial surfaces. Considering now stationary black holes, this procedure is no longer sensible, and it is necessary to inspect explicitly where the norm of the Killing vector that generates the horizon (here $\mathbf{k}$) becomes zero.

However, studying where $g_{tt} = 0$ is still worthy, and it happens if the radial coordinate takes the values

$$r_{IR}^{\pm} = \frac{\mu}{2} \pm \sqrt{\frac{\mu^2}{4} - a^2 \cos^2\theta}, \tag{1.31}$$

where it holds $r_{IR}^{-} < r_{-} < r_{+} < r_{IR}^{+}$. Of course, an observer in $(r,\theta)_{OBS}$ would measure the frequency of a signal emitted at $(r,\theta)_{EM}$ with a redshift determined by

$$\nu_{OBS} = \sqrt{\frac{g_{tt}(r,\theta)_{EM}}{g_{tt}(r,\theta)_{OBS}}}\,\nu_{EM}, \tag{1.32}$$

in such a way that a signal coming from r_{IR}^{+} undergoes an infinite redshift, and has vanishing energy according to *any* observer outside that surface. Furthermore, it is noteworthy that in the interval $r_{IR}^{-} < r < r_{IR}^{+}$ the component g_{tt} is positive. It involves that here ∂_t is a spacelike coordinate and that there can be no static observer. Thus, for

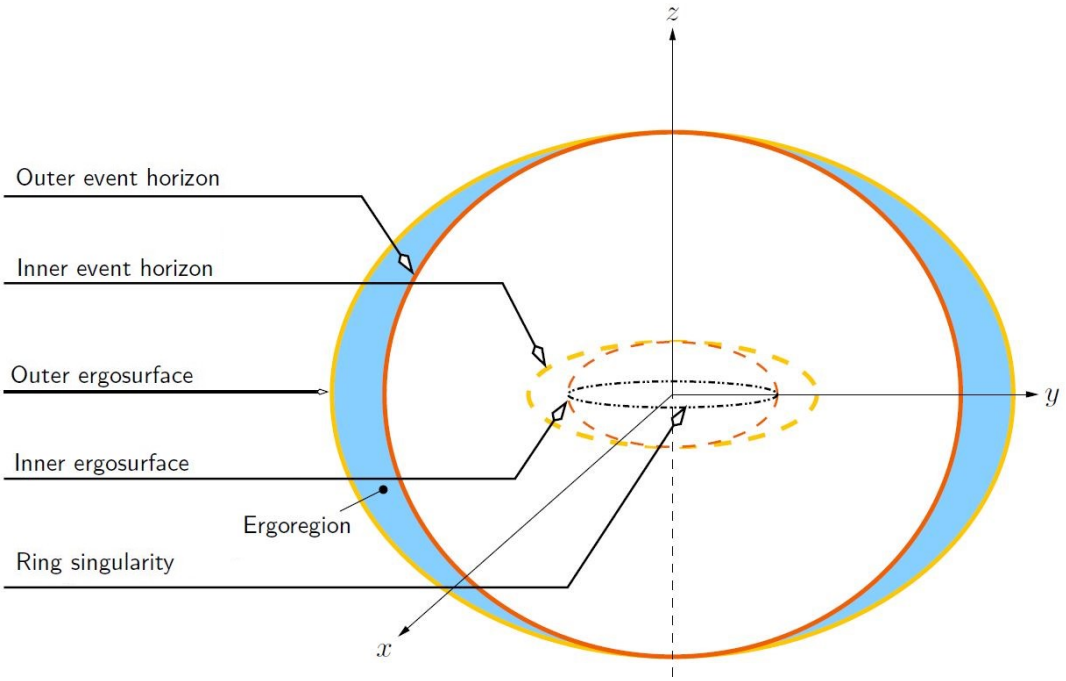

Figure 1.2: The most important features of the Kerr spacetime are shown in this cartoon [10], such as the ring curvature singularity, the horizons and the ergosphere.

rotating black holes there exists a new region $r_+ < r < r^+_{IR}$ called *ergosphere* where an observer cannot stand still, but from which he can get to spatial infinity. A summary of the above considerations is displayed in Figure 1.2.

The Kerr metric can be generalised in order to include electric charge (in such a way that it becomes an *electro-vacuum* solution). The result is the Kerr-Newman metric. It is a solution to EFE, now coupled to Maxwell equations, and it is characterized by an additional asymptotic conserved charge Q, which is of course the electric charge of the source. The *Black Hole Uniqueness Theorem* actually states that, together with well-motivated physical assumptions, the only possible asymptotically flat, stationary and axisymmetric black hole solution to Einstein-Maxwell equations in $D = 4$ is the Kerr-Newman metric. In this way, we can completely characterize such a black hole by simply pointing out its mass M, total angular momentum J and electric charge Q [12].

A remarkable assumption that underlies this work is the so-called *Cosmic Censorship Conjecture*, originally brought forth by Penrose. It states that any physical spacetime must exhibit global hyperbolicity, that is it must admit at least one Cauchy surface, leading to the predictability of the spacetime [13]. Consequently, it can be restated by saying that naked singularities cannot develop in nature from a set of regular initial

conditions. Its first consequence is a constraint on the possible range of values of the black hole parameters M, J and Q, following from the Kerr-Newman extremality bound

$$M^2 \geq a^2 + Q^2, \tag{1.33}$$

which is a simple generalization of the Kerr bound mentioned above.

1.4 Black Hole Mechanics

In 1973 Bardeen, Carter and Hawking provided a general proof of four laws that constrain the dynamic behaviour of stationary black holes [14, 11]. We now turn to a brief review of these *Four Laws of Black Hole Mechanics*.

It is possible to calculate surface gravity from equation (1.7) also for Kerr and Kerr-Newman black holes. Although being defined locally, κ is constant on the whole horizon. In fact, this statement can be proven to be a general result, simply following the assumptions of stationarity and the properties of a Killing horizon, and it is usually referred to as the *Zeroth Law*.

The *First Law* consists in a first order identity relating variations of the characteristic parameters for a stationary black hole, and it reads

$$\delta M = \frac{\kappa}{8\pi G}\delta A + \Omega_H \delta J + \Phi_H \delta Q. \tag{1.34}$$

where A is the horizon area, while Φ_H is the electric potential on the horizon.

The *Second Law* coincides with the well known Area Theorem, which was proven by Hawking requiring the strong energy condition on the energy-stress tensor and the global hyperbolicity of the spacetime. It asserts that the horizon area is a non-decreasing function of the timelike coordinate outside the horizon.

Finally, the *Third Law* states that it is impossible to make the surface gravity vanish in a finite number of steps. From the explicit form of κ, in turn it means that one cannot make a stationary black hole reach extremality in a finite number of variations involving its characteristic parameters. Then, if we consider a physical situation, it appears to be impossible to reach extremality at all.

1.5 Black Hole Thermodynamics

The first reason that compels us to think of a black hole as of a thermodynamic object is the fact that otherwise it would get very easy to violate the Second Law of Thermodynamics. In principle, it would be sufficient to let a physical system fall into a black hole horizon in order to have a decrease of the total entropy, corresponding to the loss of the entropy of the system according to an observer outside the black hole. Following the

celebrated paper by Bekenstein [15], we can estimate the subsequent increase that the black hole entropy should undergo in order not to violate the Second Law of Thermodynamics, and this led Bekenstein to associate to a black hole an entropy proportional to its horizon area.

This way of reasoning is further justified by the explicit similarity between the Four Laws of Black Hole Mechanics and the usual Laws of Thermodynamics. From this point of view, a review of the Zeroth and Third Law let us recognize an analogy between the behaviour of the temperature T of a thermodynamic system and the one followed by the surface gravity κ.

It is also customary to write the First Law of Thermodynamics in case of conserved charges N_i as

$$dU = TdS - \delta W + \sum_i \mu_i N_i. \tag{1.35}$$

Then, if we consider a situation with no work done on the system $\delta W = 0$, we see that (1.35) coincides perfectly with (1.34), once we make the black hole mass M correspond to the internal energy of the system. The conserved charges here are the angular momentum J and the charge Q, and hence the surface angular momentum and electric potential can be thought of as being their conjugated chemical potentials.

Therefore, in some sense we expect to be able to associate an entropy and a temperature to a black hole in the form

$$T_H = \lambda\kappa, \tag{1.36}$$

$$S_{BH} = \frac{A}{8\pi G\lambda}, \tag{1.37}$$

for some real constant λ. We also notice that a correspondence for the Second Law follows straightforwardly from the Area Theorem with an entropy of the form (1.37). Of course, at the moment these relations are still lacking a physical meaning. A naive interpretation may be misleading, since for instance classically the temperature of a black hole is zero. The attribution of a Statistical Mechanics and of a phase space to this black hole Thermodynamics is puzzling as well.

In fact, the meaning of the previous discussion is partly explained by a quantum mechanical effect, namely Hawking radiation. Given a spacetime with a black hole and a set of fields ϕ_i on that spacetime, at late times an observer placed at spatial infinity detects particles of the fields ϕ_i with an energy distribution following the black body spectrum with a specific temperature T_H, at leading order.

The origin of this phenomenon is essentially related to the effect that the non-trivial causal structure has on the fields propagation in the vicinity of the horizon [16]. The most standard way to find out Hawking radiation makes use of Bogoliubov formalism, inspecting the change of basis that the creation and annihilation operators of a field undergo when switching from a freely falling frame and its ground state to an asymptotic static observer. Of course, we can state that only the latter *detects particles* in the usual

Minkowski QFT meaning, since we are dealing with asymptotically flat spacetimes. An essential ingredient is then to recall that the energy of a state and, in particular, its positivity is frame-dependent in GR. As a consequence, it turns out that the ground state of the infalling observer is not a vacuum state according to the asymptotic Minkowskian observer. He actually detects particles with a Planckian number distribution

$$N(\omega) \approx \frac{1}{\exp(\frac{2\pi\omega}{\kappa}) - 1}, \tag{1.38}$$

where κ is the surface gravity, in such a way that

$$T_H = \frac{\hbar\kappa}{2\pi k_B}. \tag{1.39}$$

From relation (1.37), it also means that the entropy of a black hole is

$$S_{BH} = \frac{A}{4G}. \tag{1.40}$$

We remark that the outgoing spectrum is Planckian just at leading order, since there are several corrections that one has to take into account [17]. Here we will only mention the so called *grey-body factors*, which change the previous number distribution as

$$N(\omega) \approx \frac{f(\omega)}{\exp(\frac{2\pi\omega}{\kappa}) - 1}, \tag{1.41}$$

with $0 < f(\omega) \leq 1$ a suppression function related to the backscattering of outgoing modes. These get reflected before reaching spatial infinity due to the curvature of spacetime, which acts effectively as a potential barrier. The main outcome is an effective temperature $T_{eff} \leq T_H$ measured by an asymptotic static observer.

It is now interesting to think of the implications of Hawking radiation. First, we notice that its most immediate consequence is the fact that black holes loose mass over time and eventually evaporate. However, due to the low emitted power, it would take some $10^{50}s$ for a solar-mass black hole to evaporate. We also observe that this fact does not disagree with the requirement of a total entropy increase, even though the horizon area apparently decreases with time. As a matter of fact, at any given moment, Hawking radiation involves a decrease of the black hole entropy

$$dS_{BH} = -\frac{|dM|}{T_H}, \tag{1.42}$$

while an entropy variation

$$dS_{rad} = +\frac{|dM|}{T_{eff}} \tag{1.43}$$

corresponds to the outgoing radiation, so that the total entropy variation is

$$dS = dS_{BH} + dS_{rad} = |dM| \left(\frac{1}{T_{eff}} - \frac{1}{T_H} \right) \geq 0, \tag{1.44}$$

and the Second Law of Thermodynamics does still hold.

In conclusion, an analogy with ordinary Thermodynamics is suggested from a classical approach involving only GR. In addition, from a semiclassical point of view it is possible to obtain a physical explanation of associating a non-vanishing temperature T_H to a black hole, and this leads us to go beyond the analogy and to understand the actual presence of a black hole Thermodynamics.

One would expect the next step to consist in finding a clear Statistical Mechanics from which the Bekenstein-Hawking entropy should emerge, perhaps at the quantum gravity level. Here we will not delve into the many (promising) attempts to find these related microstates that have been pursued since the first satisfactory stringy computation by Strominger and Vafa in 1996 [18], and we will simply assume the validity of (1.40) in the following sections.

Chapter 2

Black Holes in Higher Dimensions

As we saw in Chapter 1, there are several features that are common to any $D = 4$ stationary vacuum black hole solution. For instance, they are all characterized by a spherical horizon topology and the Uniqueness Theorem strictly constraints the possible solutions of this kind. On the contrary, in this Chapter we will partly inspect how wide and populous the zoo of higher dimensional black holes is found to be. We restrict ourselves to discussing the solutions that we will make use of in the following sections, leaving aside the more complicated cases of doubly spinning black rings and multi black holes such as black saturns, bi- and di-rings.

We anticipate that for rotating higher dimensional black holes it becomes both interesting and necessary to perform a phase diagram analysis to compare different regimes and different solutions with the same conserved quantities. In order to make consistent comparisons, we intend to define a general form of the dimensionless angular momentum and horizon area depending only on the dimension D of the solution [19]. It is convenient to define

$$j^{D-3} = c_J \frac{J^{D-3}}{GM^{D-2}}, \qquad a_H^{D-3} = c_{\mathcal{A}} \frac{\mathcal{A}_H^{D-3}}{(GM)^{D-2}}, \tag{2.1}$$

with numerical constants

$$c_J = \frac{\Omega_{D-3}}{2^{D+1}} \frac{(D-2)^{D-2}}{(D-3)^{\frac{D-3}{2}}}, \qquad c_{\mathcal{A}} = \frac{\Omega_{D-3}}{2(16\pi)^{D-3}} (D-2)^{D-2} \left(\frac{D-4}{D-3}\right)^{\frac{D-3}{2}}. \tag{2.2}$$

2.1 Schwarzschild and black branes

A relatively straightforward generalization of the Schwarzschild solution was found by Tangherlini [20], and it describes the D dimensional spacetime outside a source with spherical symmetry. Its explicit form is

$$ds^2 = -\left(1 - \frac{r_0^{D-3}}{r^{D-3}}\right) dt^2 + \left(1 - \frac{r_0^{D-3}}{r^{D-3}}\right)^{-1} dr^2 + r^2 d\Omega_{D-2}^2, \tag{2.3}$$

and it can be easily understood to be a Ricci-flat metric. It is apparent that it shows the same features as the well known 4-dimensional counterpart: we have a horizon located at $r = r_0$ with $(D-2)$-spheres as spatial sections. The difference is now that the gravitational potential has a stronger radial fall-off in the Newtonian limit, with power law $1/r^{D-3}$. Due to it, we will continue to refer to this metric simply as Schwarzschild solution.

It is noteworthy that the easiest way to obtain a vacuum black hole solution in $D > 4$ dimensions is by adding extra flat directions to another known vacuum solution [19]: given a solution $\Upsilon^{(d)}$ in d dimensions with horizon spatial sections $\mathcal{H}^{(d-2)}$, one can construct a solution in $d+p$ dimensions by adding p flat directions to it, that is

$$ds^2_{d+p} = ds^2_d(\Upsilon) + \sum_{i=1}^{p}(dz^i)^2. \tag{2.4}$$

As a consequence, this new solution has horizon topology $\mathcal{H}^{(d-2)} \times \mathbb{R}^p$, or $\mathcal{H}^{(d-2)} \times \mathbb{T}^m \times \mathbb{R}^{p-m}$ if we require a periodicity of some m directions.

For example, one can consider adding extra-dimensions to the Schwarzschild-Tangherlini metric and the result is a *Schwarzschild black p-brane* (or more commonly just *black p-brane*), with metric

$$ds^2 = -\left(1 - \frac{r_0^n}{r^n}\right)dt^2 + \left(1 - \frac{r_0^n}{r^n}\right)^{-1} dr^2 + r^2 d\Omega^2_{n+1} + \sum_{i=1}^{p}(dz^i)^2, \tag{2.5}$$

where we have set $n = D-p-3$ for later convenience. Of course, Kerr black branes can be constructed in an analogous way.

2.2 Myers-Perry black holes

Myers-Perry (MP) metrics can be seen as a generalization of the Kerr solution to dimensions $D \geq 4$, and consequently they admit more than one plane of rotation [21, 22]. One finds that it is necessary to distinguish between the case of odd and even dimensions.

For $D = 2n+1$ and $D \geq 5$, the metric is usually written in the form

$$ds^2 \;=\; -dt^2 + \frac{\mu r^2}{\Pi F}\left(dt + \sum_{i=1}^{n} a_i \mu_i^2 d\phi_i\right)^2 + \frac{\Pi F}{\Pi - \mu r^2}\, dr^2 + \sum_{i=1}^{n}\left(r^2 + a_i^2\right)\left(d\mu_i^2 + \mu_i^2 d\phi_i^2\right), \tag{2.6}$$

where we have defined

$$F = 1 - \sum_{i=1}^{n} \frac{a_i^2 \mu_i^2}{r^2 + a_i^2}, \qquad \Pi = \prod_{i=1}^{n}\left(r^2 + a_i^2\right). \tag{2.7}$$

Implicitly, the coordinate system splits the $2n$ spatial dimensions onto n planes, each labelled by i. Then, μ_i is the projection of the point over the i-th plane, and ϕ_i is the angle related to it. From these definitions, not all the μ_i are independent, since the constraint $\sum_{i=1}^{n} \mu_i^2 = 1$ is present.

We identify also (μ, a_i) as the $n+1$ parameters of these solutions[1]. From the asymptotic analysis of the metric, it can be shown that they determine the mass and angular momenta of the black hole as

$$M = \frac{(D-2)\Omega_{D-2}}{16\pi G}\,\mu, \qquad J^i = \frac{\Omega_{D-2}}{8\pi G}\,\mu a_i = \frac{2}{D-2} M a_i, \tag{2.8}$$

so that μ is related to the Schwarzschild radius and a_i gives an estimate of the i-th angular momentum density per unit mass. This is in agreement with the fact that setting every $a_i = 0$ leads to the Schwarzschild-Tangherlini solution.

In the case of even dimensions $D = 2n+2$ ($D \geq 4$), there is an extra direction to take into account and the metric can be cast in the form

$$ds^2 = -dt^2 + \frac{\mu r}{\Pi F}\left(dt + \sum_{i=1}^{n} a_i \mu_i^2 d\phi_i\right)^2 + \frac{\Pi F}{\Pi - \mu r} dr^2 + \sum_{i=1}^{n} \left(r^2 + a_i^2\right)\left(d\mu_i^2 + \mu_i^2 d\phi_i^2\right) + r^2 d\alpha^2, \tag{2.9}$$

where $-1 \leq \alpha \leq 1$ and the constraint on the direction cosines clearly becomes $\alpha^2 + \sum_{i=1}^{n} \mu_i^2 = 1$.

The Kerr metric is recovered explicitly if one considers $D = 4$ dimensions and thus only one plane of rotation, i.e. $n = 1$. It can be easily shown that both metrics (2.6) and (2.9) have $n+1$ commuting Killing vectors, related to shifts in t and $SO(2)$ rotations of the n planes.

It is now useful to approach the case of solutions with a single non-vanishing spin parameter [23]. If we set $a_1 = a,\ a_{i>1} = 0$, for any $D \geq 4$ the metric reduces to

$$\begin{aligned} ds^2 = -dt^2 + \frac{\mu}{r^{D-5}\rho^2}\left(dt + a\sin^2\theta\, d\phi\right)^2 + \frac{\rho^2}{\Delta} dr^2 + \rho^2 d\theta^2 + \\ + (r^2 + a^2)\sin^2\theta d\phi^2 + r^2\cos^2\theta d\Omega_{D-4}^2, \end{aligned} \tag{2.10}$$

where we have also set $\mu_1 = \sin\theta$ and

$$\rho^2 = r^2 + a^2\cos^2\theta, \qquad \Delta = r^2 + a^2 - \frac{\mu}{r^{D-5}}. \tag{2.11}$$

[1] They are the parameters of this particular class of solutions in $D \geq 4$, but, as we will see, in general for $D > 4$ they are not enough to determine uniquely a black hole if we do not specify the class of solutions that we are considering, via some topological invariants. On the contrary, as well known, in $D = 4$ they do point out uniquely a black hole by themselves.

Let us now study the outer event horizon of the metric (2.10), focussing on the largest root r_+ of $g^{rr} = 0$, i.e.

$$\Delta(r_+) = 0 \qquad \text{iff} \qquad r_+^2 + a^2 - \frac{\mu}{r_+^{D-5}} = 0. \tag{2.12}$$

For $D = 4$, it leads to $r_+^2 - \mu r_+ + a^2 = 0$ and we recover the well known Kerr bound $a \leq \mu/2$ by imposing the reality of the horizon radius. Analogously, in $D = 5$ we find a similar bound for the angular momentum: $a^2 \leq \mu$. Again, beyond this value of a, no outer event horizon arises, and a naked singularity is present.

Instead, if we examine the case of $D \geq 6$, there is no such bound on a, since

$$\begin{aligned} \Delta(r_+) &\longrightarrow +\infty \quad \text{for} \quad r_+ \to \infty, \\ \Delta(r_+) &\longrightarrow -\infty \quad \text{for} \quad r_+ \to 0, \end{aligned}$$

and hence there is always a positive real root r_+. As a consequence, we find an admissible black hole solution for each value of a, and we can analyse the ultra-spinning regime $a \gg \mu$ of these metrics. In particular, we notice that in this limit we can give an asymptotic solution to eq. (2.12) in the form

$$r_+ \,=\, \left(\frac{\mu}{r_+^2 + a^2}\right)^{\frac{1}{D-5}} \,\approx\, \left(\frac{\mu}{a^2}\right)^{\frac{1}{D-5}} \tag{2.13}$$

for high rotation parameters a.

The horizon of this class of solutions is a $(D-2)$-surface homeomorphic to S^{D-2}, and it has size $l_\parallel = \sqrt{r_+^2 + a^2} \approx a$ along the two directions parallel to the plane of rotation, while it sweeps a radial distance $l_\perp = r_+$ along the other $D-4$ directions. The horizon area then results

$$\mathcal{A} \,=\, \Omega_{D-2}\, r_+^{D-4}\, (r_+^2 + a^2) \,\approx\, \Omega_{D-2}\, a^2 \left(\frac{\mu}{a^2}\right)^{\frac{D-4}{D-5}}, \tag{2.14}$$

and it is worth stressing that $\mathcal{A}$ decreases down to zero if we increase the angular momentum, while keeping the mass fixed. We also observe that the characteristic length scales $l_\parallel$ and $l_\perp$ of the horizon spatial sections have very different values in the ultra-spinning regime, a fact that is usually expressed by saying that the horizon gets a pancake shape along the plane of rotation.

Figure 2.1 shows the phase diagram of singly-spinning MP solutions in $D = 5, 6, 8$. The plot related to the $D = 5$ case has the same features as the one for Kerr, as already discussed. Instead, for $D \geq 6$ the reduced horizon area is still a decreasing function of the angular momentum, but we have no more a naked limit and the ultra-spinning regime $j \gg 1$ becomes accessible.

Thus, it becomes interesting to study the metric (2.10) in the so-called *black membrane limit*, by taking $j \to \infty$ in $D \geq 6$. We are interested in the case of a non vanishing

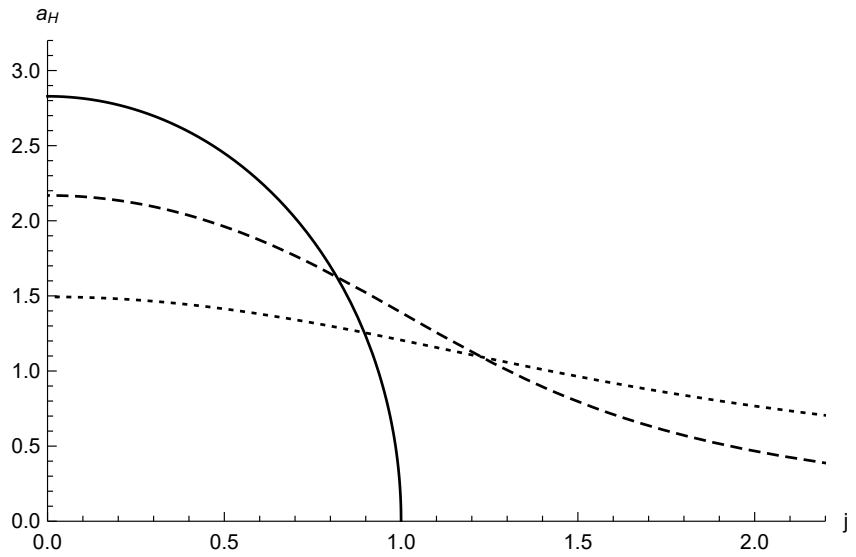

Figure 2.1: We display here the phase diagram for MP black holes in $D = 5$ (thick line), $D = 6$ (dashed line) and $D = 8$ (dotted line). In the first case, the plot has essentially the same behaviour as for a Kerr black hole (compare with Figure 1.1), while for $D \geq 6$ we obtain a range of physical angular momenta that runs up to infinity.

horizon area, and hence we cannot simply set $a \to \infty$, as seen from eq. (2.14). For instance, a suitable way to regularize this limit is by keeping $\hat{\mu} = \frac{\mu}{a^2}$ fixed, while letting $\mu \to \infty$. In order to avoid divergences of the metric components, it is also necessary to keep r finite and θ near the rotation axis $\theta \sim 0$, in such a way that

$$\begin{aligned} \sigma &= a \sin\theta \quad \text{is finite}, \\ \frac{\rho^2}{\Delta} &\approx \frac{1}{1 - \frac{\hat{\mu}}{r^{D-5}}}, \\ \rho^2 d\theta^2 &\approx d\sigma^2. \end{aligned} \tag{2.15}$$

This procedure then leads to

$$ds^2 = -\left(1 - \frac{\hat{\mu}}{r^{D-5}}\right) dt^2 + \left(1 - \frac{\hat{\mu}}{r^{D-5}}\right)^{-1} dr^2 + r^2 d\Omega_{D-4} + d\sigma^2 + \sigma^2 d\phi^2. \tag{2.16}$$

That is, we obtain the metric of a flat black 2-brane in vacuum with horizon scale $r_0 = \hat{\mu}^{\frac{1}{D-5}}$ and spatial topology $\mathbb{R}^2 \times S^{D-4}$, where the plane is described by the coordinates (σ, ϕ). The one obtained is also a static solution, as actually the component $g_{t\phi}$ related to the angular velocity vanishes once we take the limit $\frac{\sigma^2}{a} \to 0$. The result (2.16) naively agrees with the limiting condition of a pancaked horizon, and if we move away from the rotation axis, we also expect corrections to this metric to order $\frac{\sigma}{a}$, $\frac{\sigma^2}{a^2}$ and $\frac{r^2}{a^2}$.

2.3 Black rings

The black ring (BR) geometry was the first explicit higher dimensional black hole solution with a non-spherical spatial horizon topology [24, 25]. It was found in $D = 5$, and its existence can be somehow intuitively expected.

Let us take a Schwarzschild spacetime and add an extra dimension, as we did in Section 2.1. The obtained geometry is known as *black string* and has horizon topology $S^2 \times \mathbb{R}$. We can think of wrapping the extra-dimension on itself, so that the resulting topology is now $S^2 \times S^1$. However, this is an unstable condition, since the ring would tend to shrink due to its tension and gravitational self-attraction, but we foresee that making the black ring spin may then balance this contraction.

In the present section, we will see that this intuitive reasoning is well based, to some extent. We will consider first a suitable parametrization of the flat $D = 5$ Minkowski spacetime, namely one adapted to the ring shape, and then we will deform the obtained metric by adding a ring-shaped mass.

We start by dividing $\mathbb{R}^4$ into two independent planes as

$$x^1 = r_1 \cos\phi, \qquad x^2 = r_1 \sin\phi, \tag{2.17}$$

$$x^3 = r_2 \cos\psi, \qquad x^4 = r_2 \sin\psi, \tag{2.18}$$

so that

$$d\mathbf{x}^2 = dr_1^2 + r_1^2 d\phi^2 + dr_2^2 + r_2^2 d\psi^2. \tag{2.19}$$

Now we consider a foliation of this space consisting of the equipotential surfaces of a 2-form potential $B_{\mu\nu}$ with a charged circular ring of radius R as a source. Of course, $B_{\mu\nu}$ can be related to a 3-form field strength $H = dB$ with vacuum equations

$$\nabla_\mu H^{\mu\nu\rho} = 0 \qquad \text{i.e.} \qquad \partial_\mu \left(\sqrt{-g} H^{\mu\nu\rho}\right) = 0 \tag{2.20}$$

outside the ring-shaped source. We take the latter lying on the plane (x^3, x^4), with $r_1 = 0,\ r_2 = R,\ 0 \leq \psi < 2\pi$. It is also useful to work with the Hodge dual of H, defining a 1-form A via $H = *dA$, such that H is the curl of A.

With these choices and naming $\Sigma = \sqrt{(r_1^2 + r_2^2 + R^2)^2 - 4R^2 r_2^2}$, we can define the coordinate

$$y = -\frac{R^2 + r_1^2 + r_2^2}{\Sigma}, \qquad -\infty < y \leq -1, \tag{2.21}$$

corresponding to spatial surfaces with constant $B_{t\psi}$. They can be understood as toroids surrounding the ring, and, in particular, $y = -1$ identifies the axis[2] of rotation related to ψ (it means that $B_{t\psi} = 0$), while in the limit $y \to -\infty$ (where $B_{t\psi} \to \infty$) we recover the source position.

[2] It is actually a plane orthogonal to the ring, since we are in $\mathbb{R}^4$.

Analogously, we can define a second coordinate

$$x = \frac{R^2 - r_1^2 - r_2^2}{\Sigma}, \qquad -1 \leq x \leq 1, \tag{2.22}$$

which foliates the space with surfaces of constant A_ϕ. If we keep the two angular coordinates fixed, we see from the definition of x that they represent circles passing through the ring source. The circle with infinite radius is given by $x = -1$ and has vanishing A_ϕ; therefore we approach spatial infinity in the limit $x \to -1$, $y \to -1$.

Once extracted the inverse relations

$$r_1 = R\frac{\sqrt{1-x^2}}{x-y}, \qquad r_2 = R\frac{\sqrt{y^2-1}}{x-y}, \tag{2.23}$$

we can recast the metric (2.19) as

$$d\mathbf{x}^2 = \frac{R^2}{(x-y)^2}\left[\frac{dy^2}{y^2-1} + \frac{dx^2}{1-x^2} + (y^2-1)d\psi^2 + (1-x^2)d\phi^2\right]. \tag{2.24}$$

It is possible to understand more easily the geometrical meaning of this construction near the ring by making a suitable change of coordinates. In fact, at fixed ψ and ϕ we notice that surfaces at $y = const$ effectively determine different radial distances from the ring, and conversely we can use the x coordinate to define a direction on the plane. Following these ideas, we can replace (x, y) with a pair of new radial and angular coordinate (r, θ) such that

$$r = -\frac{R}{y}, \qquad \cos\theta = x, \tag{2.25}$$

$$0 \leq r \leq R, \qquad 0 \leq \theta \leq \pi. \tag{2.26}$$

This choice then leads to a spatial metric of the form

$$d\mathbf{x}^2 = \frac{1}{\left(1 + \frac{r}{R}\cos\theta\right)^2}\left[\left(1 - \frac{r^2}{R^2}\right)R^2 d\psi^2 + \frac{dr^2}{1-\frac{r^2}{R^2}} + r^2\left(d\theta^2 + \sin^2\theta d\phi^2\right)\right]. \tag{2.27}$$

We notice that spatial infinity $x \to -1$, $y \to -1$ corresponds here to $\theta = \pi$ and $r \to R$, and that we have a singularity of the coordinates at $r = R$, which corresponds to the rotation axis around ψ, in view of what observed above.

It is also easier to understand the meaning of y with this new set of coordinates. Setting $r = const$, the metric becomes of the form

$$d\mathbf{x}^2\big|_r = a(\theta; r, R)d\psi^2 + b(\theta; r, R)\left(d\theta^2 + \sin^2\theta d\phi^2\right). \tag{2.28}$$

Hence we see explicitly that surfaces at constant y (and r) have topology equal to the product $S^1 \times S^2$.

Furthermore, in the vicinity of the ring $r \ll R$ (i.e. $y \to -\infty$), the metric (2.28) reduces to

$$d\mathbf{x}^2\big|_r \approx R^2 d\psi^2 + r^2\left(d\theta^2 + \sin^2\theta d\phi^2\right). \tag{2.29}$$

In this way, ψ parametrizes a ring with radius R, the pair (θ, ϕ) describe the sphere of radius r transverse to the ring, and we recover the interpretation of r as specifying the radial distance from the ring. This all is in agreement with the intuitive picture given above.

We can now analyse the neutral singly spinning black ring in 5 dimensions. In this case, the spatial sector of the metric has the same structure as in the parametrization (2.24) of flat space, now deformed with factors accounting for the global non-zero curvature of the space-time. There appears also a mixing term $g_{t\psi}$ describing a possible spin along ϕ, that is along the circle S^1.

The solution involves two dimensionless parameters λ and ν such that $0 < \nu \leq \lambda < 1$, characterizing the shape and rotation of the solution, and the length scale R of the ring. Defining then the functions

$$F(x) = 1 + \lambda x, \tag{2.30}$$

$$G(x) = (1 - x^2)(1 + \nu x), \tag{2.31}$$

and the constant

$$C = \sqrt{\lambda(\lambda - \nu)\frac{1+\lambda}{1-\lambda}}\,, \tag{2.32}$$

one can show that

$$ds^2 = -\frac{F(y)}{F(x)}\left(dt - CR\frac{1+y}{F(y)}d\psi\right)^2 + \frac{R^2}{(x-y)^2}F(x)\left[-\frac{G(y)}{F(y)}d\psi^2 - \frac{dy^2}{G(y)} + \frac{dx^2}{G(x)} + \frac{G(x)}{F(x)}d\phi^2\right] \tag{2.33}$$

is a solution to EFE, with $-\infty < y \leq -1$ and $-1 \leq x \leq 1$ as before. It is noteworthy that one recovers the corresponding form of the flat Minkowski metric (2.24) switching off both λ and ν, which implies $F(x) = 1$, $G(x) = 1 - x^2$ and $C = 0$. A recap of the features of these coordinates is shown in Figure 2.2.

In order to get some insight on (2.33) , we can define two coordinates (r, θ) as done in (2.25) with ranges (2.26) and redefine the parameters of the solution as

$$\nu = \frac{r_0}{R}, \qquad \lambda = \frac{r_0}{R}\cosh^2\sigma. \tag{2.34}$$

We also restrict ourselves to the so-called *thin ring* or *ultra-spinning (US) limit*, considering

$$r,\, r_0,\, r_0\cosh^2\sigma \ll R \tag{2.35}$$

and setting $\psi = \frac{z}{R}$ as a new parametrization of the ring, where of course we have to identify z with period $2\pi R$. In this limit,we see by direct substitution that we recover

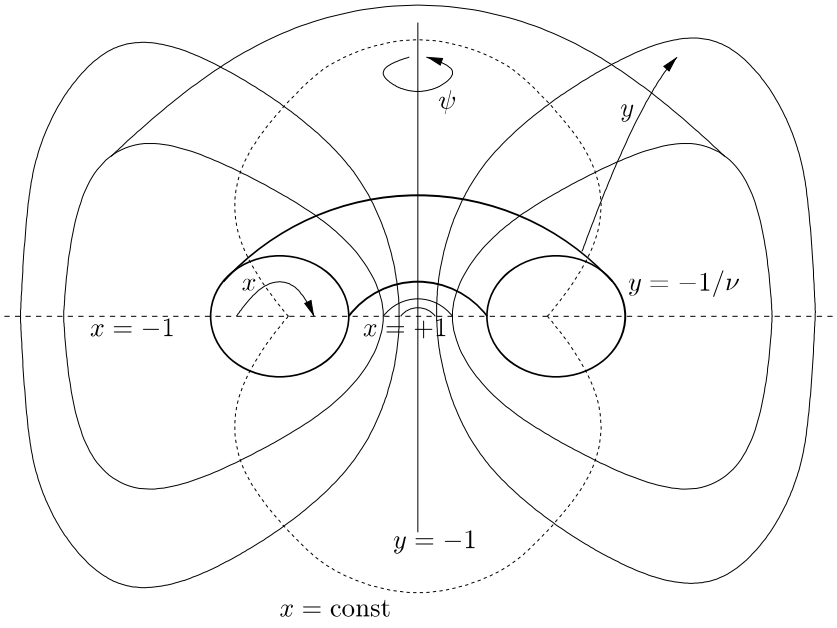

Figure 2.2: We show here the meaning of the BR coordinates (x, y) , by considering a spatial section of the spacetime while keeping ϕ constant [26]. For $x \to -1$, $y \to -1$ we approach spatial infinity, and at $y \to -\infty$ we recover the ring source. From an explicit analysis of the black ring metric, a Killing horizon is found at $y = -1/\nu$.

the metric of a boosted black string with boost parameter σ, boosted along the directions (t, z), where z is the string coordinate. In addition, it results that r_0 is the horizon scale of the black string.

On the whole, it makes sense since we are focussing on the near ring region $r \sim r_0$ with this choice of coordinates. Furthermore, we are taking the ring radius (related to S^1) to be much greater than its thickness (related to the transverse sphere S^2) $R \gg r_0$. We notice then that ν measures the ratio between these two radii, that is, the linear mass density of the ring, and we retrieve the picture of a boosted black string when $\nu, \lambda \ll 1$: smaller ν correspond to thinner rings.

Also, the ratio $\frac{\lambda}{\nu} = \cosh^2 \sigma$ clearly measures the boost of the black string and thus the spin of the ring in the non-limiting situation. From this, we can also define a local boost velocity on the black string as

$$v \,=\, \tanh \sigma \,=\, \sqrt{1 - \frac{\nu}{\lambda}}. \tag{2.36}$$

In conclusion, this discussion tells us that in some sense a black ring can be thought of as a boosted black string shaped into a circle, in agreement with the hand-waving

argument we reported above. But we have not imposed a balancing condition on the spinning ring, so that in general the described configuration will be actually unstable, for unspecified values of λ and ν. We intend to study more formally this requirement of stability of the solution. In order to achieve it, we need to demand the stability of the system over time , without any external force. This corresponds to requiring the absence of *conical singularities*.

In general [11, 8], we have come across curvature singularities, at points of the spacetime where the Kretschmann invariant $R_{\mu\nu\rho\sigma}R^{\mu\nu\rho\sigma}$ diverges. For instance, this is the case at $r = 0$ in the Schwarzschild solution, as we saw. What happens in this situation is that an observer reaching $r = 0$ disappears after a finite amount of proper time, and geometrically it translates to a geodetic incompleteness. Nonetheless, the latter can be present also for extendible spacetimes, a class of solutions that refers to spacetimes that cannot be embedded as a subset into another larger spacetime. For example, it is the case if we remove a point from a regular solution.

But we can have a singular behaviour also without any curvature divergence, even if the spacetime is inextendible. This can happen due to conical singularities, that can be thought of as unbalanced external stresses. The most clear example is obtained by considering Minkowski in spherical coordinates

$$ds^2 = -dt^2 + dr^2 + r^2\left(d\theta^2 + \sin^2\theta d\phi^2\right) \tag{2.37}$$

if we remove a wedge of the manifold, restricting ϕ to $0 \leq \phi < \tilde{\phi}$ for some $\tilde{\phi} < 2\pi$. Then, if we restore a periodicity by identifying the points with $\phi = 0$ and $\phi = \tilde{\phi}$, it is easy to show with arguments using neighbourhoods that we can recover a flat metric at all points of the new manifold, except for $r = 0$. There we have no more a smooth behaviour if an observer approaches that point, and we say that a conical singularity is present[3].

For example, usually there is one in black hole solutions where the mass parameter enters the angular sector of the metric, and it can bring about angular defects. This is our situation with the metric (2.33), but we can easily trace and remove conical singularities by evaluating the proper length of the orbits where a specific angular coordinate is constant.

In this case, one can check that

- at infinity $x = -1$, $y = -1$, we must impose a periodicity of the angular variables

$$\Delta\phi = \Delta\psi = -4\pi\frac{\sqrt{F(-1)}}{G'(-1)} = 2\pi\frac{\sqrt{1-\lambda}}{1-\nu}; \tag{2.38}$$

- near the ring at $x = 1$, we must identify the points along the orbits of ∂_ϕ with

[3]And it is now clear the origin of the name itself.

periodicity

$$\Delta\phi = 2\pi\frac{\sqrt{1+\lambda}}{1+\nu}. \tag{2.39}$$

We see that these conditions are compatible if and only if the *balancing condition* holds:

$$\lambda = \frac{2\nu}{1+\nu^2}. \tag{2.40}$$

The non-singular periodicity of ϕ and ψ is then

$$\Delta\phi = \Delta\psi = \frac{2\pi}{\sqrt{1+\nu^2}}. \tag{2.41}$$

From a physical point of view, the meaning of (2.40) is remarkable. Once the mass of the ring r_0 and its radius R are known, namely once we know ν, the angular velocity of the black ring (which is related to λ) must be chosen in such a way that the centrifugal force balances its gravitational self-attraction. It implies the absence of conical defects inside the ring that prevent it from collapsing. In turn, the angular velocity gets fixed and consequently the free parameters of the solution become just r_0 and R.

Singularities and Observables

The metric (2.33) exhibits also a singularity for $y \to -\infty$, which actually corresponds to a spacelike curvature singularity located on the ring source. On the other hand, $G(y)$ vanishes at $y = -1/\nu$ and here the metric becomes singular (while $G(x)$ can never be zero, thanks to the domain of x). It is possible to show straightforwardly with a change of coordinates that this is not a physical singularity. Instead, we have a Killing horizon with spatial topology $S^2 \times S^1$ and with Killing generator

$$\mathbf{k} = \partial_t + \Omega\,\partial_{\tilde{\psi}}, \tag{2.42}$$

where $\tilde{\psi} = \frac{2\pi}{\Delta\psi}\psi$ is the asymptotic ring coordinate with periodicity 2π. Ω is the horizon angular velocity, and reads

$$\Omega = \frac{1}{R}\sqrt{\frac{\lambda-\nu}{\lambda(\lambda+1)}} = \frac{1}{\sqrt{2}R}\sqrt{\frac{1-\nu+\nu^2-\nu^3}{\nu+1}} \tag{2.43}$$

for a black ring in equilibrium. We stress for later interest that

$$\Omega \approx \frac{1}{\sqrt{2}R} \tag{2.44}$$

in the US limit (2.35). Keeping in mind the balancing condition (2.40), a computation of the horizon area and of the surface gravity shows that

$$\mathcal{A} = 8\pi^2 R^3 \frac{\nu^{3/2}\sqrt{\lambda(1-\lambda^2)}}{(1-\nu)^2(1+\nu)}, \tag{2.45}$$

$$T = \frac{1}{4\pi R}(1+\nu)\sqrt{\frac{1-\lambda}{\lambda\nu(1+\lambda)}}. \tag{2.46}$$

If we now turn to spatial infinity, an ADM analysis of g_{tt} and $g_{t\psi}$ from (2.33) shows[4] that the conserved charges are

$$M = \frac{3\pi R^2}{4G}\frac{\lambda}{1-\nu}, \tag{2.47}$$

$$J = \frac{\pi R^3}{2G}\frac{\sqrt{\lambda(\lambda-\nu)(1+\lambda)}}{(1-\nu)^2}. \tag{2.48}$$

By making use of the definitions (2.1), it is possible to study the phase diagram of such a singly-spinning black ring in equilibrium. The dimensionless parameters result in

$$j = \frac{(1+\nu)^{3/2}}{\sqrt{8\nu}}, \qquad a_H = 2\sqrt{\nu(1-\nu)}, \tag{2.49}$$

and we can plot them parametrically in terms of the linear mass density ν, as displayed in Figure (2.3).

The cusp is located at $j_0 = \frac{3\sqrt{3}}{4\sqrt{2}}$, and it implies that there can be two different black ring solutions with the same characteristic parameters M and J within the whole interval $j_0 \leq j < 1$. This is enough to exclude a possible generalization of the Uniqueness Theorem to $D > 4$, or at least to $D = 5$. But furthermore, if we compare this phase diagram with the one related to a 5-dimensional MP black hole, we observe that also a MP black hole is present for each value of M and J in that same interval of j.

We can divide conveniently black rings into two classes, one for each branch of the phase diagram. We call *fat rings* the ones that live in $j_0 < j < 1$, and that have consequently a relatively low j, implying that $r_0 \sim R$. We label *thin rings* the ones that live in the interval $j_0 < j < \infty$ and that can access the ultra-spinning regime $r_0 \ll R$ (as in (2.35)). Finally, we call *minimally spinning black ring* the one with $j = j_0$ (which corresponds to $\nu = 1/2$).

The extremal limit for singly-spinning black rings corresponds to a naked singularity at $(j, a_H) = (1, 0)$. The same happens for $D = 5$ MP black holes.

[4] We will provide a set of coordinates suitable for this task in Section 5.3.

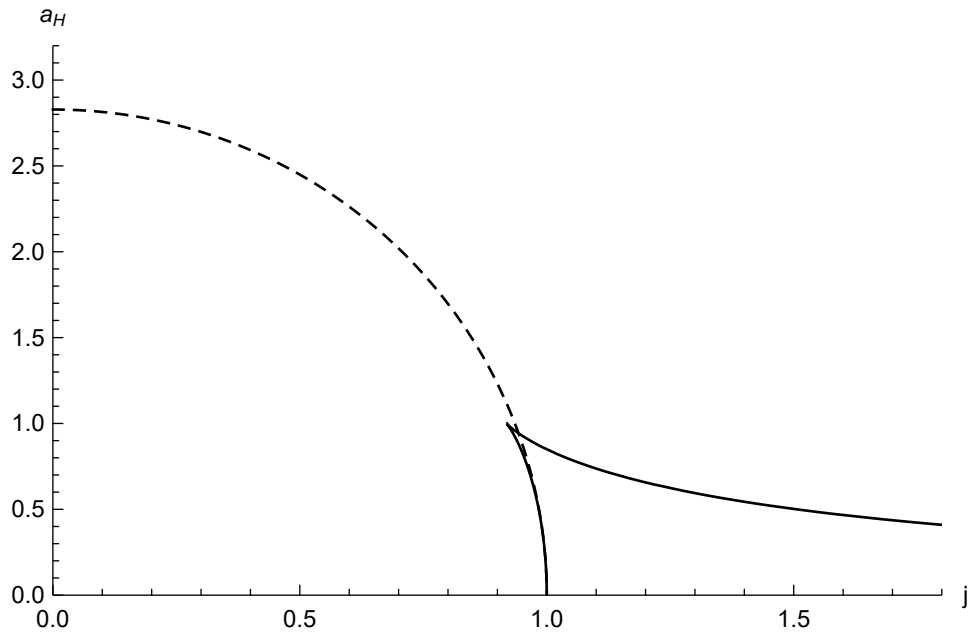

Figure 2.3: We compare here the phase diagram of a black ring (solid line) with the one for a MP black hole in $D = 5$ (dashed line). Noticeably, the existence of a MP black hole, a fat and a thin ring for each dimensionless angular momentum j in the interval $\frac{3\sqrt{3}}{4\sqrt{2}} \leq j < 1$ precludes the possibility of a generalization of the Uniqueness Theorem to higher dimensional black holes.

Chapter 3

The Blackfold Approach

We saw in Chapter 2 that singly spinning MP black holes in $D \geq 6$ develop a pancake horizon and exactly approach the shape of a black membrane when we increase the angular momentum of the solution up to the ultra-spinning limit. Something similar happens to black rings. We saw that thinner rings correspond to higher angular momenta, and we recover the metric of a black string in the thin ring limit, again if we focus on the near horizon region. This can be shown to be the case also for multi-spinning solutions [23]. It hints at the fact that, in some particular regime, neutral rotating higher dimensional black holes exhibit similar features as those of black branes.

We observe that this happens in the cases studied previously when a distinct hierarchy of length scales arises. For MP black holes, we see it in the presence of an angular momentum scale $l_{\parallel}$ (which goes to infinity in the ultra-spinning limit) and of a much smaller mass scale $l_{\perp}$, related to the radius of the transverse sphere S^{D-4}. Black rings behave in a similar way, with $R \gg r_0$ in the thin ring limit, where, as we remarked, R becomes the length scale associated to rotation, after imposing the balancing condition.

Therefore, the picture that emerges suggests that one could treat *any* rotating higher dimensional black hole solution admitting an ultra-spinning regime as a series expansion in l_M/l_J, whose leading order is locally a black brane with the right dimensions D. Each term that follows in the expansion is then understood as a correction proportional to powers of l_M/l_J that allows us to consider lower and lower angular momenta and to capture the behaviour of that solution away from the ultra-spinning limit. The black brane approximation is clearly valid only in the horizon vicinity, as we inspected explicitly for black rings and MP black holes.

We consider a flat Schwarzschild black p-brane in D dimensions of the same form as in (2.5). As we saw in Section 2.1, it can be build by adding a set of p flat directions to each point of a Schwarzschild-Tangherlini solution in $n+3$ dimensions. On the other hand, we can identify a worldvolume $\mathcal{W}_{p+1}$ described by the flat metric η_{ab} and spanned by the p-brane during its evolution along t. We define $\sigma^a = (t, z^i)$, $a = 0, 1 \ldots p$ as the directions parallel to the worldvolume, and (r, Ω_{n+1}) as the directions orthogonal to the

worldvolume. The parameter r_0 is the constant radius of the transverse sphere horizon.

We can make a more general construction by boosting the points of the p-brane along the worldvolume with homogeneous velocity u^a. These components are not all independent, due to the constraint $u^a u^b \eta_{ab} = -1$, so we take the spatial u^i as the independent ones. The metric can then be recast in the form

$$ds^2 = \left(\eta_{ab} + \frac{r_0^n}{r^n} u_a u_b\right) d\sigma^a d\sigma^b + \frac{dr^2}{1 - \frac{r_0^n}{r^n}} + r^2 d\Omega_{n+1}, \tag{3.1}$$

where the parameters of this solution are the horizon transverse radius r_0, the p independent components of u^a, and the $D - p - 1$ coordinates $\{X^\perp\}$ fixing the position on the worldvolume within the transverse space (i.e. along the radial and angular directions). For simplicity, we are collectively setting them to zero, assuming (3.1) to lie in the origin of the transverse space.

Our purpose will be to build perturbatively new black holes solutions in higher dimensions and to study their stability by slowly perturbing the black brane parameters along both worldvolume and transverse directions, such that the perturbative length scale R is much larger than the brane thickness r_0, that is $R \gg r_0$. In general, R is either related to the gradient of the worldvolume parameters (as $\ln r_0$ and u^i) or to the smallest extrinsic curvature radius of $\mathcal{W}_{p+1}$. The requirement of slow variations over length scales R ensures in particular that all the higher-derivative terms are suppressed by factors $O\big(\frac{r_0}{R}\big)$.

Therefore, the scale hierarchy mentioned above allows us to split the gravitational degrees of freedom of the considered spacetime into short and long wavelength components as

$$g_{\mu\nu} = \{g_{\mu\nu}^{(short)}, g_{\mu\nu}^{(long)}\}, \tag{3.2}$$

where $g_{\mu\nu}^{(short)}$ describes the geometry in the horizon vicinity for $r \ll R$, while $g_{\mu\nu}^{(long)}$ describes it far away from the black brane, namely for $r \gg r_0$. Then, considering perturbations over the scale R, we can simply think of a thin brane (locally described by $g_{\mu\nu}^{(short)}$) embedded into a curved background spacetime $g_{\mu\nu}^{(long)}$. For consistency, we require the matching of these two metrics in the interval $r_0 \ll r \ll R$. For the moment, we discuss this framework at the *probe brane* level, that is we neglect any backreaction of the brane on the background spacetime, considering them decoupled from each other.

It is also convenient to introduce a set of coordinates $\{X^\mu\}$, obtained by adding redundant degrees of freedom to the transverse coordinates $\{X^\perp\}$. Its convenience resides in having manifest covariance and in being able to fix completely the embedding $X^\mu(\sigma)$ of the submanifold determined by the worldvolume inside the background spacetime[1]. Hence, we can consider

$$\gamma_{ab} = g_{\mu\nu}^{(long)} \partial_a X^\mu \partial_b X^\nu \tag{3.3}$$

[1] We refer the reader to Appendix A for some useful results and derivations related to submanifold calculus.

as the induced metric of this embedding on $\mathcal{W}_{p+1}$.

We restrict now to the study of perturbations to first order in the perturbative expansion, and this makes it possible to analyse separately intrinsic and extrinsic fluctuations, as they decouple. We can build perturbations around flat configurations longitudinally and transversely to $\mathcal{W}_{p+1}$ by allowing $\{r_0(\sigma), u^i(\sigma)\}$ and $\{X^\mu(\sigma)\}$ to vary over the worldvolume respectively. The black brane metric under this kind of perturbations will assume the form

$$ds^2 = \left(\gamma_{ab}(X^\mu(\sigma)) + \frac{r_0^n(\sigma)}{r^n} u_a(\sigma) u_b(\sigma)\right) d\sigma^a d\sigma^b + \frac{dr^2}{1 - \frac{r_0^n(\sigma)}{r^n}} + r^2 d\Omega_{n+1} + h_{\mu\nu}(x) dx^\mu dx^\nu, \tag{3.4}$$

where $h_{\mu\nu}(x)$ gathers terms of order $O\left(\frac{r_0}{R}\right)$ in derivatives of $\ln(r_0), u^i$ and $X^\perp$, which are necessary to ensure that ds^2 is a solution to EFE. Here $x^\mu = (\sigma^a, r, \theta, \Omega_{n+1})$ in such a way that these extra-terms are added to each component of the metric, in principle. In view of the considerations above, the metric (3.4) is descriptive of the geometry at short distances, playing the role of $g_{\mu\nu}^{(short)}$. The term *blackfolds* will denote then black branes whose worldvolume is treated as a submanifold within a background spacetime.

3.1 The effective stress-tensor

In this framework, we can build an effective theory where the presence of the source is encoded at long distances into an effective stress-energy tensor [27]. We proceed in this way by considering the quasilocal stress-energy tensor provided by the Brown-York formalism [28]: let us consider a boundary surface with constant $r = L$, with $L \gg r_0$ and induced metric $\tilde{\gamma}_{\alpha\beta}$ obtained as

$$\tilde{\gamma}_{\alpha\beta} = e^\mu{}_\alpha e^\nu{}_\beta \, g_{\mu\nu}^{(short)}. \tag{3.5}$$

Then we define the Brown-York (BY) energy-stress tensor as

$$8\pi G \, T_{\alpha\beta}^{(BY)} = K_{\alpha\beta} - \tilde{\gamma}_{\alpha\beta} K - \left(K_{\alpha\beta}^{(0)} - \tilde{\gamma}_{\alpha\beta} K^{(0)}\right). \tag{3.6}$$

Here $K_{\alpha\beta} = K_{\alpha\beta}{}^r$ refers to the extrinsic curvature of the boundary surface, which has codimension 1, so it can be simply expressed as

$$K_{\alpha\beta} = -\frac{1}{2} \pounds_n \tilde{\gamma}_{\alpha\beta}, \tag{3.7}$$

naming n the unitary normal vector to the surface, which is proportional to ∂_r; conversely, the scalar K identifies the trace of $K_{\alpha\beta}$ computed with $\tilde{\gamma}^{\alpha\beta}$. In (3.6) we are also subtracting the flat spacetime contribution from the usual BY stress tensor in order to neglect the divergent flat parts of $T_{\alpha\beta}^{(BY)}$. That is, we take

$$K_{\alpha\beta}^{(0)} = -\frac{1}{2} \left. \pounds_n \eta_{\alpha\beta} \right|_{r=L}, \tag{3.8}$$

which coincides with turning off the sources in equation (3.7).

For the flat brane (3.1), the hypersurface at $r = L$ involves a set of $p+1$ flat directions, with a transverse $(n+1)$-sphere of radius L at each point. We are considering a boundary surface with topology $\mathbb{R}^{p+1} \times S^{n+1}$, and consequently the induced metric reads

$$\tilde{\gamma}_{\alpha\beta} = \begin{pmatrix} \eta_{ab} + \frac{r_0^n}{r^n} u_a u_b & \\ & r^2 \end{pmatrix}, \tag{3.9}$$

where we put the worldvolume directions in the first row and column, followed by the $n+1$ angular directions in the second row and column. Using (3.7), it leads to

$$K_{\alpha\beta} = \sqrt{1 - \frac{r_0^n}{r^n}} \begin{pmatrix} \frac{n}{2r}\frac{r_0^n}{r^n} u_a u_b & \\ & -r \end{pmatrix}. \tag{3.10}$$

After computing the inverse induced metric (3.9) and finding the mean extrinsic curvature $K_{\alpha\beta}$, we obtain

$$K = -\left[\frac{n}{2r}\frac{r_0^n}{r^n} + \frac{n+1}{r}\left(1 - \frac{1}{2}\frac{r_0^n}{r^n}\right)\right] + O\left(\frac{r_0^{2n}}{r^{2n}}\right). \tag{3.11}$$

The background quantities read then

$$K^{(0)}_{\alpha\beta} = \begin{pmatrix} 0 & \\ & -r \end{pmatrix}, \qquad K^{(0)} = -\frac{n+1}{r}, \tag{3.12}$$

and the BY-tensor to first order in $\frac{r_0^n}{r^n}$ is

$$T^{(BY)}_{ab} = \frac{r_0^n}{16\pi G}\frac{1}{r^{n+1}}\left(n u_a u_b - \eta_{ab}\right). \tag{3.13}$$

In this perturbative setup, perturbations along transverse spheres and flat directions decouple. This fact allows us to focus on the stress tensor living on the thin brane worldvolume, by performing an integration of the tensor in (3.6) over the transverse sphere:

$$T_{ab} = \int_{S^{n+1}} r^{n+1} d\Omega_{n+1}\, T^{(BY)}_{\alpha\beta}. \tag{3.14}$$

A straightforward calculation leads to a perfect fluid energy-stress tensor, with form

$$T_{ab} = (\varepsilon + P)\, u_a u_b + P\eta_{ab} = \frac{\Omega_{(n+1)}}{16\pi G}\, r_0^n \left(n u_a u_b - \eta_{ab}\right), \tag{3.15}$$

where Ω_{n+1} identifies the volume of a $(n+1)$-sphere. Explicitly, the pressure and energy density read

$$\varepsilon = \frac{\Omega_{(n+1)}}{16\pi G}(n+1)\, r_0^n \qquad P = -\frac{\varepsilon}{n+1} = -\frac{\Omega_{(n+1)}}{16\pi G}\, r_0^n. \tag{3.16}$$

To sum up, our procedure consisted in integrating out the short-distance behaviour of the brane and substituting it with an effective source that reproduces the brane effects as if observed from outside the boundary surface. An observer placed far enough from the brane would see its intrinsic dynamics described by a perfect fluid one at leading order.

As a consequence, we find a thermodynamic behaviour for our higher dimensional black hole. Let us compare it with the well-known black hole Thermodynamics inspected in Section 1.5, by assuming its validity locally at each point σ^a of our black brane worldvolume. It means that we require the Bekenstein-Hawking relation between the horizon area and the entropy density to hold locally:

$$s = \frac{\Omega_{(n+1)}}{4G} r_0^{n+1}, \tag{3.17}$$

as well as the relation by Hawking between surface gravity and temperature, which reads in the case of a Schwarzschild black brane

$$\mathcal{T} = \frac{\kappa}{2\pi} = \frac{n}{4\pi r_0}. \tag{3.18}$$

We see these choices to be consistent since both the First Law of Thermodynamics

$$d\varepsilon = \mathcal{T} ds \tag{3.19}$$

and the Euler relation

$$\varepsilon + P = \mathcal{T} s \tag{3.20}$$

are satisfied as a consequence.

3.2 Blackfolds equations

In this section we find a set of equations defining both the intrinsic and extrinsic dynamics of the black brane worldvolume. They follow as constraints from EFE, after imposing variations of the metric with either intrinsic or extrinsic perturbations.

Intrinsic Equations

Following [27], we can impose slow variations of the parameters along the worldvolume directions, keeping fixed the embedding X^μ [2]. In this way, the unperturbed velocity field $u^a = (1, 0 \dots 0)$ and horizon radius r_0 become

$$u^0(\sigma) = 1 + O(\epsilon^2), \qquad u^i(\sigma) = \epsilon \sigma^a \partial_a u^i + O(\epsilon^2), \tag{3.21}$$

[2] It is also possible to impose metric fluctuations as intrinsic perturbations related to the induced Ricci tensor on the submanifold $\mathcal{W}_{p+1}$. But this involves second derivatives of the induced metric components, and in turn it results in negligible terms, again as long as we perform an up to first order analysis.

$$r_0(\sigma) = r_0(0) + \epsilon\sigma^a \partial_a r_0(0), \tag{3.22}$$

with ϵ being a small parameter accounting for the order in the perturbative expansion. It is also convenient to switch to Eddington-Finkelstein coordinates in order to recover the manifest regularity of the metric at the horizon. After renaming $\sigma^a = (v, z^i)$, the short range metric reads

$$\begin{aligned} ds^2 = &- \left(1 - \frac{r_0(\sigma)^n}{r^n}\right) u_a(\sigma) u_b(\sigma) d\sigma^a d\sigma^b - 2u_a(\sigma) d\sigma^a dr + \\ &+ \left(\eta_{ab} + u_a(\sigma) u_b(\sigma)\right) d\sigma^a d\sigma^b + r^2 d\Omega_{n+1}^2 + \epsilon f_{\mu\nu}(r) dx^\mu dx^\nu + O(\epsilon^2), \end{aligned} \tag{3.23}$$

where $f_{\mu\nu}(r)$ are further first order corrections needed to ensure that this metric is a solution to EFE, in the same fashion as equation (3.4).

If we now turn to solving vacuum Einstein's Equations, an explicit calculation shows that the components $R^r{}_a = 0$ do not depend on second derivatives of the metric components, and so are not to be considered dynamic equations but simply constraints on the evolution of $u^a(\sigma)$ and $r_0(\sigma)$. They are independent of the corrections $f_{\mu\nu}(r)$ and they can be rewritten in terms of the effective stress-energy tensor as

$$D_a T^{ab} = 0, \tag{3.24}$$

where D_a indicates the submanifold covariant derivative compatible with γ_{ab}. We notice then that equations (3.24) defines the intrinsic dynamics of the brane, seen as the continuity equation for the effective fluid living on the worldvolume itself.

The other independent EFE $R_{\mu\nu} = 0$ are indeed dynamic equations, and it is possible to solve them explicitly in order to find $f_{\mu\nu}(r)$ and hence obtain the complete perturbed metric under intrinsic perturbations to first order in ϵ. After this, it is possible to go ahead in the perturbative expansion proper of the blackfold approach by performing the BY computation for this new metric, and it leads to a perturbed stress-energy tensor of the form

$$T_{ab} = \frac{\Omega_{(n+1)}}{16\pi G} r_0^n(\sigma) \left(n u_a(\sigma) u_b(\sigma) - \gamma_{ab}(\sigma)\right) + O(\partial u, \partial r_0). \tag{3.25}$$

We can interpret these extra-terms as viscous corrections to the perfect fluid behaviour of the brane, recasting them as

$$T_{ab} = \rho u_a u_b + P \Delta_{ab} - \zeta \theta \Delta_{ab} - 2\eta \sigma_{ab}, \tag{3.26}$$

where

$$\Delta_{ab} = \eta_{ab} + u_a u_b \tag{3.27}$$

is the orthogonal projector to the boost direction, and

$$\theta = \partial_a u^a, \qquad \sigma_{ab} = \Delta_a{}^c \left(\partial_{(c} u_{d)} - \frac{1}{p} \Delta_{cd}\right) \Delta^d{}_b \tag{3.28}$$

are the expansion and the shear tensor of the velocity field, respectively. The coefficients η and ζ are the shear and bulk viscosity, with explicit form

$$\eta = \frac{\Omega_{(n+1)}}{16\pi G} r_0^{n+1}, \qquad \zeta = \frac{2}{p}\left(1+\frac{p}{n+1}\right)\eta = \frac{\Omega_{(n+1)}}{8\pi G}\left(\frac{1}{p}+\frac{1}{n+1}\right) r_0^{n+1}. \tag{3.29}$$

We will not delve further into this computation, and we refer to [27] for a more complete discussion.

Extrinsic Equations

Following [29],we now study the extrinsic behaviour of the brane, and we proceed by considering extrinsic perturbations. In particular, our aim is to find another local relation akin to (3.24), describing the dynamics of the black brane within the background spacetime.

The extrinsic curvature tensor has the general form

$$K_{\mu\nu}{}^{\rho} = \gamma_{\nu}{}^{\sigma}\,\overline{\nabla}_{\mu}\gamma_{\sigma}{}^{\rho}. \tag{3.30}$$

Here we have the first fundamental form $\gamma_{\alpha\beta}$ of the worldvolume, which expresses the induced metric γ_{ab} in terms of the background coordinates:

$$\gamma^{\alpha\beta} = \gamma^{ab}\partial_a X^{\alpha}\partial_b X^{\beta}. \tag{3.31}$$

We have also defined the tangential covariant derivative $\overline{\nabla}_{\mu}$ as the projection of the background covariant derivative (built with $g_{\mu\nu}$) on the worldvolume, in such a way that $\overline{\nabla}_{\mu} = \gamma_{\mu}{}^{\sigma}\nabla_{\sigma}$.

Restricting ourselves to a first order analysis in derivatives, we observe that extrinsic fluctuations of the metric do contribute. Indeed, they must involve the extrinsic curvature tensor (3.30), which only contains first derivatives of the first fundamental form components.

On more general grounds, for later convenience, we think of the worldvolume $\mathcal{W}_{p+1}$ spanned by a classical p-brane in a background spacetime as a submanifold moved away from flatness by intrinsic and extrinsic curvature perturbations. We define R as the length scale for extrinsic perturbations, and it holds that $K_{ab}{}^{i} \sim \frac{1}{R}$. Analogously, we introduce the intrinsic curvature radius R_{int}, whose size determines the intrinsic perturbations scale, once we keep fixed r_0 and u_a.

It is also possible to build first order intrinsic fluctuations around flatness, with a choice of normal coordinates σ_a on $\mathcal{W}_{p+1}$ such that first derivatives of the metric are zero, and $\Gamma^{c}_{ab} = 0$. Defining also y^i as the transverse directions to the worldvolume and setting $\mathcal{W}_{p+1}$ at $y^i = 0$, the metric reads [29]

$$ds^2 = \eta_{ab}d\sigma^a d\sigma^b + \delta_{ij}dy^i dy^j + O\left(y/R\right) + O\left(\sigma^2/R_{int}^2\right), \tag{3.32}$$

where $O(y/R)$ identifies the extrinsic curvature perturbations, while $O(\sigma^2/R_{int}^2)$ the intrinsic ones, which are negligible to first order, as explained above.

We intend to study explicitly the first order $O(y/R)$, and we proceed by considering a set of Fermi normal coordinates associated to an observer on the worldvolume, in order to make calculations more straightforward. In general, Fermi coordinates are the natural choice of coordinates system based on a particular observer in a certain spacetime, and, as a consequence, they are defined only in a neighbourhood of his trajectory. A common and non-trivial example is the set of Rindler coordinates, which are the Fermi coordinates for an accelerated observer in Minkowski spacetime; as well known, they are not defined globally but only in the right sector of Minkowski.

If we generalize Fermi coordinates to the motion of a p-brane within a background spacetime, they will naturally make use of the affine parameters related to geodesics orthogonal to $\mathcal{W}_{p+1}$ as coordinates y^i along the transverse directions. Since y^i parametrize geodesics, it holds that

$$\Gamma^{\mu}_{ij} = (\nabla_j e_i)^{\mu} = 0 \quad \text{for } \mu = a, i. \tag{3.33}$$

Recalling that the woldvolume lies at $y^i = 0$, from (A.18), the extrinsic curvature tensor has components

$$K_{ab}{}^{i} = D_a e_b{}^{i} + \Gamma^{i}_{\mu\nu} e_a{}^{\mu} e_b{}^{\nu} = \Gamma^{i}_{ab}, \tag{3.34}$$

where as usual X^μ are the embedding coordinates and $e_b{}^{\mu} = \partial_b X^\mu$ are the tangent vectors to the submanifold.

It is now important to understand how the extrinsic curvature should contribute to the metric. For $p = 0$, we recover the standard geodesic motion of a point particle, with the worldvolume indices reducing to $a = t$: in this case, we have simply $K_{tt}{}^{i} = a^i$, with a^i acceleration of the particle within the background spacetime. Then, as well known [9], such an acceleration contribution has to fit into the worldvolume sector of the metric.

In general, we could also have terms of first order in derivatives of the same form as (3.34), but mixing worldvolume and transverse directions. They are linked to the holonomies of the connection considered, and must be proportional to the twist or external rotation coefficients defined as

$$\omega_{\mu}{}^{\nu}{}_{\rho} = \perp^{\nu}{}_{\sigma} n_{\rho}{}^{i} \overline{\nabla}_{\mu} n^{\sigma}{}_{i}, \tag{3.35}$$

which tells how the angle between two normal vectors vary when they are moved along a curve of direction μ on a given submanifold (here $\mathcal{W}_{p+1}$). Recalling the choices made so far, it is easy to see that these coefficients reduce to

$$\omega_{\mu}{}^{\nu}{}_{\rho} = \perp^{\nu}{}_{\sigma} n_{\rho}{}^{i} \gamma_{\mu}{}^{\lambda} \left(\partial_\lambda n_{\rho}{}^{i} + \Gamma^{\sigma}_{\lambda\alpha} n_{\alpha}{}^{i} \right) = \Gamma^{\nu}_{\mu\rho}, \tag{3.36}$$

where we notice that the indices ν and ρ are orthogonal to the worldvolume, while μ is parallel to it. Then we can safely state that in our case it holds that

$$\omega_{a}{}^{i}{}_{j} = \Gamma^{i}_{aj}. \tag{3.37}$$

They are clearly first order terms, which must be included.

On the whole, the perturbed metric reads

$$ds^2 = \left(\eta_{ab} - 2K_{ab}{}^i y_i\right) d\sigma^a d\sigma^b + 2\,\omega_{a\,j}^{\ i} y_i\, d\sigma^a dy^i + dy_i dy^i + O\left(y^2/R^2\right) + O\left(\sigma^2/R_{int}^2\right), \quad (3.38)$$

where the new terms are of order $O\left(y/R\right)$. However, it can be shown that mixed contributions like (3.37) can be gauged away by simply performing a rotation along the transverse directions:

$$y^i \longmapsto y^i - \sigma^a \omega_{a\,i}^{\ j} y_j + O(\sigma^2). \quad (3.39)$$

Eventually, we can rewrite the perturbed metric of any classical brane as

$$ds^2 = \left(\eta_{ab} - 2K_{ab}{}^i y_i\right) d\sigma^a d\sigma^b + dy_i dy^i + O\left(y^2/R^2\right) + O\left(\sigma^2/R_{int}^2\right). \quad (3.40)$$

Therefore, if we restrict ourselves to a boosted Schwarzschild black p-brane, the contributions from extrinsic curvature lead to

$$\begin{aligned} ds^2 \;=\; & \left(\eta_{ab} - 2K_{ab}{}^i y_i + \frac{r_0^n}{r^n} u_a u_b\right) d\sigma^a d\sigma^b + \frac{dr^2}{1-\frac{r_0^n}{r^n}} + r^2 d\Omega_{n+1}^2 + \\ & + h_{\mu\nu}(y^i) dx^\mu dx^\nu + O\left(y^2/R^2\right) + O\left(\sigma^2/R_{int}^2\right), \end{aligned} \quad (3.41)$$

where the radial coordinate can be restated in terms of the transverse directions as $r = \sqrt{y_i y^i}$. We are also gathering all the other first-order extrinsic fluctuations inside the symmetric tensor $h_{\mu\nu}(y^i)$ in order to ensure that (3.41) is a solution to EFE.

Since we are working to first order, we can make use of the decoupling of transverse fluctuations from each other. It means that we can study them individually, assuming for example $K_{ab}{}^i$ to be non-zero only along one orthogonal direction $\hat{i}$. As a consequence, we can introduce an angle θ related to $y^{\hat{i}}$ as

$$y^{\hat{i}} = r\cos\theta, \quad (3.42)$$

so that we can extract it from the angular part $d\Omega_{n+1}^2$ and recast $h_{\mu\nu}(y^i) = h_{\mu\nu}(r,\theta)$. The metric reads then

$$\begin{aligned} ds^2 \;=\; & \left(\eta_{ab} - 2K_{ab}{}^{\hat{i}} r\cos\theta + \frac{r_0^n}{r^n} u_a u_b\right) d\sigma^a d\sigma^b + \frac{dr^2}{1-\frac{r_0^n}{r^n}} + \\ & + r^2\left(d\theta^2 + \sin^2\theta d\Omega_n^2\right) + h_{\mu\nu}(r,\theta) dx^\mu dx^\nu + O\left(y^2/R^2\right) + O\left(\sigma^2/R_{int}^2\right). \end{aligned} \quad (3.43)$$

Furthermore, working at this perturbative order also allows us to express $h_{\mu\nu}$ as a dipole of the natural spherical foliation of the spacetime, in such a way that

$$\begin{aligned} h_{\mu\nu}(r,\theta) dx^\mu dx^\nu \;&=\; \cos\theta\, \hat{h}_{\mu\nu}(r) dx^\mu dx^\nu = \\ &=\; \cos\theta \left[\hat{h}_{ab}(r) d\sigma^a d\sigma^b + \hat{h}_{rr}(r) dr^2 + \hat{h}_{\theta\theta}(r)\left(d\theta^2 + \sin^2\theta d\Omega_n^2\right)\right], \end{aligned} \quad (3.44)$$

where we took advantage of the gauge freedom to choose $h_{r\theta} = h_{\theta r} = 0$ [30].

We can expand the metric (3.43) far away from our black brane source, focussing on the sector $r \gg r_0$, and the result is

$$\begin{aligned} ds^2 \;=\; & \left(\eta_{ab} - 2K_{ab}{}^{\hat{i}} r\cos\theta + \frac{r_0^n}{r^n}u_a u_b\right) d\sigma^a d\sigma^b + \left(1 + \frac{r_0^n}{r^n}\right) dr^2 + \\ & + r^2\left(d\theta^2 + \sin^2\theta d\Omega_n^2\right) + \cos\theta \hat{h}_{\mu\nu}(r)\, dx^\mu dx^\nu + O\left(\frac{r_0^{2n}}{r^{2n}}\right), \end{aligned} \tag{3.45}$$

where we are now keeping explicit only the order of the mass/distance ratio r_0^n/r^n.

But, as we know from the intrinsic analysis, the effective energy-stress tensor (3.15) accounts for the dynamics of a Schwarzschild black brane as seen from far away. Therefore, it is wise to recast r_0 (which is the only free parameter of this solution) in terms of T_{ab}. We also remark that in this case the Brown-York energy-stress tensor must be evaluated on a boundary surface with radius L such that $r_0 \ll L \ll R$, in order to have a weak gravitational field from the background and ensure in turn that T_{ab} is considering only the black brane effects. From eq. (3.15) it follows that

$$T \;=\; \eta_{ab}T^{ab} = -\frac{\Omega_{(n+1)}}{16\pi G} r_0^n (D-2), \tag{3.46}$$

and hence

$$\begin{aligned} r_0^n \;&=\; -\frac{16\pi G}{\Omega_{(n+1)}}\frac{T}{D-2}, \\ r_0^n\, u_a u_b \;&=\; \frac{16\pi G}{n\,\Omega_{(n+1)}}\left(T_{ab} - \frac{T}{D-2}\eta_{ab}\right). \end{aligned} \tag{3.47}$$

In this way, after substituting into (3.45), we obtain [29]:

$$\begin{aligned} ds^2 = & \left(\eta_{ab} - 2K_{ab}{}^{\hat{i}} r\cos\theta + \frac{16\pi G}{n\,\Omega_{(n+1)}}\left(T_{ab} - \frac{T}{D-2}\eta_{ab}\right)\frac{1}{r^n}\right) d\sigma^a d\sigma^b + \\ & + \left(1 - \frac{16\pi G}{\Omega_{(n+1)}}\frac{T}{D-2}\frac{1}{r^n}\right) dr^2 + r^2\left(d\theta^2 + \sin^2\theta d\Omega_n^2\right) + \\ & + \cos\theta\, \hat{h}_{\mu\nu}(r) dx^\mu dx^\nu + O\left(\frac{T_{ab}^2}{r^{2n}}\right). \end{aligned} \tag{3.48}$$

We denote this form as the *Camps-Emparan form* of the metric for a Schwarzschild black brane. Later on we will see the convenience of making a black brane solution dependent only on its related effective energy-stress tensor. In fact, it will be shown that it is possible to recast a very general class of black branes into eq. (3.48) form, with very few modifications.

We intend now to extract a set of constraint describing the extrinsic evolution of the perturbed p-brane within the background spacetime. Again, we will restrict ourselves to an analysis up to first order in the ratio r_0/R, where the mass scale is $r_0^n \sim T_{ab}$ and the extrinsic radius is such that $R \sim \frac{1}{K_{ab}{}^{\hat{i}}}$; we also consider $h_{\mu\nu}$ of order 1 in this ratio.

After some computations, one can observe that a particular combination of $G_{r\theta}$ and G_{rr} does not involve the perturbations $\hat{h}_{\mu\nu}$, and can be thought of as acting as a constraint for each transverse direction $y^{\hat{i}}$:

$$G_{r\theta} - \frac{r\tan\theta}{n+1} G_{rr} = \frac{n+2}{n+1}\frac{\sin\theta}{r^n}\frac{8\pi G}{\Omega_{(n+1)}} T^{ab} K_{ab}{}^{\hat{i}}. \tag{3.49}$$

We can interpret this result in this way: since we have a vacuum condition, the l.h.s. must be zero; it means that, if the extrinsic constraint

$$T^{ab} K_{ab}{}^{\hat{i}} = 0 \tag{3.50}$$

holds, then the geometry does not develop other singularities. Otherwise, it could develop conical or curvature singularities at $\sin\theta = 0$, that is on the axis $\theta = 0, \pi$. These singularities can be thought of as arising from unbalanced stresses.

Finally, we observe that one can find $\hat{h}_{\mu\nu}(r)$ explicitly by requiring (3.48) to be a solution to the whole set of vacuum equations $R_{\mu\nu} = 0$, in the same way as it was done for $f_{\mu\nu}(r)$ in (3.23).

Remarkably, we can give a very intuitive interpretation to blackfold extrinsic equations. After expanding the extrinsic curvature tensor (3.30) in terms of the connection, we can recast it in the form

$$T^{ab} \perp_{\sigma}^{\rho} \left(\partial_a \partial_b X^{\sigma} + \Gamma^{\sigma}_{\mu\nu} \partial_a X^{\mu} \partial_b X^{\nu}\right) = 0, \tag{3.51}$$

where $\perp_{\rho\sigma}$ is the orthogonal projector to the worldvolume submanifold as usual. It has now the same form as Newton's Second Law $m\vec{a} - \vec{F} = 0$ considered along the transverse direction ρ, and thus equation (3.50) can be seen as a generalization of the geodesic equation to p-brane dynamics.

Observations

To sum up, we started with a worldvolume-flat Schwarzschild black brane, and it was possible to find a set of D constraints on the evolution of the brane under long wavelength perturbations (both intrinsic and extrinsic) once we stayed at the leading order, since

- it allowed us to neglect dissipative effects on the worldvolume. It led to an effective perfect fluid description of the brane, with T_{ab} satisfying the $p+1$ *intrinsic blackfold equations*

$$D_a T^{ab} = 0; \tag{3.52}$$

- neither the backreaction of the brane on the background spacetime nor bending effects appear at this perturbative order. Consequently, we obtain the $D-p-1$ *extrinsic blackfold equations*

$$T^{ab}K_{ab}{}^{\hat{i}}=0. \tag{3.53}$$

In [31] it was also shown that this set of D constraints follow directly from the properties of EFE. We refer to $T_{\mu\nu}$ as the push-forward of T_{ab} on the background spacetime, and it can be considered as an energy-stress tensor with support on the worldvolume. Being the Einstein tensor divergenceless, $T_{\mu\nu}$ must satisfy the D equations

$$\overline{\nabla}_\mu T^{\mu\nu}=0. \tag{3.54}$$

It is easy to see that this relation contains the whole set of both intrinsic and extrinsic blackfold equations. If we project (3.54) onto the orthogonal and tangential directions, we obtain

$$\begin{aligned}\overline{\nabla}_\mu T^{\mu\rho} &= \overline{\nabla}_\mu\left(T^{\mu\nu}\gamma_\nu{}^\rho\right) = T^{\mu\nu}\,\overline{\nabla}_\mu\gamma_\nu{}^\rho+\gamma_\nu{}^\rho\,\overline{\nabla}_\mu T^{\mu\nu}= \\ &= T^{\mu\sigma}\gamma_\sigma{}^\rho\,\overline{\nabla}_\mu\gamma_\nu{}^\rho+\gamma_\nu{}^\rho\,\overline{\nabla}_\mu T^{\mu\nu}= \\ &= T^{\mu\nu}K_{\mu\nu}{}^\rho+\left(\partial_b X^\rho\right)D_a T^{ab},\end{aligned} \tag{3.55}$$

where ρ is meant to be orthogonal to $\mathcal{W}_{p+1}$ in the first term and parallel to $\mathcal{W}_{p+1}$ in the second one. As a consequence, we can decompose (3.54) into two independent sets of equations, namely (3.52) and (3.53). But it is also possible to reverse this argument and observe that equation (3.54) has the same meaning as blackfold equations, presenting them in an often more useful form.

In connection with this, it is relevant to approach the issue of backreaction. So long we have disregarded it, but one could think of going beyond the approximation of test branes by adding a coupling between the brane and the background. As observed above, T_{ab} describes the short wavelength gravitational degrees of freedom of the brane as seen from far away. Accordingly, it also accounts for the effects of the brane on the background geometry. Then, one can add a new set of equations to the intrinsic and extrinsic blackfold equations:

$$R^{(long)}_{\mu\nu}-\frac{1}{2}R^{(long)}\,g^{(long)}_{\mu\nu}=8\pi G\,T_{\mu\nu} \tag{3.56}$$

with $R^{(long)}_{\mu\nu}$ and $R^{(long)}$ evaluated with the background metric $g^{(long)}_{\mu\nu}$.

In summary, at the leading order, one has to consider only equations (3.24) and (3.50), and this is the way we follow in the rest of this dissertation. Otherwise, up to a generic order, one has to consider also (3.56), with $g^{(long)}_{\mu\nu}$, $T_{\mu\nu}$ and $K_{ab}{}^i$ of the suitable order.

The definition we gave of the effective stress-energy tensor guarantees that the short wavelength metric $g^{(short)}_{\mu\nu}$ describing the brane is well matched with the background

$g_{\mu\nu}^{(long)}$ in the range $r_0 \ll r \ll R$, since it reproduces the correct Physics of the brane in this range. We point out once more that asymptotically the only relevant quantity gathering all the short wave-length behaviour of a Schwarzschild black brane is its ADM mass, through T_{ab} and r_0.

3.3 Stationary blackfolds

In the previous sections we studied how the effective behaviour of a black brane can be captured by an effective fluid (a perfect one, at the leading order) that an observer far away describes as living on the brane itself. We can then demand the stationarity of this relativistic fluid, by requiring it to have a 4-velocity field u^a whose flow lines are invariant according to the class of observers following orbits of a certain timelike vector $\mathbf{k}$ defined on $\mathcal{W}_{p+1}$. From a GR point of view, this requirement will be related to considering a stationary black hole spacetime, with some Killing vector $\mathbf{k}$.

Furthermore, it can be shown that the intrinsic worldvolume velocity must be proportional to this Killing vector, once we neglect dissipative effects within the fluid:

$$\mathbf{u} = \frac{\mathbf{k}}{\mathrm{k}}, \tag{3.57}$$

where $\mathrm{k} = \sqrt{-\gamma_{ab}k^a k^b}$, and with $\mathbf{k}$ satisfying the intrinsic Killing equations

$$D_{(a}k_{b)} = 0. \tag{3.58}$$

Remarkably, equation (3.57) embodies the connection between the black hole picture and the effective fluid paradigm in this stationary case: the velocity field of the effective fluid is strictly related to the vector field $\mathbf{k}$ encoding the symmetries of the considered spacetime.

Furthermore, it is possible to enlarge the presence of this Killing vector to the background, or at least to some region close enough to the worldvolume, when the condition on the mass scale $r_0 \ll R$ holds with r_0 finite. In this case, there is a timelike Killing vector $\mathbf{k} = k^\mu \frac{\partial}{\partial X^\mu}$ on the background, satisfying

$$\nabla_{(\mu}k_{\nu)} = 0, \tag{3.59}$$

whose pullback on $\mathcal{W}_{p+1}$ coincides with $k^a\partial_a$. Indeed, we impose the existence of such a timelike Killing vector on the background (describing the geometry at infinity) matching with the one on the worldvolume since we want to describe a stationary black hole solution.

It is also convenient to rewrite the blackfold equations more explicitly. We allow all the parameters of our brane to vary, that is $u^a(\sigma)$, $r_0(\sigma)$ on the worldvolume, and also the embedding X^μ due to a generally non-null extrinsic curvature $K_{ab}{}^i$.

Applying equation (3.54) to the case of a deformed Schwarzschild black brane with effective energy-stress tensor (3.25), we obtain

$$\begin{aligned}\overline{\nabla}_\nu T^{\mu\nu} \;=\; & u^\mu u^\nu \left(\overline{\nabla}_\nu \epsilon + \overline{\nabla}_\nu P\right) + (\epsilon + P)\left(\dot{u}^\mu + u^\mu \overline{\nabla}_\nu u^\nu\right) + \\ & + \gamma^{\mu\nu}\overline{\nabla}_\nu P + P\overline{\nabla}_\nu \gamma^{\mu\nu},\end{aligned} \tag{3.60}$$

where we have defined $\dot{u}^\mu = u^\nu \overline{\nabla}_\nu u^\mu$. From definition (3.30), the mean extrinsic curvature is

$$K^\rho = \gamma^{\mu\nu} K_{\mu\nu}{}^\rho = \gamma^{\mu\nu}\gamma^\alpha{}_\nu \overline{\nabla}_\mu \gamma^\rho{}_\alpha = \overline{\nabla}_\mu \gamma^{\mu\rho}. \tag{3.61}$$

Then we can rewrite equation (3.54) as

$$u^\mu u^\nu \overline{\nabla}_\nu \varepsilon + \left(u^\mu u^\nu + \gamma^{\mu\nu}\right)\overline{\nabla}_\nu P + (\epsilon + P)\left(\dot{u}^\mu + u^\mu \overline{\nabla}_\nu u^\nu\right) + P K^\mu = 0. \tag{3.62}$$

Taking into account the energy density and pressure in (3.16), an explicit form of the blackfold equations can be found. Projecting (3.62) orthogonally to the worldvolume results in

$$K^\rho = n \perp^\rho{}_\nu \dot{u}^\nu, \tag{3.63}$$

while projecting it along $\mathcal{W}_{p+1}$ leads to

$$\dot{u}_a + \frac{1}{n+1} u_a D_b u^b = \partial_a \ln r_0. \tag{3.64}$$

Contracting now the background Killing equation (3.59) with $k^\mu k^\nu$ brings us to the relation $k^\mu \partial_\mu \mathrm{k} = 0$. In view of this, we obtain

$$\dot{u}^\mu = u^\nu \overline{\nabla}_\nu u^\mu = \frac{k^\nu}{\mathrm{k}} \overline{\nabla}_\nu \frac{k^\mu}{\mathrm{k}} = \frac{k^\nu}{\mathrm{k}^2} \overline{\nabla}_\nu k^\mu. \tag{3.65}$$

Using again equation (3.59) brings us to

$$\dot{u}^\mu = \partial^\mu \ln \mathrm{k}. \tag{3.66}$$

With respect to the intrinsic blackfold equations (3.64), we also notice that the velocity field expansion $D_a u^a$ vanishes thanks to the worldvolume Killing equation. On the whole, it means that

$$\partial_a \ln \mathrm{k} = \partial_a \ln r_0, \tag{3.67}$$

which has solution

$$\frac{r_0}{\mathrm{k}} = const \tag{3.68}$$

over the whole worldvolume.

One can fix this constant by studying the norm k close to the p-brane. Here the geometry is well described by metric (3.4), so that in this region of the transverse space we have

$$k^\mu k^\nu g^{(short)}_{\mu\nu} = \left(\gamma_{ab} + \frac{r_0^n}{r^n} u_a u_b\right) k^a k^b = -\left(1 - \frac{r_0^n}{r^n}\right) \mathrm{k}, \tag{3.69}$$

since $\mathbf{k}$ properly lives on the worldvolume. This tells us that actually a Killing vector living on the wordlvolume of a Schwarzschild black brane is the generator of the whole Killing horizon of the solution, as it becomes null when $r \to r_0$. Furthermore, one can easily evaluate its surface gravity, which results in

$$\kappa = \frac{n\mathrm{k}}{2r_0}. \tag{3.70}$$

It means that the surface gravity is proportional to the constant over $\mathcal{W}_{p+1}$ that we found in equation (3.68), and, in turn, κ is constant over the entire horizon; of course, this hints at a well defined thermodynamics.

As a matter of fact, equations (3.70) and (3.18) jointly tell us that we can define a global temperature $T = \mathrm{k}\mathcal{T}$ constant on the whole worldvolume. Conversely, we can make explicit the dependence of the local temperature $\mathcal{T}$ on the point σ^a as

$$\mathcal{T}(\sigma) = \frac{T}{\mathrm{k}}, \tag{3.71}$$

that is, it is equal to the redshifted global one. Also, we can interpret this result by stating that the brane thickness varies on $\mathcal{W}_{p+1}$ as

$$r_0(\sigma) = \frac{n}{4\pi T}\,\mathrm{k}, \tag{3.72}$$

in such a way that T remains constant there.

It is well established that black hole thermodynamics has a global nature: its laws involve only global quantities, such as the ADM mass, the event horizon area and the temperature, and they must be evaluated by an observer at infinity. On the other hand, ordinary thermodynamics holds at any point of a given system. Thus, it is interesting to see how in this picture the ordinary (that is, local) thermodynamics of the effective fluid on the worldvolume allows us to reconstruct the global and geometrical nature of black hole thermodynamics as seen from the background, through red-shifted global quantities like T.

Turning back to solving the blackfold equations, from the above discussion we can give automatically an expression for the parameters u_a and r_0 in the stationary case, once we know the explicit form of the Killing vector $\mathbf{k}$. In particular, we can choose a vector field basis $\{\xi, \chi_i\}$ formed by $p+1$ orthogonal vectors[3] from the background

[3]Originally $\mathbf{k}$ was a vector on the worldvolume, and consequently it has at most $p+1$ degrees of freedom.

spacetime. We will generally assume that it is possible to pick them up in such a way that ξ is the generator of time translations at infinity, and that χ_i are the generators of asymptotic rotations. With these choices, we can write on the background

$$\mathbf{k} = \xi + \sum_{i=1}^{p} \Omega_i \chi_i, \tag{3.73}$$

with Ω_i independent of the coordinates. Furthermore, even if not strictly required, we also assume that $\{\xi, \chi_i\}$ are Killing vectors individually.

It is convenient to introduce $p+1$ functions $R_a(\sigma)$ on the worldvolume, defined as the moduli

$$R_0(\sigma) = \sqrt{-\xi^2}\,\Big|_{\mathcal{W}_{p+1}} \qquad\qquad R_i(\sigma) = \sqrt{-\chi_i^2}\,\Big|_{\mathcal{W}_{p+1}}, \tag{3.74}$$

which effectively describe the embedding as much as X^μ do. With the basis chosen above, we can give a clear interpretation of these quantities. Apparently, $R_0(\sigma)$ measures the redshift between background infinity and the point σ^a of the worldvolume. On the other hand, a function $R_i(\sigma)$ represents the proper radius of the orbit generated by χ_i passing through σ^a. As a consequence, we see that Ω_i is the related angular velocity of the horizon, and equivalently it describes the angular velocity along the direction χ_i of static observers following orbits of ξ on the horizon.

Starting from the functions in (3.74), we can define a set of $p+1$ vectors on the worldvolume, with the property of being orthonormal according to the worldvolume induced metric γ_{ab}:

$$\frac{\partial}{\partial t} = \frac{1}{R_0}\,\xi\,\Big|_{\mathcal{W}_{p+1}}, \qquad\qquad \frac{\partial}{\partial z^i} = \frac{1}{R_i}\,\chi_i\,\Big|_{\mathcal{W}_{p+1}}. \tag{3.75}$$

Defining then

$$V_i(\sigma) = \frac{u \cdot \partial_{z^i}}{-u \cdot \partial_t} = \frac{\Omega_i R_i(\sigma)}{R_0(\sigma)} \tag{3.76}$$

as the spatial velocities of the effective fluid along the direction z^i at the point σ^a, we can recast the Killing vector $\mathbf{k}$ in terms of the coordinates of $\mathcal{W}_{p+1}$. In turn, it leads to a more explicit form of the intrinsic parameters r_0 and u_a: on the worldvolume, it holds that

$$\begin{aligned} \mathbf{k} \;&=\; \xi + \sum_{i=1}^{p} \Omega_i \chi_i = R_0 \frac{\partial}{\partial t} + \sum_i \Omega_i R_i \frac{\partial}{\partial z^i} = \\ &=\; R_0(\sigma) \left(\frac{\partial}{\partial t} + \sum_i V_i(\sigma) \frac{\partial}{\partial z^i} \right), \end{aligned} \tag{3.77}$$

which means that

$$\mathrm{k} = \sqrt{-\gamma_{ab}k^a k^b} = R_0(\sigma)\sqrt{1-V^2(\sigma)}\,, \tag{3.78}$$

with

$$V^2(\sigma) = \sum_i V_i^2 = \frac{1}{R_0^2}\sum_i \Omega_i^2 R_i^2(\sigma). \tag{3.79}$$

It is clear in this form that $\mathrm{k}(\sigma)$ incorporates the total redshift both gravitational (through $R_0(\sigma)$) and kinematic (through $\sqrt{1-V^2(\sigma)}$) that a static observer on an orbit of ξ at infinity would see with respect to the point σ^a of the effective fluid on $\mathcal{W}_{p+1}$.

In conclusion, we obtain straightforwardly the explicit solutions to the intrinsic equations (3.52) in the stationary case, and they read

$$\mathbf{u}(\sigma) = \frac{\mathbf{k}}{\mathrm{k}} = \frac{1}{\sqrt{1-V^2(\sigma)}}\left(\frac{\partial}{\partial t} + \sum_i V_i(\sigma)\frac{\partial}{\partial z^i}\right), \tag{3.80}$$

$$r_0(\sigma) = \frac{n}{2\kappa}R_0(\sigma)\sqrt{1-V^2(\sigma)}\,, \tag{3.81}$$

once we fix the horizon Physics of the solution through κ and Ω_i.

From a more practical point of view, one can actually reverse this argument. Let us think of a background spacetime with a Killing vector k^μ. We also assume that its pull-back on the worldvolume is a Killing vector. As a consequence, we know automatically the velocity field u^a of the effective fluid due to equation (3.57). Then we can solve for r_0 the intrinsic equation (3.64), and it is proportional to the Killing vector modulus k.

Since r_0 and u^a completely determine the effective energy stress tensor (3.15), now the set of extrinsic equations (3.63) can be solved, and this leads to

$$K^\rho \;= \perp^{\rho\mu}\,\partial_\mu \ln\left(\mathrm{k}^n\right) \;=\; n\,\perp^{\rho\mu}\,\partial_\mu \ln\left(R_0\sqrt{1-V^2(\sigma)}\right). \tag{3.82}$$

In this way, an up to first order solution for the whole set of free parameters in our effective theory follows automatically from stationarity. As we will inspect first in Chapter (3.7), the requirement of stationarity allows us to generate very easily new classes of higher dimensional black hole solutions.

3.4 Horizon topology and blackfolds with boundaries

With the blackfold construction, the transverse sphere S^{n+1} corresponding to the Schwarzschild horizon can be thought of being mapped to each point σ^a of the worldvolume. It is parametrized by Ω_{n+1} in (3.1) and it has radius $r_0(\sigma)$, depending on the point. Given the hypersurface-orthogonal timelike vector ξ^a, we can foliate the worldvolume in space-like slices $\mathcal{B}_p$, each of which is orthogonal to ξ^a and has topology $\mathsf{T}(\mathcal{B}_p)$. Then the

topology of the entire blackfold horizon is $\mathsf{T}(\mathcal{B}_p) \times S^{n+1}$, where r_0 is the parameter which determines how much this product is warped, due to its variation over $\mathcal{B}_p$.

This picture changes if we have boundaries within the worldvolume. Let us assume to have a boundary ∂W_{p+1} determined by a function $f(\sigma)$ such that $f|_{\partial W_{p+1}} = 0$. We demand that the effective fluid stays within this boundary on any spatial slice $\mathcal{B}_p$, and hence the velocity field must maintain itself parallel to it

$$u^a \ \partial_a f|_{\partial W_{p+1}} = 0. \tag{3.83}$$

By multiplying equation (3.52) by f, reverting the derivative on f and evaluating the result on ∂W_{p+1}, it follows that the intrinsic blackfold equations read on the boundary

$$[(\varepsilon + P)u_a u_b + P\gamma_{ab}] \ \partial_a f|_{\partial W_{p+1}} = 0. \tag{3.84}$$

Then, comparing this equation with (3.83), we observe that the pressure must be null on the boundary, which is a well understood consequence of perfect fluid dynamics in case of bounded fluids. The specific form of pressure (3.16) implies that the thickness r_0 of the horizon must approach a zero size at the boundary

$$r_0|_{\partial W_{p+1}} = 0, \tag{3.85}$$

and consequently the horizon of the blackfold must close at its edge.

In turn, this fact also implies through equation (3.72) that k $\to 0$ at the boundary as well. It can happen in case of

- $V^2 \to 1$, that is the fluid locally moves at the speed of light near the boundary. It is the most common case, and in the known cases the blackfold solutions that one can obtain in this situation do match at the boundary with EFE analytical solutions with regular horizons. We will see an example of this in Section 3.7.2;
- $R_0 \to 0$, that is the blackfold ends on a surface of infinite redshift, that is the worldvolume meets another horizon at its boundary. This can happen when the background exhibits a horizon and when the scale hierarchy allows the two horizons to meet. Contrary to the previous case, it can happen that the corresponding known solutions are not endowed with a regular horizon at the boundary.

However, we are still lacking a general understanding or proof of the conditions that lead to a regular horizon at the edge of the blackfold[4].

If worldvolume boundaries are present, it means that r_0 shrinks to zero there, and in turn it does not lead anymore to a horizon topology $\mathsf{T}(\mathcal{B}_p) \times S^{n+1}$, but instead we have a non-trivial fibration, and it will be necessary to discuss it on a case by case basis.

[4]I am grateful to Roberto Emparan for an interesting discussion on this issue.

3.5 The observables

We intend now to study the main features of the blackfold construction, by analysing the observables quantities. Let us consider first the horizon area, which of course involves short wavelength physics at distances $r \sim r_0$. Thus we need to focus on $g_{\mu\nu}^{(short)}$ of equation (3.4).

To the lowest order in $\frac{r_0}{R}$, its spatial horizon sections have metric

$$ds_H^2 = (\delta_{ij} + u_i u_j)\, dz^i dz^j + r_0^2 d\Omega_{(n+1)}^2, \tag{3.86}$$

where $u^i = \mathbf{u}\cdot\partial_{z^i}$ as before. We name $a_H(\sigma)$ the local horizon area at each point $\sigma^a \in \mathcal{B}_p$, and it is only related to the transverse sphere S^{n+1}. Therefore, to the lowest order we have

$$a_H(\sigma) = \Omega_{(n+1)} r_0^{n+1} \sqrt{1 + \delta_{ij} u^i u^j}\,. \tag{3.87}$$

Recalling the definitions given above, one has

$$u_i = \mathbf{u}\cdot\partial_{z^i} = \frac{\Omega_i R_i}{R_0\sqrt{1-V^2}}, \tag{3.88}$$

and in turn we can rewrite

$$\sqrt{1+\delta_{ij}u^i u^j} = \sqrt{1 + \sum_i \frac{R_i^2\Omega_i^2}{R_0^2(1-V^2)}} = \frac{1}{\sqrt{1-V^2}}, \tag{3.89}$$

in such a way that

$$a_H(\sigma) \;=\; \frac{\Omega_{(n+1)}}{\sqrt{1-V^2}}\, r_0^{n+1} \;=\; \Omega_{(n+1)} \left(\frac{n}{2\kappa}\right)^{n+1} \big(1-V^2\big)^{\frac{n}{2}}\, R_0^{n+1}(\sigma), \tag{3.90}$$

where we made use of the intrinsic solution for r_0 given in (3.81).

But we know that the local area $a_H(\sigma)$ involves only the area of the transverse sphere of radius $r_0(\sigma)$. Consequently, the global area of the horizon will be

$$A_H = \int_{\mathcal{B}_p} dV_{(p)} a_H(\sigma), \tag{3.91}$$

where $dV_{(p)}$ refers to a volume element on $\mathcal{B}_p$. This definition means that the global entropy is

$$S = \frac{A_H}{4G}, \tag{3.92}$$

once assumed the validity of the Bekenstein-Hawking relation.

We are now able to interpret this result from the effective fluid theory point of view. First, we define the local entropy current $s^a = s(\sigma)u^a$ of the fluid, with $s(\sigma)$ given by

(3.17). As usual, the related conserved charge can be interpreted as the global entropy of the fluid

$$S = -\int_{\mathcal{B}_p} dV_{(p)} s_a n^a = \int_{\mathcal{B}_p} dV_{(p)} \frac{R_0}{\mathrm{k}} s(\sigma), \tag{3.93}$$

where we have also introduced for convenience the unit timelike vector orthogonal to $\mathcal{B}_p$ as

$$n^a \;=\; (\partial_t)^a \;=\; \frac{1}{R_0}\xi^a, \tag{3.94}$$

so that $\xi^a = R_0\, n^a$. We see that this global entropy matches perfectly with (3.92).

Analogously, let us assume to be working with a type of black branes with a transverse angular momentum. It would be the case if we started from a Kerr black brane, whose horizon has an angular momentum along the transverse sphere. In such a situation, we could find a local current $\mathcal{J}^a = \mathcal{J} u^a$ from the short wavelength physics as we did for s^a. In fact, we can extract $\mathcal{J}^a$ from the mixing component of the metric $g_{\mu\nu}^{(short)}$, according to the ADM prescription. After that, it is possible to define a global angular momentum $\hat{J}$ as the integral over the spacelike slice $\mathcal{B}_p$ of this current. We will make use of this kind of procedures in the Chapter 6.

Returning to the study of Schwarzschild black branes, we notice that the intrinsic equations (3.53) allow us to define in principle up to $p+1$ conserved global charges of the fluid, one for each direction of $\mathcal{W}_{p+1}$. We have the (ADM) mass

$$M = \int_{\mathcal{B}_p} dV_{(p)} T_{\mu\nu} n^\mu \xi^\nu, \tag{3.95}$$

related to the component T_{00}. From the definitions given in Section 3.3, we can give a more explicit form of it as

$$M = \frac{\Omega_{(n+1)}}{16\pi G}\left(\frac{n}{2\kappa}\right)^n \int_{\mathcal{B}_p} dV_{(p)}\, R_0^{n+1}\big(1-V^2\big)^{\frac{n}{2}-1}\big(n+1-V^2\big)\,. \tag{3.96}$$

Also, we can find the worldvolume angular momenta J_i from T_{0i} as

$$\begin{aligned} J_i \;&=\; -\int_{\mathcal{B}_p} dV_{(p)} T_{\mu\nu} n^\mu \chi_i^{\ \nu} = \\ &= \frac{\Omega_{(n+1)}}{16\pi G}\left(\frac{n}{2\kappa}\right)^n n\Omega_i \int_{\mathcal{B}_p} dV_{(p)}\, R_0^{n-1} R_i^2 \big(1-V^2\big)^{\frac{n}{2}-1}\,. \end{aligned} \tag{3.97}$$

So, in summary, worldvolume isometries lead to conserved charges from the effective energy stress tensor. One can have further conserved currents on the transverse space, and they lead to other corresponding charges.

We conclude this section with a remark on a possible way to measure the validity of the blackfold approach in case of stationary configurations [32]. As explained at the beginning of this chapter, in general one must require at each order that at any point of the

worldvolume the local horizon thickness r_0 is much smaller than the length scales related to the intrinsic and extrinsic geometry at the next order in the perturbative expansion. This is necessary to ensure that we recover locally the description of a Schwarzschild black brane, and, according to the analysis above, it means that r_0 must be smaller than any possible curvature scalar radius that can be made up with the induced Riemann tensor $\mathcal{R}$, the extrinsic curvature tensor $K_{ab}{}^{i}$ and the derivatives of the collective brane variables. As a consequence, if we work at the leading order, in general it is necessary to require that at each point of $\mathcal{W}_{p+1}$

$$r_0 \ll \min\left(|\mathcal{R}|^{-\frac{1}{2}}, \left|u^a u^b \mathcal{R}_{ab}\right|^{-\frac{1}{2}}, \left|K^i K_i\right|^{-\frac{1}{2}}, \left|K^{abi} K_{abi}\right|^{-\frac{1}{2}}, \left|u^a u^b K_a{}^{ci} K_{bci}\right|^{-\frac{1}{2}}, \left|\frac{\nabla_a \nabla^a \mathrm{k}}{\mathrm{k}}\right|^{-\frac{1}{2}}\right). \tag{3.98}$$

3.6 The effective action formalism

The splitting of the gravitational degrees of freedom (3.2) into the long wavelength and the short wavelength sectors can also be analysed in terms of actions. Actually, the complete Hilbert-Einstein action in vacuum for the system can be separated as

$$I_{HE}[g] = \frac{1}{16\pi G}\int d^D x\sqrt{-g}\; R \approx \frac{1}{16\pi G}\int d^D x\sqrt{-g^{(long)}}\, R^{(long)} + I_{eff}\left[g^{(long)}_{\mu\nu}, \phi\right], \tag{3.99}$$

where R and $R^{(long)}$ refer to the Ricci scalars computed with $g_{\mu\nu}$ and $g^{(long)}_{\mu\nu}$ respectively. The first term in the r.h.s. is the one that accounts for the background dynamics, and it involves the backreaction of the brane (as one can see for example from equation (3.56)).

On the other hand, the second term describes the effective brane dynamics related to the fluid endowed with the energy stress tensor T_{ab}. From an action-based point of view, it can be interpreted as the result of integrating out the short wavelength gravitational degrees of freedom in $I_{HE}[g]$, and it matches with the meaning of the effective stress energy tensor description that we gave in Section 3.1. As a consequence, I_{eff} shows a dependence only on the long wavelength metric and on the effective brane dynamics parameters, called $\phi = \{r_0, u^i, X^\mu\}$ in equation (3.99).

This action-based formalism will be equivalent to the one previously showed involving the explicit metrics $g^{(short)}_{\mu\nu}$, $g^{(long)}_{\mu\nu}$ if and only if it allows to recover the equations of motion (3.52) and (3.53).

As far as it concerns the intrinsic equations, given I_{eff} we can define an effective energy stress tensor

$$T_{\mu\nu} = -\frac{2}{\sqrt{g^{(long)}}}\left.\frac{\delta I_{eff}}{\delta g^{\mu\nu}_{(long)}}\right|_{\mathcal{W}_{p+1}}, \tag{3.100}$$

in the same fashion as the stress tensor that one usually defines in GR. Remarkably, it can be shown to be equal to the one defined in Section 3.1, and also to satisfy a conservation equation analogous to (3.53) [31]. Therefore we recover perfectly the intrinsic behaviour of the brane.

In order to obtain the extrinsic equations from (3.99), we need to carry out a leading order analysis concerning the explicit form of I_{eff} for stationary configurations [33]. The dynamics is completely fixed by the induced metric γ_{ab} and the Killing vector k^a in this case, which means that in general the only scalars that one can build are functions of the modulus $\mathrm{k} = \left|\gamma_{ab}\, k^a k^b\right|^{1/2}$. We can then assume without restrictions that at this order the effective action is a generalization of the Polyakov action, with form

$$I_{eff}\left[r_0, u^i, X^\mu, \gamma_{ab}\right] = \int_{\mathcal{W}_{p+1}} d^{p+1}\sigma\ \mathcal{L}_{eff}(\gamma_{ab}, \mathrm{k}) = \int_{\mathcal{W}_{p+1}} d^{p+1}\sigma\ \sqrt{-\gamma}\,\lambda(\mathrm{k}), \tag{3.101}$$

where the dependence on $g^{(long)}$ is just through γ_{ab} at this order, while the embedding X^μ also encodes the dependence on $R_a(\sigma)$, as mentioned above. It means in turn that in (3.101) the true dependence is only on X^μ and γ_{ab}, since we were able to express r_0 and u^i in terms of R_a in the stationary case.

Recasting the definition of effective energy stress tensor above as

$$T^{ab} = -\frac{2}{\sqrt{-\gamma}}\frac{\delta \mathcal{L}_{eff}}{\delta \gamma_{ab}}, \tag{3.102}$$

and noticing that

$$\frac{\delta\sqrt{-\gamma}}{\delta\gamma_{ab}} \;=\; -\frac{1}{2\sqrt{-\gamma}}\frac{\delta\gamma}{\delta\gamma_{ab}} \;=\; \frac{\sqrt{-\gamma}}{2}\gamma^{ab} \tag{3.103}$$

and that

$$\frac{\delta\lambda(\mathrm{k})}{\delta\gamma_{ab}} \;=\; \lambda'(\mathrm{k})\frac{\delta \mathrm{k}}{\delta\gamma_{ab}} = -\frac{\lambda'(\mathrm{k})}{2\mathrm{k}}k^a k^b = -\frac{1}{2}\,\lambda'(\mathrm{k})\,\mathrm{k}u^a u^b, \tag{3.104}$$

we obtain explicitly

$$T^{ab} = \lambda'(\mathrm{k})\,\mathrm{k}u^a u^b - \lambda(\mathrm{k})\gamma^{ab}. \tag{3.105}$$

We see that (3.105) describes a perfect fluid, with

$$P = -\lambda(\mathrm{k}), \tag{3.106}$$

$$\varepsilon + P = \lambda'(\mathrm{k})\,\mathrm{k}. \tag{3.107}$$

Hence, the local entropy and the local free energy result in

$$s \;=\; \frac{\mathrm{k}}{\mathcal{T}}\lambda'(\mathrm{k}), \tag{3.108}$$

$$\mathcal{F} \;=\; \varepsilon - \mathcal{T}s \;=\; -P \;=\; \lambda(\mathrm{k}). \tag{3.109}$$

Therefore, we can define a global free energy F as the integral over the worldvolume

$$F \;=\; \int_{\mathcal{W}_{p+1}} d\sigma^{p+1}\sqrt{-\gamma}\,\mathcal{F}, \tag{3.110}$$

where of course we must think of the time direction as Wick rotated in order to make this integration sensible. We also remark that the Euclidean rotation is trivial since we are dealing with a foliation of $\mathcal{W}_{p+1}$ into time-independent slices $\mathcal{B}_p$. Consequently,

$$F \;=\; -\beta\int_{\mathcal{B}_p} dV_{(p)}\; R_0\, P, \tag{3.111}$$

where the redshift factor R_0 comes from integrating over the Euclidean asymptotic (that is, background) time span β.

This framework is constructed consistently since now we can verify the following relation between global quantities

$$F = M - TS - \sum_i \Omega_i J_i, \tag{3.112}$$

and we observe again that the angular momenta Ω_i have the same role as a set of chemical potentials related to the conserved charges J_i. Furthermore, if we take as usual $dF|_{\Omega_i,T} = 0$ as variational principle, we can easily obtain the First Law

$$dM = TdS + \sum_i \Omega_i\, dJ_i. \tag{3.113}$$

If we return now to the effective action, we can consider to integrate it over an asymptotic span of time $\Delta\tau = \Delta t/R_0$, again in view of the relation (3.75) between background and worldvolume time translations. In this way, we find

$$I_{eff} = -\Delta\tau\int_{\mathcal{B}_p} dV_{(p)}\; R_0 P, \tag{3.114}$$

from which we see explicitly the equivalence with the free energy (3.110). Noticeably, by using equation (3.16) and (3.72) it is possible to rewrite the pressure as

$$P = -\frac{\Omega_{(n+1)}}{16\pi G}\left(\frac{n}{4\pi T}\right)^n \mathrm{k}^n = -\frac{\Omega_{(n+1)}}{16\pi G}\left(\frac{n}{4\pi T}\right)^n R_0^n\left(1-V^2\right)^{n/2}, \tag{3.115}$$

which means that, up to a numerical factor, we can consider a variational principle based on the effective action

$$\tilde{I}_{eff}[X^\mu] = \int_{\mathcal{B}_p} dV_{(p)}\; R_0\,\mathrm{k}^n = \int_{\mathcal{B}_p} dV_{(p)}\; R_0^{n+1}\big(1-V^2\big)^{n/2}. \tag{3.116}$$

Then, thanks to the result (A.32), we note that this action actually leads to the extrinsic equations in the form (3.82), as desired. Of course, we can also recast the variational principle in terms of the free energy as

$$\frac{\delta \tilde{I}_{eff}}{\delta X^{\mu}} = 0, \tag{3.117}$$

and it corresponds to demanding

$$\frac{\delta M}{\delta X^{\mu}} = T \frac{\delta S}{\delta X^{\mu}} + \sum_i \Omega_i \frac{\delta J_i}{\delta X^{\mu}}. \tag{3.118}$$

Then we have proven the equivalence between the approach followed in the previous sections and the one based on an effective action. In fact, it is remarkable that one can consider the pressure as found in the effective energy stress tensor, integrate it as in (3.110) and straightforwardly recover the full thermodynamics of Section 3.5 by simply performing the following derivatives:

$$S = -\left.\frac{\partial F}{\partial T}\right|_{\Omega_i}, \qquad J_i = -\left.\frac{\partial F}{\partial \Omega_i}\right|_{T,\Omega_{j\neq i}}. \tag{3.119}$$

As we will see, it is often a shorter and more viable computation to go through.

3.7 Examples of blackfolds

In this section, we consider some basic examples of blackfold solutions. In particular, we intend to show the usefulness of this approach by describing how both MP black holes and black rings in the US regime are easily recovered as specific cases.

3.7.1 Black one-folds

In this section we give a basic demonstration of the power of the blackfold setup, by studying the whole set of possible stationary $p = 1$ blackfolds at once [34, 32]. This will also give us the chance to appreciate the advantages related to the two approaches shown in Chapter 3 at the perfect fluid level, namely solving explicitly the blackfold equations and deriving the observables from an effective action.

We are dealing here with $p = 1$ and then with a two dimensional worldvolume, endowed with coordinates $\sigma^a = (t, z)$. We can choose to parametrize the vector space related to this worldsheet with two tangential orthonormal vectors u^a and v^a, where v^a is spacelike and u^a is the timelike unit vector describing the velocity field of the effective fluid. As a consequence, we have

$$u^2 = -1, \qquad v^2 = 1, \qquad u^a v_a = 0. \tag{3.120}$$

The first fundamental form associated to the worldsheet can be simply written as

$$h^{\mu\nu} = -u^\mu u^\nu + v^\mu v^\nu, \tag{3.121}$$

in agreement with the fact that $h^{\mu\nu} + u^\mu u^\nu$ is the projector on the direction orthogonal to the fluid boost u^a. If we consider their push-forwards u^μ and v^ν, it follows that we can rewrite the pull-back of the perfect fluid stress tensor (3.15) as

$$T^{\mu\nu} = \varepsilon u^\mu u^\nu + P v^\mu v^\nu. \tag{3.122}$$

The worldsheet origin of u^μ and v^ν implies of course that $[u, v]$ must lie again in the vector algebra of the worldsheet, that is

$$\perp^\mu_{\ \rho} [u, v]^\rho = 0. \tag{3.123}$$

We are dealing with stationary solutions, and thus u^a must be proportional to a certain Killing vector k^a. Recalling the machinery presented in Section 3.3, we consider the vectors $\xi = \partial_t$ (restrincting to $R_0 = 1$) and $\zeta = \partial_z$. Then we can perform a change of basis on the worldsheet vector space defined uniquely by a real parameter α such that

$$\begin{aligned} \mathbf{u} &= \cosh\alpha\, \xi + \sinh\alpha\, \zeta, \\ \mathbf{v} &= \sinh\alpha\, \xi + \cosh\alpha\, \zeta. \end{aligned} \tag{3.124}$$

We notice that this change of basis simply corresponds to switching from static observers following orbits of ∂_t to the fluid-comoving ones, via a boost with α as parameter.

We can now turn to the explicit solution of the extrinsic equations. By using relation (A.15), it is easy to show that they correspond to

$$\perp^\rho_{\ \mu} (\varepsilon \nabla_u u^\mu + P\, \nabla_v v^\mu) = 0. \tag{3.125}$$

In terms of ξ and ζ, they read then

$$\perp^\rho_{\ \mu} \nabla_u u^\mu = \perp^\rho_{\ \mu} \left[\cosh\alpha\, \nabla_\xi (\cosh\alpha\, \xi^\mu + \sinh\alpha\, \zeta^\mu) + \sinh\alpha\, \nabla_\zeta (\cosh\alpha\, \xi^\mu + \sinh\alpha\, \zeta^\mu)\right]. \tag{3.126}$$

It is reasonable to assume that ξ is a Killing vector by itself; furthermore, it is normalized and hence its integral curves must satisfy $\nabla_\xi \xi = 0$, that is they must be geodesics. We can also assume that ζ is parallel-transported along these curves, which means that $\nabla_\xi \zeta = 0$. Since we are considering a zero-torsion spacetime, these assumptions imply that

$$\nabla_\zeta \xi \ = \ - [\zeta, \xi]\,. \tag{3.127}$$

Recalling that the worldsheet vector algebra must close according to (3.123), it holds that

$$\perp^\rho_{\ \mu} (\nabla_\zeta \xi)^\mu = 0 \tag{3.128}$$

as well. Hence, on the whole,

$$\perp^{\rho}_{\ \mu} \nabla_u u^{\mu} = \perp^{\rho}_{\ \mu} \sinh^2 \alpha \, (\nabla_\zeta \zeta)^{\mu}, \tag{3.129}$$

and analogously

$$\perp^{\rho}_{\ \mu} \nabla_v v^{\mu} = \perp^{\rho}_{\ \mu} \cosh^2 \alpha \, (\nabla_\zeta \zeta)^{\mu}, \tag{3.130}$$

in such a way that the extrinsic equations can be recast in the form

$$\left(\varepsilon \sinh^2 \alpha + P \cosh^2 \alpha\right) \nabla_\zeta \zeta = 0. \tag{3.131}$$

Consequently, they lead to $\varepsilon \sinh^2 \alpha + P \cosh^2 \alpha = 0$, i.e.

$$\tanh^2 \alpha = -\frac{P}{\varepsilon} = \frac{1}{n+1}. \tag{3.132}$$

By comparing with equation (4.10), we conclude that the local effective fluid velocity $\beta = \tanh \alpha$ is equal to the propagation speed of transverse perturbations on the 1-brane, independently of the worldsheet point σ^a. Furthermore, we can consider ζ in terms of a background spacelike vector χ describing an asymptotic isometry as

$$\zeta = \frac{1}{R} \chi, \tag{3.133}$$

where R is the norm of χ on the worldsheet, and in general it depends on σ^a. By introducing the spatial velocity field $V = R\Omega$ as above, thanks to relation (3.132), it is possible to obtain the constraint between the angular velocity and the orbits radius $R(\sigma)$

$$V = \Omega R = \frac{1}{\sqrt{n+1}}, \tag{3.134}$$

which clearly reminds us of the balance condition (2.44) for ultra-spinning black rings in $D = 5$. In particular, we notice that the radius R is independent of the worldsheet point, namely there is just one possible radius for the orbits, once we fix the angular velocity Ω.

Let us now inspect how to obtain (3.134) with the effective action formalism. We start by taking two background vectors ξ and χ tangent to the worldsheet, on such a way that they are timelike and spacelike respectively, with χ describing orbits of periodicity 2π. Here we can consider their norms R_0 and R on the worldsheet to be constant form the start, since we can always choose their push-forwards as the vector basis of the worldsheet. Explicitly, we have again

$$\xi = R_0 \partial_t, \qquad \chi = R \partial_z. \tag{3.135}$$

From (3.114) and neglecting the time span factor, we obtain the effective action

$$I = 2\pi R R_0 \left[R_0^2 - \Omega^2 R^2\right]^{n/2}, \tag{3.136}$$

and we can vary it along the transverse radial direction to find the solution to extrinsic equations, namely

$$\Omega R = \frac{R_0}{\sqrt{n+1}}, \tag{3.137}$$

which reduces to (3.134) for $R_0 = 1$. Once more, we interpret it as the necessary condition on the radius in order to have a stationary configuration.

Instead of picking up a specific one-fold configuration and computing its observables, it was noticed that it possible to gather the whole zoo of $p = 1$ blackfolds into a general discussion if we choose a Minkowski background with $R_0 = 1$ [34].

With this choice of background, requiring stationarity with respect to asymptotic observers corresponds to taking ξ and χ_i as the Minkowski time translations and rotations generators, respectively. We also choose the 1-dimensional spatial sections of the world-sheet to be invariant under background translations generated by ∂_x, with associated coordinate x describing compact orbits of length $2\pi R_x$. For later convenience, we also introduce an angular coordinate $\phi_x = x/R_x$ with standard periodicity 2π.

Let us now consider the subspace of Minkowski spacetime over which the 1-fold embedding is non-trivial, that is where the 1-fold actually lies, in such a way that the other embedding coordinates can be set identically to zero. Following the exact solutions discussed in Sections (2.2) and (2.3), we parametrize the spatial slices of this subspace as

$$dl^2 = R_x^2 d\phi_x^2 + \sum_{i=1}^{m} \left(dr_i^2 + r_i^2 d\phi_i^2 \right). \tag{3.138}$$

In this way, we are splitting them onto the direction x and onto m planes over which the projection of the 1-fold is invariant under translations ∂_x and rotations χ_i respectively. In general, we have $2m \leq D-1$, and not $D-2$ since the x direction can also collapse into a point. In addition, we notice that by construction the m radial directions r_i are orthogonal to the 1-fold itself, as well as the $D-(1+2m) = n+3-2m$ trivial embedding directions. Thus, we see that these total $n+3-m$ coordinates must account for the transverse sphere s^{n+1} of radius r_0.

This choice allows to simply parametrize the spatial curve the string lies along as

$$\phi_x = n_x \sigma, \qquad \phi_i = n_i \sigma, \tag{3.139}$$

where we also set the embedding $r_i = R_i$, with σ characterizing the proper length of the 1-fold in the interval $0 \leq \sigma < 2\pi$. Then, any ϕ_a can span up to $2\pi n_a$, with $a = x, 1 \ldots m$. Of course, if the 1-fold closes on itself, the n_a must be all integers, and in particular we think of $n_a \geq 0$. It means in turn that each ratio n_i/n_j is rational. Furthermore, if we want to restrict ourselves to single-covering parametrizations of the 1-fold, we observe that it necessary to require that the smallest winding n_{min} is coprime with respect to all the remaining n_a.

We can now proceed with a complete classification of stationary 1-folds, consisting of

- *black strings*, for $n_x \neq 0$, $n_i = 0\ \forall i$. The resulting curve has no winding, as a consequence;

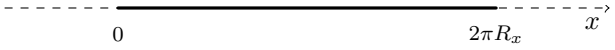

- *black rings*, for $n_x = 0$ and $n_i = 1\ \forall i$. The direction x collapses to a point, and in particular we impose $n_i = 1$ in order to avoid multiple coverings. The radius of these black rings will be given by $R^2 = \sum_i R_i^2$;

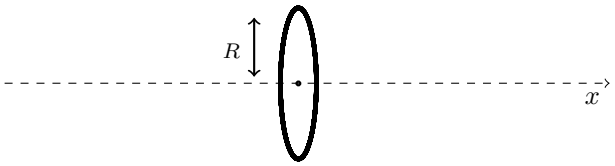

- *helical black strings*, for $n_x \neq 0$ and $n_i > 0$ for some planes i. Clearly, the number of $n_i > 0$ specifies the dimensionality of the spatial non-trivial subspace. We depict here the case of $n_1 > 0$ only, in such a way that the spatial subspace is 3-dimensional and that we have two characteristic length scales, namely R_1 and R_x;

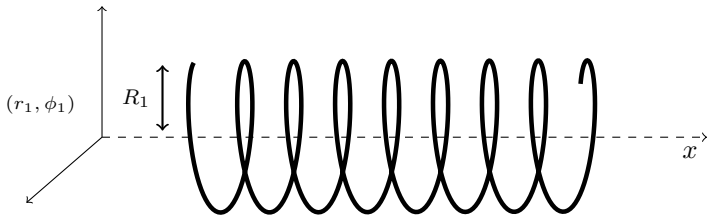

- *helical black rings*, if $n_x = 0$, $n_i \neq 0$ for at least two distinct i, j such that $0 < n_i < n_j$. In this case, we obtain a configuration like

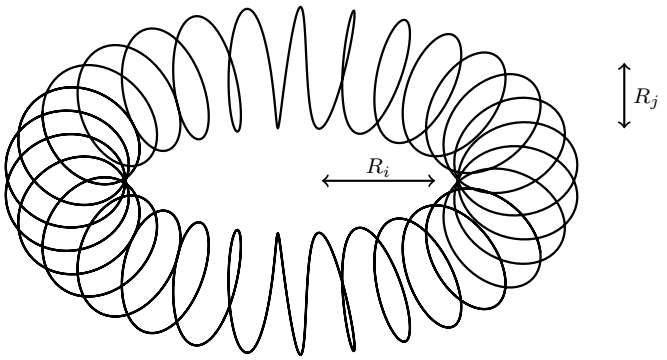

where the number of windings is n_j/n_i. We can recover a helical black string by performing a suitable limit of large R_i.

We notice that the constraint on m discussed above implies that

$$m \leq \left[\frac{n+3}{2}\right]. \tag{3.140}$$

As we know, we need at least a plane for helical black strings and two of them for helical black rings to be present. This means that it is possible to find both of these configurations already in $n = 1$, according to that constraint. In Chapter 2 we analysed the exact analytic solutions for black strings and black rings in $D = 5$, while the explicit solution for helical black strings and rings (which have the same horizon topology as those known solutions) has not been found yet.

Let us now consider the spatial fluid velocity V, whose value is fixed by (3.134). We can decompose it along the directions related to the chosen rotational and translational Killing vectors dividing V into the components $\Omega_i R_i$ and $V_x = \Omega_x R_x$. In this way, its modulus reads

$$V^2 \,=\, \sum_a \Omega_a^2 R_a^2 \,=\, \frac{1}{n+1}, \tag{3.141}$$

due to the balancing condition.

We can now turn to the evaluation of the relevant thermodynamic quantity both from the free energy functional and from the conserved currents. After observing that the 1-fold length is simply

$$L = 2\pi R, \tag{3.142}$$

where $R = \sqrt{\sum_a n_a^2 R_a^2}$, the observables result in

$$S = \frac{\pi \Omega_{(n+1)}}{2G}\sqrt{\frac{n+1}{n}} r_0^{n+1} R, \tag{3.143}$$

$$M \,=\, \frac{\Omega_{(n+1)}}{8G}(n+2) r_0^n R, \tag{3.144}$$

$$J_a = \pm \frac{\Omega_{(n+1)}}{8G}\sqrt{n+1} r_0^n n_a R_a^2, \tag{3.145}$$

where we defined the horizon radius conveniently as

$$r_0 = \frac{n^{3/2}}{\sqrt{n+1}}\,\frac{1}{4\pi T}. \tag{3.146}$$

It is remarkable that they coincide with the corresponding singly-spinning $D = 5$ black ring quantities discussed in Section 2.3 if we take the ultra-spinning limit in $n = 1$, and define the radius of the ring as R. Of course, we have to set $n_x = 0$ and $n_{\hat{i}} = 1$ for

only one specific $\hat{i}$ (since we are considering a singly-spinning BR). We also notice that we have fully recovered the intuitive black ring picture of a black string bent to form a circle. In addition, we observe that these results hint at the existence of black rings in any $D \geq 5$, since we found a well-defined thermodynamics of their US counterparts.

This is an outstanding check of the blackfold approach, which was precisely conceived in order to grasp the dynamics of solutions in higher dimensions with high angular momenta. At this point, we can be persuaded that also helical black rings and strings describe exact solutions in the US regime, with the thermodynamic properties above.

If we now turn to the analysis of relations (3.143)-(3.145), after disregarding numerical factor except for the n_a, we can easily combine these quantities into

$$S^n \sim \frac{M^{n+2}}{\sum_a n_a J_a}, \tag{3.147}$$

which relates the behaviour of entropy to the conserved charges. We see that entropy tends to decrease if we increase the winding numbers n_a of the solution while keeping fixed its conserved charges. This is an interesting check of our analysis, since effectively we are making the string longer and hence we are decreasing its mass density (a fact that causes an entropy decrease in NG classic strings as well). From these considerations, we also understand that black rings are the most favourable singly spinning 1-folds.

Finally, we observe that these solutions are endowed with the $m+1$ conserved charges M and J_i. On the other hand, a helical black ring described at the perfect fluid level has $2m$ independent parameters, that is the horizon scale r_0, the radii R_i and the m independent winding numbers ratios n_i/n_{min}. We can then conclude that we are in presence of an infinite non-uniqueness, as for each observable helical black ring configuration with some M and J_i, there is an infinite class of solutions parametrized by $m-1$ rational numbers with the same mass and angular momenta.

3.7.2 Black discs

We give now another example of the solution-generating power of the blackfold approach by considering a Schwarzschild black 2-brane within a Minkowski background [34, 32]. We take the embedding map to be

$$\begin{gathered} X^0 = \tau, \\ X^1(\rho,\phi) = \rho\cos\phi, \qquad X^2(\rho,\phi) = \rho\sin\phi, \\ X^i = 0 \qquad \text{for each } \; i = 3\ldots D-1, \end{gathered} \tag{3.148}$$

with $\rho \geq 0$ and $0 \leq \phi < 2\pi$. With these choices, the induced metric on the spatial section $\mathcal{B}_2$ of the worldvolume reads

$$ds^2 \;=\; -d\tau^2 + d\rho^2 + \rho^2 d\phi^2. \tag{3.149}$$

We observe that this is a minimal surface embedding with $K_{ab}{}^{i} = 0$, and hence the extrinsic equations are automatically solved.

To implement a rotation of $\mathcal{B}_2$, it is sufficient to introduce a Killing vector field

$$\mathbf{k} = \partial_\tau + \Omega\partial_\phi \qquad \text{with norm} \qquad \mathrm{k} = \sqrt{1-\Omega^2\rho^2}\,, \tag{3.150}$$

where we notice that $R_0 = 1$ here, since we are dealing with a flat background. As explained in Section 3.4, this leads to a limiting surface at $\mathrm{k} = 0$, that is for $\rho_+ = \frac{1}{\Omega}$. Therefore the worldvolume geometry becomes compact due to this circular boundary of radius ρ_+.

Thanks to the formalism developed above for stationary blackfolds, this setup is enough to evaluate the observables related to that configuration.

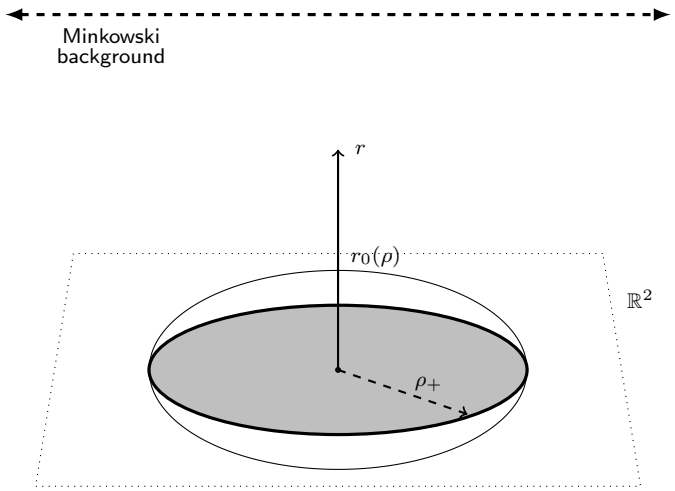

Figure 3.1: We show here a cartoon of the black disc setup, considering a space $D-1$ dimensional slice at $t = const$. The boundary around the disc is at $\rho = \rho_+$, while the solid line over the disc represents the pancaked horizon with spatial topology S^{D-2}. At spatial infinity, the dashed line represents a space slice of Minkowski background.

First, we notice that the horizon has the geometry of a 2-ball (that is, a disc) $\mathbb{D}$ with $(n+1)$-spheres fibered over, each with radius $r_0(\rho)$ depending on the worldvolume point. As one can see from Figure 3.1, it consists in a $n+1+2 = D-2$ dimensional surface, and the fibration leads to a S^{D-2} topology.

The horizon width has explicit form

$$r_0(\rho) \;=\; \frac{n}{4\pi T}\mathrm{k} \;=\; \frac{n}{4\pi T}\sqrt{1-\Omega^2\rho^2}\,. \tag{3.151}$$

Then it gets to zero at the boundary $r_0(\rho_+) = 0$, while it is maximal at the centre of the disc, where

$$r_+ = r_0(\rho = 0) = \frac{n}{4\pi T}. \tag{3.152}$$

Interestingly, this horizon topology is the same as for a singly spinning MP black hole in the US regime, where it has a pancaked shape. Arguably, we can expect our observables to match the ones of this configuration for $D \geq 6$ (where the US regime actually exists for MP black holes).

Applying the validity analysis of the blackfold approach in Section 3.3 to this case, we stress that both the Riemann curvature tensor and the extrinsic curvature vanish here, so that the requirement (3.98) reduces to demanding

$$r_0 \ \ll \ \left|\frac{\nabla_a \nabla^a \mathrm{k}}{\mathrm{k}}\right|^{-\frac{1}{2}} \ = \ \frac{1}{\Omega}\,\frac{1-\Omega^2\rho^2}{\sqrt{2-\Omega^2\rho^2}}. \tag{3.153}$$

Recalling that $r_0 = r_+\sqrt{1-\Omega^2\rho^2}$, we see that near the rotation axis at $\rho \to 0$ equation (3.153) is equivalent to requiring $r_+ \ll \frac{1}{\Omega}$, i.e. $r_+ \ll a$ making use of the definitions of Section 2.2. Thus, we recognize the usual form of the US limit, with the angular momentum length scale much bigger than the horizon scale, and this agrees with the correspondence suggested above.

On the other hand, close to the boundary at $\rho \to \rho_+$, one finds from (3.153) that

$$r_+ \ \ll \ \frac{1}{\Omega}\sqrt{\frac{1-\Omega^2\rho^2}{2-\Omega^2\rho^2}} \ \xrightarrow[\rho\to\rho_+]{} 0, \tag{3.154}$$

which is not satisfied by any positive r_+. As a consequence, it is wise to introduce a small parameter $\epsilon \ll 1$ describing the radial distance from the boundary. We consider then the blackfold approach to be valid in the range $0 \leq \rho \leq \rho_+ - \epsilon$, but we assume the existence of a regular limit of the blackfold observables for $\epsilon \to 0$.

We can now safely deal with the observables, and we start by evaluating the free energy functional. The pressure of the effective fluid is

$$P = -\frac{\Omega_{(n+1)}}{16\pi G}\, r_0^n = -\frac{\Omega_{(n+1)}}{16\pi G}\, r_+^n \left(1-\Omega^2\rho^2\right)^{\frac{n}{2}}, \tag{3.155}$$

and subsequently the free energy (3.111) reads

$$\begin{aligned} F \ &= \ \frac{\Omega_{(n+1)}}{16\pi G}\, r_+^n \int_0^{2\pi} d\phi \int_0^{\rho_+-\epsilon} d\rho\, \rho \left(1-\Omega^2\rho^2\right)^{\frac{n}{2}} = \\ &= \ \frac{\Omega_{(n+1)}}{8G}\, r_+^n\, \frac{1-\left[\,\epsilon\,\Omega\,(2-\epsilon\,\Omega)\,\right]^{\frac{n}{2}+1}}{(n+2)\,\Omega^2} = \\ &= \ \frac{\Omega_{(n+1)}}{8G}\, r_+^n \left(\frac{1}{(n+2)\,\Omega^2} + O\left(\epsilon^{\frac{n}{2}+1}\right)\right). \end{aligned} \tag{3.156}$$

Of course, we can calculate the free energy for a MP black hole in the US regime from the known thermodynamics relations and the observables from Section 2.2. It can be easily seen to coincide to first order in ϵ with (3.156), and then it is guaranteed that the observables will match as well, as anticipated. Therefore we can conclude that the blackfold approach allows to describe the US regime of another class of known analytic exact solutions, that is MP black holes, in addition to black rings, as we found in Section 3.7.1.

Chapter 4

Black Ring Stability and Blackfolds

Besides generating new solutions, another interesting application of the blackfold approach consists in studying the dynamic stability of higher dimensional black holes, which basically reduces to the analysis of effective fluid perturbations. In this chapter, we approach black ring stability with the blackfold formalism. As we noticed in Section 3.7, solutions with the same topology as the five-dimensional black ring are present in any $D \geq 5$. Consequently, we will analyse the case in generic dimensions.

We first review static black branes stability by considering the quasinormal modes propagating transversally and longitudinally to the worldvolume. Then, we turn to boosted black strings, and finally we tackle a more realistic modelling of black rings by introducing a finite extrinsic radius R. We evaluate also the viscous corrections to the boosted black string modes.

4.1 Stability of static blackfolds

In this section, we present the most simple instance of stability analysis making use of blackfolds. We consider a Schwarzschild black brane with a flat, non-compact $(p+1)$-dimensional worldvolume, endowed with the properties outlined in the previous sections [31, 35].

We take then an effective fluid with energy-stress tensor (3.15) with the known uniform energy density ε and pressure P. We set the initial velocity to be $u^a = (1, 0 \dots 0)$, in such a way that the initial fluid is static and the worldvolume is not boosted. Finally, we consider conveniently a static embedding of the worldvolume into flat space as

$$X^0 = t, \qquad X^i = z^i, \quad \text{with } \; i = 1 \dots p, \tag{4.1}$$

while initially we keep the transverse coordinates X^m, $m = p+1 \dots D$ fixed to a constant value independent of σ^a. Accordingly, the unperturbed effective energy-stress tensor has form

$$T^{ab} \;=\; (\varepsilon + P)\, u^a u^b + P \eta^{ab} \;=\; \mathrm{diag}(\varepsilon, P \dots P). \tag{4.2}$$

Let us introduce perturbations with characteristic wavelength in the interval $r_0 \ll r \ll R$ where the blackfold framework is valid. In that range, we can work at the leading order as before, in such a way that the worldvolume can be considered flat (${K_{ab}}^{\rho} \approx 0$), while intrinsic and extrinsic dynamics decouple. The fluid parameters are r_0 and the velocity field u^a. If we impose a variation of r_0 dependent on σ^a, it will bring about a $\delta\varepsilon(\sigma)$ and a $\delta P(\sigma) = \frac{dP}{d\varepsilon}\delta\varepsilon$, once given the known equation of state. We also impose a variation of the velocity field, which now reads $\tilde{u}^a = (1, v^i(\sigma))$, and it is still unit-normalized, since $v^i v_i \approx 0$ at first order. We also introduce perturbations of the embedding $\delta X^m = \xi^m(\sigma)$.

First, we notice that we still have a flat induced metric η^{ab}, because its components do not involve the coordinates and we are not perturbing the embedding along the worldvolume directions. Consequently, the perturbed energy-stress tensor reads

$$T^{ab} = \left[\varepsilon + P + \left(1 + \frac{dP}{d\varepsilon}\right)\delta\varepsilon\right] u^a u^b + (\varepsilon + P)\left(u^a \delta u^b + u^b \delta u^a\right) + \left(P + \frac{dP}{d\varepsilon}\delta\varepsilon\right)\eta^{ab}, \quad (4.3)$$

or, more explicitly, we can write its non-zero components as

$$T^{00} = \varepsilon + \delta\varepsilon, \qquad T^{0i} = (\varepsilon + P)v^i, \qquad T^{ii} = P + \frac{dP}{d\varepsilon}\delta\varepsilon. \quad (4.4)$$

Due to the embedding perturbations, the extrinsic curvature is no more vanishing. It results in

$${K_{ab}}^{\rho} = D_a \partial_b X^\rho + \Gamma^\rho_{\mu\nu}\partial_a X^\mu \partial_b X^\nu, \quad (4.5)$$

where now $\tilde{X}^\mu = X^\mu + \xi^\mu(\sigma)$, and so $\Gamma^\rho_{\mu\nu}\partial_a X^\mu \partial_b X^\nu$ is a second order term and we can neglect it. Analogously, since the worldvolume geometry is flat for this interval of wavelength, the perturbed extrinsic curvature has non-vanishing components with simple form

$${K_{ab}}^{m} = \partial_a \partial_b \xi^m. \quad (4.6)$$

As we mentioned, extrinsic and intrinsic perturbations decouple in this setup, and it means that we can deal with the intrinsic and extrinsic blackfold equations separately. Let us now turn to the former. Requiring the validity of (3.53) coincides with demanding

$$T^{ab}_{(0)} {K_{ab}}^{m} = 0, \quad (4.7)$$

since we are working at first order. After substituting, we obtain

$$\left(\varepsilon\partial_t^2 + P\partial_i^2\right)\xi^m = 0, \quad (4.8)$$

which is a well-known dispersion equation. If we take a plane-wave behaviour of the variations

$$\xi^m(\sigma) = \xi^m\, e^{i(-wt + k_i z^i)}, \quad (4.9)$$

it tells us that transverse elastic perturbations of the worldvolume have group velocity

$$c_T^2 = -\frac{P}{\varepsilon} = \frac{1}{n+1}. \tag{4.10}$$

It means that $c_T > 0$ and hence we have simply an oscillatory evolution of the perturbations, corresponding to an extrinsic stability of Schwarzschild flat black branes at the leading order.

Let us now inspect the dynamics of longitudinal modes with the p intrinsic equations

$$D_a T^{ab} = 0, \tag{4.11}$$

from which it is customary to extract the second order differential equation

$$\partial_t^2 T^{00} - \partial_i \partial_j T^{ij} = 0. \tag{4.12}$$

After substituting, it reads

$$\left(\partial_t^2 - \frac{dP}{d\varepsilon}\partial_i^2\right)\delta\varepsilon = 0. \tag{4.13}$$

If we consider

$$\delta\varepsilon(\sigma) = \delta\varepsilon\, e^{i(-wt+k_i z^i)}, \tag{4.14}$$

then equation (4.13) implies an imaginary sound speed, that is

$$c_L^2 = \frac{d\varepsilon}{dP} = -\frac{1}{n+1}. \tag{4.15}$$

It means that we have a real exponential amplitude influencing the propagation of sound-modes on the worldvolume, and hence we can conclude that an intrinsic instability is present for Schwarzschild black branes at the leading order.

Indeed, these results agree with the well-known longitudinal instability that Gregory and Laflamme found for low frequency perturbations of black branes by linearising the whole set of EFE [36, 37]. Instead, we observe that here it was just necessary to take into account the constraints (3.52) and (3.53), thanks to the blackfold machinery. In view of the discussion above, this fact also means that we expect any higher dimensional black hole admitting an ultraspinning regime to be unstable for perturbations along the directions corresponding to the worldvolume in the blackfold approach. Numerical simulations actually show that this is what happens for very high angular momenta.

By making use of the duality developed so far between dynamical behaviour and thermodynamics of the effective fluid, it can be interesting to compare these results with the thermodynamic stability of the fluid. From equation (3.19) and (3.20) we can find the Gibbs-Duhem relation

$$dP = s d\mathcal{T}, \tag{4.16}$$

which leads to

$$\frac{dP}{d\varepsilon} = \frac{dP}{d\mathcal{T}}\frac{d\mathcal{T}}{d\varepsilon} = \frac{s}{c_v}, \tag{4.17}$$

where c_v is the specific heat at constant volume. It is well-known that a thermodynamic system is unstable if $c_v < 0$. Since $s > 0$, we see a perfect relation between the two pictures: the local Thermodynamics of the effective fluid is unstable ($c_v < 0$) if and only if the dynamics of the black brane is unstable under long wavelength soundmode perturbations ($c_L^2 < 0$), as it was found to be in (4.15).

4.2 Stability of boosted black strings

We study now the dynamics of a boosted black string under perturbations. In comparison with the setup of Section 4.1, we have an additional boost, described by the Killing vector

$$k^a\partial_a = \partial_t + \beta\partial_z, \qquad \mathrm{k} = \sqrt{1-\beta^2}, \tag{4.18}$$

which entails a velocity field

$$u^a = \frac{k^a}{\mathrm{k}} = \left(\frac{1}{\sqrt{1-\beta^2}}, \frac{\beta}{\sqrt{1-\beta^2}}\right). \tag{4.19}$$

The unperturbed energy-stress tensor has now components

$$T^{00}_{(0)} = \frac{\varepsilon}{n+1}\left(\frac{n}{1-\beta^2}+1\right), \tag{4.20}$$

$$T^{01}_{(0)} = \frac{\varepsilon}{n+1}\frac{n\beta}{1-\beta^2}, \tag{4.21}$$

$$T^{11}_{(0)} = \frac{\varepsilon}{n+1}\left(\frac{n\beta^2}{1-\beta^2}-1\right). \tag{4.22}$$

We introduce the perturbations $\delta\varepsilon(\sigma)$, $\delta u^a(\sigma)$, $\xi^m(\sigma)$ with explicit form

$$\begin{aligned}\delta\xi^m(\sigma) &= \delta\xi^m\, e^{i(-wt+kz)},\\ \delta u^1(\sigma) &= \delta u^1\, e^{i(-wt+kz)},\\ \delta\varepsilon(\sigma) &= \delta\varepsilon\, e^{i(-wt+kz)}.\end{aligned} \tag{4.23}$$

Of course, we notice that δu^0 will be simply related to δu^1 according to

$$\delta u^0(\sigma) = \frac{u^1}{u^0}\,\delta u^1(\sigma). \tag{4.24}$$

In this way,

$$\delta T^{ab} = \frac{\varepsilon}{n+1}\left[\left(nu^au^b - \eta^{ab}\right)\frac{\delta\varepsilon}{\varepsilon} + n(u^a\delta u^b + u^b\delta u^a)\right], \tag{4.25}$$

while

$$K_{ab}{}^m = \partial_a\partial_b\xi^m. \tag{4.26}$$

Extrinsic equations. For each ξ^m, we obtain the equation

$$\left(\frac{n}{1-\beta^2}+1\right)w^2-2\,\frac{n\beta}{1-\beta^2}wk+\left(\frac{n\beta^2}{1-\beta^2}-1\right)k^2=0, \tag{4.27}$$

leading to

$$w_{1,2}(k)\;=\;\frac{n\beta\pm\sqrt{n+1}\,(1-\beta^2)}{1+n-\beta^2}\,k. \tag{4.28}$$

We can specialize them to the boosted black string obtained as a US limit of a black ring in equilibrium, by setting $\beta=\frac{1}{\sqrt{n+1}}$, as found in Section 3.7.1. The resulting frequencies are

$$w_{1,2}(k)\;=\;0\,,\;\frac{2\sqrt{n+1}}{n+2}\,k\;=\;0\,,\;\frac{2\sqrt{2}}{3}\,k \tag{4.29}$$

in the specific case of $n=1$ and $\beta=\frac{1}{\sqrt{2}}$.

Intrinsic equations. They simply read $\partial_a\delta T^{ab}=0$, leading to

$$\left[-\left(n(u^0)^2+\frac{1}{n}\right)w+u^0u^1k\right]\frac{\delta\varepsilon}{\varepsilon}+\left[-2u^1w+\left(u^0+\frac{(u^1)^2}{u^0}\right)k\right]\delta u^1=0, \tag{4.30}$$

$$\left[-u^0u^1w+\left((u^1)^2-\frac{1}{n}\right)k\right]\frac{\delta\varepsilon}{\varepsilon}+\left[-\left(u^0+\frac{(u^1)^2}{u^0}\right)w+2u^1k\right]\delta u^1=0. \tag{4.31}$$

Setting the determinant related to this system to zero, we find the frequencies

$$w_{3,4}\;=\;\frac{\beta(n+2)\pm i\sqrt{n+1}(1-\beta^2)}{1+n+\beta^2}\,k. \tag{4.32}$$

We can consider again $\beta=\frac{1}{n+1}$, which leads to

$$w_{3,4}\;=\;(n+2\pm n\,i)\,\frac{\sqrt{n+1}}{n^2+2n+2}\,k\;=\;(3\pm i)\frac{\sqrt{2}}{5}\,k, \tag{4.33}$$

once we choose $n=1$.

Then, as for the static black string, we find elastic stability, while we have a Gregory-Laflamme instability under longitudinal perturbations. This is shown explicitly by the presence of an imaginary part in the frequencies (4.33), and we notice that they are no longer purely imaginary as in (4.15), due to the presence of a boost.

4.3 Black rings leading order stability

We start with a generic $D = n + p + 1 = n + 4$ Schwarzschild boosted black string, and, as mentioned above, we intend to bend it into a ring. Thus, naming as usual X^μ the background coordinates, we choose the Minkowski metric

$$ds^2 = -d(X^0)^2 + d(X^1)^2 + (X^1)^2 d(X^2)^2. \tag{4.34}$$

as the worldvolume embedding, with $X^1 = r$ and X^2 playing the role of a radial and angular coordinate, respectively. The transverse coordinates $X^3, X^4 \dots X^{D-1}$ are set identically to zero. The only non-vanishing components of the connection are

$$\Gamma^1_{22} = -X^1, \qquad \Gamma^2_{12} = \Gamma^2_{21} = \frac{1}{X^1}. \tag{4.35}$$

We consider the embedding map

$$X^0 = t, \qquad X^1 = R, \qquad X^2 = \phi,$$

with R being the radius of the ring. The induced metric γ_{ab} then reads

$$ds^2\big|_R = -dt^2 + R^2 d\phi^2, \tag{4.36}$$

and the induced connection is now zero: $\Gamma^c_{ab} = 0$. We notice that the tangent vectors $e^\mu_a = \partial_a X^\mu$ and the normal vector n^μ_i are essentially Kronecker deltas with this choice of embedding. Finally, since we want to describe a rotating solution, we introduce a worldvolume Killing vector $\mathbf{k}$. Due to the balancing condition in the US limit, we know that it must have form

$$\mathbf{k} = \partial_t + \Omega \partial_\phi = \partial_t + \frac{1}{R\sqrt{n+1}} \partial_\phi, \tag{4.37}$$

with modulus $\mathrm{k} = \sqrt{\frac{n}{n+1}}$.

It is now possible to evaluate the extrinsic curvature

$$K_{ab}{}^\rho = D_a \partial_b X^\rho + \Gamma^\rho_{\mu\nu} \partial_a X^\mu \partial_b X^\nu. \tag{4.38}$$

The first term in the r.h.s vanishes, and then it follows that the only non-zero component is $K_{\phi\phi}{}^r = -R$. Furthermore, we take an initial energy-stress tensor of the usual form

$$T^{ab}_{(0)} = \frac{\varepsilon}{n+1} \left(n u^a u^b - \gamma^{ab} \right), \tag{4.39}$$

where the specific values of the velocity field components $u^a = (u^0, u^1)$ are dictated by the Killing vector $\mathbf{k}$ as

$$u^a_{(0)} = \frac{k^a}{\mathrm{k}} = \left(\sqrt{\frac{n+1}{n}}, \frac{1}{R\sqrt{n}} \right). \tag{4.40}$$

Let us now perform a variation of the embedding only along the radial direction:

$$X^r \mapsto X^r + \xi^r(\sigma), \tag{4.41}$$

implying a perturbed position of the worldvolume $R+\delta R(\sigma)$. Introducing $e^\mu{}_a = \partial_a X^\mu$ as the tangent vectors to the worldvolume (see Appendix A and [38]), one has the variations

$$\delta e^\mu{}_a = \partial_a \xi^\mu = \delta_{\mu r}\partial_a \xi^r, \tag{4.42}$$

$$\delta\gamma_{ab} = 2e^\mu{}_a e^\nu{}_b \nabla_{(\mu}\xi_{\nu)} = -2K_{ab}{}^r\xi_r, \tag{4.43}$$

so that the only new contribution is $\delta\gamma_{\phi\phi} = 2R\delta R$. We can read this variation also on the background metric as

$$\delta g_{\mu\nu} = \xi^r \partial_r g_{\mu\nu}, \tag{4.44}$$

and we get a non-vanishing connection on the worldvolume of the perturbed configuration. Explicitly, on the surface we have

$$\Gamma^r_{\phi\phi} = -R - \delta R, \qquad \Gamma^\phi_{r\phi} = \Gamma^\phi_{\phi r} = \frac{1}{R}\left(1 - \frac{\delta R}{R}\right),$$

$$\Gamma^t_{\phi\phi} = R\,\partial_t \delta R, \qquad \Gamma^\phi_{t\phi} = \Gamma^\phi_{\phi t} = \partial_t \frac{\delta R}{R}, \qquad \Gamma^\phi_{\phi\phi} = \partial_\phi \frac{\delta R}{R}.$$

We can now compute the perturbed extrinsic curvature tensor. Again, from (A.18) we have

$$\delta K_{ab}{}^r = \partial_a \delta e^r{}_b - e^r{}_c \delta\Gamma^c_{ab} - \Gamma^c_{ab}\delta e^r{}_c + e^\mu{}_a e^\nu{}_b \delta\Gamma^r_{\mu\nu} + \Gamma^r_{\mu\nu}\left(e^\mu{}_a \delta e^\nu{}_b + e^\nu{}_b \delta e^\mu{}_a\right). \tag{4.45}$$

From the choices above and keeping to the linear order in the perturbations, the only non-vanishing terms result in

$$\delta K_{ab}{}^r = \partial_a\partial_b \delta R - \delta R\,\delta_{\phi a}\delta_{\phi b}. \tag{4.46}$$

After perturbing also the energy density and the velocity field with $\delta\varepsilon(\sigma)$ and $\delta u^a(\sigma)$, the stress tensor variation results in

$$\delta T^{ab} = \frac{\varepsilon}{n+1}\left[\left(nu^a u^b - \gamma^{ab}\right)\frac{\delta\varepsilon}{\varepsilon} + n(u^a\delta u^b + u^b \delta u^a) - \delta\gamma^{ab}\right], \tag{4.47}$$

where we have that

$$\delta\gamma^{ab} = -\gamma^{ac}\gamma^{bd}\delta\gamma_{cd}. \tag{4.48}$$

As usual, we consider the variation of the δu^1 component of the velocity as independent, thanks to the normalization $u_a u^a = -1$, which actually entails

$$\delta u^0 = \frac{(u^1)^2}{2u^0}\delta\gamma_{\phi\phi} + \frac{\gamma_{\phi\phi}}{\gamma_{tt}}\frac{u^1}{u^0}\delta u^1. \tag{4.49}$$

Finally, it is convenient to define a dimensionless perturbation of the velocity $\delta\bar{u}^1 = R\delta u^1$, in order to deal more easily with the limit of large radii R.

We can now turn to the extrinsic equation along the direction r, which reads

$$\delta T^{11} K^{(0)\,r}_{\phi\phi} + T^{00}_{(0)} \delta K_{tt}{}^{r} + 2T^{01}_{(0)} \delta K_{t\phi}{}^{r} = 0. \tag{4.50}$$

After substituting the relations above together with the on-shell velocities, and taking a plane-wave behaviour of the perturbations

$$\begin{aligned} \delta R(\sigma) &= \delta R\, e^{i(-wt+kR\phi)}, \\ \delta\bar{u}^1(\sigma) &= \delta\bar{u}^1\, e^{i(-wt+kR\phi)}, \\ \delta\varepsilon(\sigma) &= \delta\varepsilon\, e^{i(-wt+kR\phi)}, \end{aligned} \tag{4.51}$$

we find

$$\frac{\sqrt{n(n+1)}}{R}\delta\bar{u}^1 + \left[\frac{\sqrt{n+1}}{R^2} + w\sqrt{n+1}\left(\left(\frac{n}{2}+1\right)w - \sqrt{n+1}\,k\right)\right]\delta R = 0. \tag{4.52}$$

On the other hand, the two intrinsic equations $D_a T^{ab} = 0$ have the form

$$\partial_t T^{00} + \partial_\phi T^{10} + \Gamma^{\phi}_{t\phi} T^{00}_{(0)} + \Gamma^{\phi}_{\phi\phi} T^{10}_{(0)} = 0, \tag{4.53}$$

$$\partial_t T^{01} + \partial_\phi T^{11} + 3\Gamma^{\phi}_{t\phi} T^{01}_{(0)} = 0, \tag{4.54}$$

and, more explicitly, they read

$$\begin{aligned} \sqrt{n+1}\,\left[k\sqrt{n+1} - (n+2)w\right]\frac{\delta\varepsilon}{\varepsilon} + \sqrt{n}\left[(n+2)k - 2\sqrt{n+1}w\right]\delta\bar{u}^1 + \\ + \frac{k(n+2) - \sqrt{n+1}(n+4)w}{R}\,\delta R = 0, \end{aligned} \tag{4.55}$$

$$-(n+1)w\frac{\delta\varepsilon}{\varepsilon} + \sqrt{n}\left[\sqrt{n+1}k - (n+2)w\right]\delta\bar{u}^1 + \frac{2\sqrt{n+1}k - (4+3n)w}{R}\,\delta R = 0. \tag{4.56}$$

First, we observe that intrinsic and extrinsic equations are coupled in this case, and it is related primarily to an initial non-zero extrinsic curvature. Secondly, we notice that equation (4.52) decouples from the intrinsic sector for large R. Furthermore, it readily reduces to (4.27) once we set $\beta = \frac{1}{\sqrt{n+1}}$, which is the boost of the black string that we obtain in the thin ring limit. In the same way, (4.55) and (4.56) reduce to (4.30) and (4.31) respectively in the thin ring limit, and they decouple from the variations δR. On the whole, this is again consistent with the picture of a black ring seen locally as a boosted black string.

We intend to find the dispersion relation related to these fluctuations, and therefore we set the determinant of this three-equation system to zero. It is possible to write the four solutions with a generic n as

$$w_{1,2}(k) \,=\, 0\,,\, \frac{2\sqrt{n+1}}{n+2}\, k, \tag{4.57}$$

$$w_{3,4}(k) \,=\, \sqrt{n+1}\, \frac{(n+2)kR \pm \sqrt{2(n^2+2n+2) - n^2k^2R^2}}{(n^2+2n+2)R}. \tag{4.58}$$

We notice that $w_{1,2}(k)$ coincide exactly with the extrinsic stable modes found for the boosted black string, and hence they do not get corrections in $1/R$ at the perfect fluid level. On the other hand, we also expect $w_{3,4}(k)$ to recover the intrinsic (unstable) behaviour of the boosted black string in the limit of large R. After expanding them, actually we find

$$\begin{aligned} w_3 \,=& \sqrt{n+1}\, \left[\frac{n+2+n\,i}{n^2+2n+2}\, k - \frac{i}{nkR^2} - \frac{i(n^2+2n+2)}{2n^3k^3R^4}\right] + O\left(\frac{1}{m^6}\right) = \\ =& \sqrt{n+1}\frac{n+2+ni}{n^2+2n+2}k\left[1 - \frac{n+i(n+2)}{2n\,k^2R^2} - \frac{(n+i(n+2))\,(n^2+2n+2)}{4n^3\,k^4R^4}\right] + O\left(\frac{1}{m^6}\right), \end{aligned} \tag{4.59}$$

and similarly for its complex conjugated w_4. From the first line, we observe that only the imaginary part of the frequency gets corrected.

It is interesting to observe that (4.58) implies that $w_{3,4}(k)$ are real if the mode $m = kR$ satisfies

$$m < m_{min} = \frac{\sqrt{2}}{n}\sqrt{n^2+2n+2}. \tag{4.60}$$

The behaviour of m_{min} is shown in Figure 4.1, and we remark that it is $O(1)$ for each n. In particular, we have $m_{min}(1) = \sqrt{10}$, while its asymptotic value for large n is $\sqrt{2}$. The mode $m = 1$ leads to real $w_{3,4}$ for each n, while the modes $m \geq 2$ corresponds to complex frequencies for $n \geq 3$.

From numerical analyses, we would expect to find intrinsic instability and hence complex frequencies. But this contradiction comes as no surprise, since we know that the blackfold approach is valid at the perfect fluid order if the fluctuations considered have wavelength such that $r_0 \ll \lambda \ll R$, where R is here precisely the extrinsic curvature scale. This means in turn that we should trust our computations for modes

$$m \,=\, kR \,\sim\, \frac{R}{\lambda} \,\gg 1. \tag{4.61}$$

Equation (4.60) means that we can associate to each n a lower boundary m_{min} above which $w_{3,4}$ are real, but conceivably we should trust our results only for larger modes

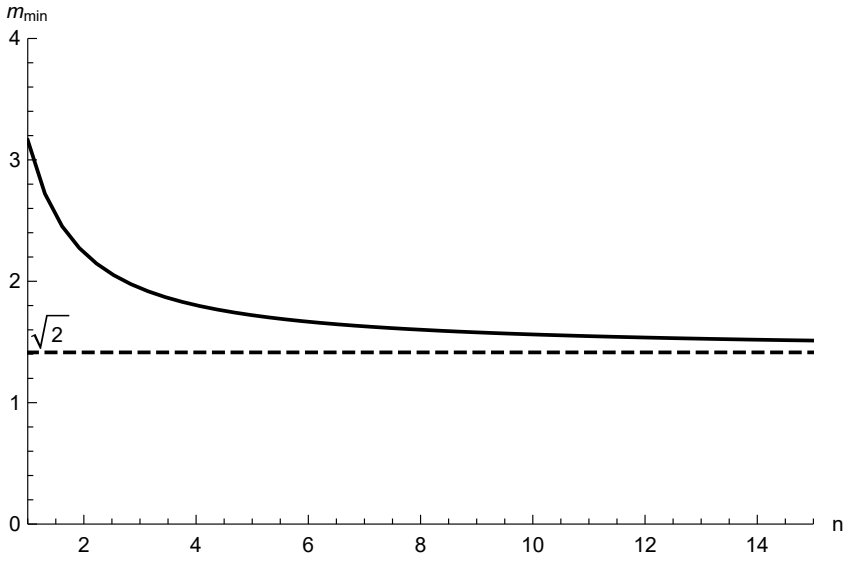

Figure 4.1: We display here the behaviour of the threshold mode $m_{min}(n)$, below which the frequencies $w_{3,4}$ are real.

$m \gg m_{min}$ and we should consider the frequencies $w_{3,4}$ only in the perturbative form of equation (4.59) .

It is interesting to compare our large R results in any n with the ones resulting from a large dimensions analysis. In [5] it was found that for $n \gg 1$ the elastic and intrinsic instability of a black ring could be described, up to $O(1/n)$, by the characteristic frequencies[1]

$$w_{1,2}^{(T)} = 0,\, 2\frac{\sqrt{R^2 - r_0^2}}{R}\,\frac{k}{\sqrt{n}} + O\left(\frac{1}{n}\right), \tag{4.62}$$

$$w_{3,4}^{(T)} = \frac{\sqrt{R^2 - r_0^2}}{R}\,\frac{kR \pm i\sqrt{k^2R^2 - 2}}{\sqrt{n}R} + O\left(\frac{1}{n}\right). \tag{4.63}$$

If we now expand $w_2^{(T)}$ and $w_3^{(T)}$ at large R, we obtain

$$w_2^{(T)} = \frac{2k}{\sqrt{n}} - \frac{k}{\sqrt{n}}\,\frac{r_0^2}{R^2} - \frac{k}{4\sqrt{n}}\,\frac{r_0^4}{R^4} + O\left(\frac{r_0^6}{R^6}, \frac{1}{n}\right), \tag{4.64}$$

[1]The dictionary with respect to that paper is $m_\Phi \to m = kR$ and $\hat{m} \to \frac{m}{\sqrt{n}R}$. It was also considered $r_0 = 1$ as definition of length scales there. Modes with $\ell = 0$ correspond to our longitudinal frequencies, while $\ell = 1$ are translated into our elastic modes.

$$
\begin{aligned}
w_3^{(T)} &= (1+i)\frac{k}{\sqrt{n}} - \frac{1}{R^2}\left[\frac{i}{k\sqrt{n}} + \frac{(1+i)kr_0^2}{2\sqrt{n}}\right] - \\
&- \frac{1}{2R^4}\left[\frac{i}{k^3\sqrt{n}} - \frac{ir_0^2}{k\sqrt{n}} - \frac{(1+i)kr_0^4}{4\sqrt{n}}\right] + O\left(\frac{r_0^6}{R^6}, \frac{1}{n}\right).
\end{aligned}
\tag{4.65}
$$

On the other hand, we can expand our frequencies (4.57) and (4.58) for large n and find

$$
w_2 = \frac{2k}{\sqrt{n}} + O\left(\frac{1}{n}\right), \tag{4.66}
$$

$$
w_3 = (1+i)\frac{k}{\sqrt{n}} - \frac{i}{\sqrt{n}kR^2} - \frac{i}{2\sqrt{n}k^3R^4} + O\left(\frac{1}{m^6}, \frac{1}{n}\right), \tag{4.67}
$$

that is, we find the same terms as Tanabe's, up to $O\left(\frac{r_0}{R}\right)$ contributions. This makes sense, since we are assuming the scale hierarchy $r_0 \ll \lambda \ll R$, and we are imposing fluctuations on the leading order effective stress-energy tensor. In this way, we can inspect the dynamics of fluctuations with new contributions to the boosted black string behaviour with form $\frac{\lambda^j}{R^j}$, while we neglect corrections like $\frac{r_0^j}{R^j}$, coming from the near horizon physics. The latter are related to thickness effects of the black ring, and it is conceivable that we could access instabilities at smaller angular momenta by considering the first order viscous effective stress tensor.

Finally, until now we have assumed that radial and longitudinal perturbations does not couple with the dynamics along the other embedding transverse directions X^m, with $m \neq r$. We intend now to check this.

Let us calculate the variation of the extrinsic curvature along such a generic transverse direction X^m under embedding variations

$$
X^r \mapsto X^r + \xi^r(\sigma), \tag{4.68a}
$$

$$
X^m \mapsto X^m + \xi^m(\sigma). \tag{4.68b}
$$

The general form of this variation is

$$
\begin{aligned}
\delta K_{ab}{}^m &= \delta\left(D_a\partial_b X^m + \Gamma^m_{\mu\nu}\partial_a X^\mu \partial_b X^\nu\right) = \\
&= \partial_a\, \delta e^m{}_b - e^m{}_c \delta\Gamma^c_{ab} - \Gamma^c_{ab}\delta e^m{}_c + \delta\Gamma^m_{\mu\nu} e^\mu{}_a e^\nu{}_b + \Gamma^m_{\mu\nu}\left(e^\mu{}_a \delta e^\nu{}_b + e^\nu{}_b \delta e^\mu{}_a\right),
\end{aligned}
\tag{4.69}
$$

where $\delta e^\mu{}_a = \partial_a \xi^\mu$. We have again

$$
\delta\gamma_{ab} = e^\mu{}_a e^\nu{}_b\left(\nabla_\mu \xi_\nu + \nabla_\nu \xi_\mu\right) = -2K^r_{ab}\xi_r, \tag{4.70}
$$

which means that the perturbed induced connection Γ^c_{ab} is the same as well. If we turn to the embedding metric $g_{\mu\nu}$, it is easy to see that

$$
\delta g_{\mu\nu} = \xi^r \partial_r g_{\mu\nu}, \tag{4.71}
$$

as well as before. Since the unperturbed transverse directions are flat, we recall that for the unperturbed connection it holds $\Gamma^m_{\mu\nu} = 0$, while

$$\delta\Gamma^m_{\mu\nu} = \frac{1}{2} g^{m\alpha} \left(\nabla_\mu \delta g_{\alpha\nu} + \nabla_\nu \delta g_{\alpha\mu} - \nabla_\alpha \delta g_{\mu\nu} \right), \tag{4.72}$$

where

$$\delta g_{m\nu} = \xi^\nu \partial_r g_{m\nu} = 0, \tag{4.73}$$

and

$$\nabla_m \delta g_{\mu\nu} = \partial_m \delta g_{\mu\nu} = 0. \tag{4.74}$$

As a consequence, $\delta\Gamma^m_{\mu\nu} = 0$, which means in turn that

$$\delta K_{ab}{}^m \;=\; \partial_a \partial_b \xi^m. \tag{4.75}$$

We have no unperturbed extrinsic curvature $K_{ab}{}^m$ and also $T^{11}_{(0)} = 0$, in such a way that the associated extrinsic equation simply reads

$$T^{ab} K_{ab}{}^m \;=\; T^{00}_{(0)} \delta K_{00}{}^m + 2T^{01}_{(0)} \delta K_{01}{}^m = 0, \tag{4.76}$$

that is

$$\left[T^{00}_{(0)} \partial_t^2 + 2T^{01}_{(0)} \partial_t \partial_\phi \right] \xi^m = 0, \tag{4.77}$$

leading to the known flat boosted black string dispersion relation, with frequencies

$$w(k) \;=\; 0\,,\; \frac{2\sqrt{n+1}}{n+2}\, k. \tag{4.78}$$

Hence these transverse perturbations do couple neither with the ones along the radial direction r, nor with the intrinsic equations, as we found no additional variation of the induced metric.

4.4 Viscous boosted black strings stability

We consider now the stability of a boosted black string endowed with the first order viscous effective stress tensor

$$T_{ab} = \rho u_a u_b + P \Delta_{ab} - \zeta \theta \Delta_{ab} - 2\eta \sigma_{ab} \tag{4.79}$$

that we saw in Section (3.2). We start by considering homogeneous velocity field and energy density on the worldvolume. It implies that the unperturbed stress tensor T^{ab} is just the same as for the leading order discussion, since the first order terms are proportional to the derivatives of the fields. We also expect intrinsic and extrinsic equations to be still uncoupled.

In order to prevent unphysical frequencies from appearing, we can proceed by solving perturbatively these dispersion equations at the viscous order. We assume then the modes to have form

$$w_i = w_i^{(PF)} + \frac{r_0}{R}\,\widetilde{w}_i, \tag{4.80}$$

where $i = 1 \ldots 4$ and $w_i^{(PF)}$ are the frequencies that we obtained at the perfect fluid level.

If we perturb the embedding as

$$X^m \mapsto X^m + \xi^m(\sigma), \tag{4.81}$$

and the energy density and velocity field[2] with $\delta\varepsilon(\sigma)$ and $\delta u^1(\sigma)$, we find $\delta K_{ab}{}^m = \partial_a\partial_b\xi^m$, just as before. Therefore, since we have a vanishing unperturbed extrinsic curvature, the extrinsic equations will read

$$T^{ab}_{(0)}\,\partial_a\partial_b\xi^m = 0, \tag{4.82}$$

leading to the elastic frequencies $w_{1,2}$ (4.28) and (4.29) previously found.

Of course, we expect new contributions to the intrinsic equations. From their explicit form, we notice first that we can rewrite the variations of the shear and bulk viscosities as

$$\frac{\delta\eta}{\eta} = \frac{\delta\zeta}{\zeta} = \frac{n+1}{n}\,\frac{\delta\varepsilon}{\varepsilon}. \tag{4.83}$$

From these definitions, and considering $\beta = \frac{1}{\sqrt{n+1}}$ together with perturbations of the form

$$\begin{aligned}\delta u^1(\sigma) &= \delta u^1\, e^{i(-wt+kz)},\\ \delta\varepsilon(\sigma) &= \delta\varepsilon\, e^{i(-wt+kz)},\end{aligned} \tag{4.84}$$

it is straightforward to see that the intrinsic equations $\partial_a T^{ab} = 0$ read

$$\begin{aligned}&\frac{-k\sqrt{1+n}+(2+n)w}{n+1}\frac{\delta\varepsilon}{\varepsilon}+\\ &+\frac{ik^2(1+n)^2\zeta + w\left(2n\sqrt{n(1+n)}\varepsilon + i(1+n)w\zeta\right) - k\left(n\sqrt{n}(n+2)\varepsilon + 2i(n+1)\sqrt{n+1}w\zeta\right)}{n(1+n)^{3/2}\varepsilon}\delta u^1 = 0,\\ &\frac{w}{\sqrt{1+n}}\frac{\delta\varepsilon}{\varepsilon}+\\ &\frac{ik^2(1+n)^2\zeta - 2k\left(n\sqrt{n}\varepsilon + i(1+n)\sqrt{n+1}w\zeta\right) + w\left(n\sqrt{\frac{n}{n+1}}\,(n+2)\,\varepsilon + i(1+n)w\zeta\right)}{n(1+n)\varepsilon}\delta u^1 = 0.\end{aligned}$$

After setting the determinant of this system to zero and after expanding the solutions up to $O(k^2)$, we obtain the longitudinal frequencies

$$w_{3,4} = \frac{(1\pm i)\sqrt{1+n}}{(1\pm i)+n}\,k - \frac{i\sqrt{n}(1+n)^{5/2}\zeta}{2((1\pm i)+n)^3\varepsilon}\,k^2 + O(k^3). \tag{4.85}$$

[2]As usual, we consider δu^1 as the independent variation and $\delta u^0 = \frac{u^1}{u^0}\delta u^1$.

First, we notice that we have no dependence on the shear viscosity η, and this is consistent with the results concerning static black strings. We recall that we are dealing with an effective fluid in a single spatial dimension, so intuitively we can say that there is no way to shear through it.

We recognize immediately that $w_{3,4}$ have the same linear order as the longitudinal frequencies found from the leading order analysis. In addition, it is possible to check that they recover the known values for a static black string by inspecting the corresponding solutions with general β in the limit $\beta \to 0$.

From the explicit forms of ε and ζ, and after setting $n = 1$, these longitudinal frequencies can be written as

$$w_{3,4} = \frac{\sqrt{2}}{5}\,(3 \pm i)\,k + \frac{3\sqrt{2}}{125}\,(11 \pm 2i)\,r_0\,k^2 + O(k^3). \tag{4.86}$$

This form makes clear the fact that we are now considering contributions coming from the near-horizon dynamics, with terms in $r_0/\lambda \ll 1$, where λ is the wavelength associated to the wave-number k.

We can also compare our longitudinal frequencies with the ones following from the large-D expansion of boosted black strings [5]. After defining the boost parameter $\alpha = \sqrt{n}\beta$, the elastic modes (4.28) can be expanded for large n as

$$w_{1,2} = \frac{\mp 1 + \alpha}{\sqrt{n}}\,k \pm \frac{1 \mp 2\alpha + 2\alpha^2}{2n\sqrt{n}}\,k + O\left(k^3, n^{5/2}\right), \tag{4.87}$$

while the expansion of our generic β longitudinal modes is

$$\begin{aligned} w_{3,4} \;=\; & \frac{\pm i + \alpha}{\sqrt{n}}\,k - \frac{i}{n}\,r_0 k^2 \mp \frac{i \mp 2\alpha + 2i\alpha^2}{2n\sqrt{n}}\,k + \frac{-2i \pm 6\alpha + 3i\alpha^2}{2n^2}\,r_0 k^2 \pm \\ & \pm \frac{3i \mp 8\alpha - 4i\alpha^2 \mp 8\alpha^3}{8n^2\sqrt{n}} + O\left(k^3, n^3\right), \end{aligned} \tag{4.88}$$

and they match perfectly with the corresponding known frequencies[3].

[3] In [5], the Killing vector related to boost symmetry is written as

$$\mathbf{k} = \partial_t + \beta\partial_z = \partial_t + \frac{\alpha}{R}\,\partial_\phi,$$

in such a way that our linear coordinate z gets translated into $z = R\Phi = \sqrt{n}R\phi$.

Chapter 5

Extrinsic Equations for Spinning Blackfolds

In this chapter, we show how it is possible to obtain the blackfold extrinsic equations by perturbing branes endowed with transverse angular momenta. We start with a Kerr black string, then we analyse the multi-spinning case with the doubly-spinning MP black strings, which has two transverse angular momenta. Finally, we introduce a new set of coordinates suitable for dealing with the asymptotic region of black ring spacetimes, and we recover the extrinsic equations for black ring black strings as well. We will also discuss how to generalize these procedures to configurations with a higher number of worldvolume dimensions.

5.1 Kerr black strings

We consider first a singly-spinning MP black hole in $D \geq 5$, with metric (2.10), and we add a new direction described by a coordinate l. Then, (t, l) represents the worldvolume while the whole metric

$$\begin{aligned} ds^2 = -dt^2 + \frac{\mu}{r^{D-6}\rho^2}\left(dt + a\sin^2\theta\, d\phi\right)^2 + \frac{\rho^2}{\Delta}dr^2 + \rho^2 d\theta^2 + \\ + (r^2 + a^2)\sin^2\theta d\phi^2 + r^2\cos^2\theta d\Omega_{D-5}^2 + dl^2 \end{aligned} \tag{5.1}$$

describes a so called *singly-spinning MP black string*. For convenience, we also report here the functions

$$\rho^2 = r^2 + a^2\cos^2\theta, \qquad \Delta = r^2 + a^2 - \frac{\mu}{r^{D-6}}. \tag{5.2}$$

We can boost this metric along the worldvolume directions, by considering

$$\sigma^a = \Lambda^a{}_b\, \sigma'^b, \qquad \text{with} \qquad \Lambda^a{}_b = \begin{pmatrix} u^0 & -u^1 \\ -u^1 & u^0 \end{pmatrix}, \tag{5.3}$$

and $u_a u^a = \eta_{ab} u^a u^b = -u_0^2 + u_1^2 = -1$ as before. After a direct substitution and after deleting the primes from the boosted coordinates, we obtain the compact form

$$\begin{aligned} ds^2 = &\left(\eta_{ab} + \frac{\mu}{r^{D-6}\rho^2} u_a u_b\right) d\sigma^a d\sigma^b - 2a\frac{\mu}{r^{D-6}\rho^2} u_a \sin^2\theta d\sigma^a d\phi + \\ &+ \left(r^2 + a^2 + \frac{\mu}{r^{D-6}\rho^2} a^2 \sin^2\theta\right) \sin^2\theta d\phi^2 + \frac{\rho^2}{\Delta} dr^2 + \\ &+ \rho^2 d\theta^2 + r^2 \cos^2\theta d\Omega_{D-5}^2. \end{aligned} \tag{5.4}$$

Thus, we observe that the main difference here is the spin-related mixing term $g_{a\phi}$, involving both transverse and worldvolume directions, if we compare this metric with the boosted Schwarzschild black brane (3.1). We remark that, in turn, rotation also implies a deviation of the angular part from sphericity.

We now turn to the case of a Kerr black string, setting $D = 5$. This choice makes calculations more straightforward but it does not influence the results; furthermore, a generalization to any dimension will be immediate. Explicitly, metric (5.4) reduces to

$$\begin{aligned} ds^2 = &\left(\eta_{ab} + \frac{\mu r}{\rho^2} u_a u_b\right) d\sigma^a d\sigma^b - 2\frac{J_a r}{\rho^2} \sin^2\theta d\sigma^a d\phi + \\ &+ \left(r^2 + a^2 + \frac{\mu r}{\rho^2} a^2 \sin^2\theta\right) \sin^2\theta d\phi^2 + \frac{\rho^2}{\Delta} dr^2 + \rho^2 d\theta^2, \end{aligned} \tag{5.5}$$

with

$$\rho^2 = r^2 + a^2 \cos^2\theta, \qquad \Delta = r^2 + a^2 - \mu r. \tag{5.6}$$

We have also defined the angular momentum current

$$J_a = \frac{1}{2} J_{ADM}\, u_a = a\mu\, u_a, \tag{5.7}$$

which, up to an integration constant, coincides with the ADM angular momentum [10]. We also notice that with these definitions we have $\mu = 2M_{ADM}$, as expected.

Following the path paved by [29] and as explained in Section 3.2, we now focus on studying how to find a set of constraints (analogous to (3.50)) after introducing extrinsic perturbations of this metric on scales larger than the characteristic lengths of the system (here a^2 and r_0).

First, we expand this metric asymptotically, considering up to $1/r^n$ contributions, with $n = 1$ [1]. Then $\rho^2 \approx r^2$ and, on the whole, the expanded metric reads

$$\begin{aligned} ds^2 \approx &\left(\eta_{ab} + \frac{\mu}{r} u_a u_b\right) d\sigma^a d\sigma^b - 2a\frac{\mu}{r} u_a \sin^2\theta d\sigma^a d\phi + \\ &+ r^2 \sin^2\theta d\phi^2 + \left(1 + \frac{\mu}{r}\right) dr^2 + r^2 d\theta^2. \end{aligned} \tag{5.8}$$

[1] It makes sense since this is the power law in r that we find in g_{ab}, and furthermore it is the value of $n = D - p - 3$ that we recover in the Schwarzschild-Tangherlini limit $a \to 0$.

It is remarkable that in this regime of expansion the presence of an angular momentum density a does not affect any component, except for the mixing $g_{a\phi}$, where it appears inside the momentum current J_a.

Our aim now is to perturb this metric along the transverse directions by adding contributions of the form (3.40), which we recall to hold for any classical brane. Once eliminated the holonomies from the metric, we obtain

$$\begin{aligned} ds^2 \approx & \left(\eta_{ab} - 2K_{ab}{}^i y_i + \frac{\mu}{r} u_a u_b\right) d\sigma^a d\sigma^b - 2a\frac{\mu}{r} u_a \sin^2\theta d\sigma^a d\phi + \\ & + r^2 \sin^2\theta d\phi^2 + \left(1 + \frac{\mu}{r}\right) dr^2 + r^2 d\theta^2 + h_{\mu\nu}(y^i) dx^\mu dx^\nu + O\left(y^2/R^2\right), \end{aligned} \tag{5.9}$$

where y^i are the transverse directions. We do not want to break the symmetries on the rotational plane, and thus, thanks to the decoupling of the perturbations at this order, we can introduce a perturbation along any single direction $y^{\hat{i}}$. One can argue that here the explicit expression of $y^{\hat{i}}$ must be different from the one in the Schwarzschild case (3.42), including for example extra-contributions from the angular momentum inside the radial part (as $\rho = \sqrt{r^2 + a^2\cos^2\theta}$ instead of r), but asymptotically we recover $y^{\hat{i}} = r\cos\theta$ as well as before.

Making the same assumptions as above, the perturbed metric can then be written as

$$\begin{aligned} ds^2 \approx & \left(\eta_{ab} - 2K_{ab}{}^i\, r\cos\theta + \frac{\mu}{r} u_a u_b\right) d\sigma^a d\sigma^b - 2a\frac{\mu}{r} u_a \sin^2\theta d\sigma^a d\phi + \\ & + r^2\left(d\theta^2 + \sin^2\theta d\phi^2\right) + \left(1 + \frac{\mu}{r}\right) dr^2 + \cos\theta\, \hat{h}_{\mu\nu}(r)\, dx^\mu dx^\nu, \end{aligned} \tag{5.10}$$

where we consider the same non-null components of $\hat{h}_{\mu\nu}$ as in (3.44). One could actually consider off-diagonal perturbation as $h_{a\phi}$, h_{ar} or $h_{a\theta}$, which correspond to adding extra-momentum along the transverse directions, but they neither enter nor influence the final result, as one can see from the explicit calculations.

We can now turn to the evaluation of the Brown-York tensor up to first order in the mass scale μ, in order to get to the Camps-Emparan form of this metric. We start from the unperturbed and expanded metric (5.8); the consequent extrinsic curvature tensor and related quantities are the same as in equations (3.10)-(3.12) at this order, once we change r_0^n with μ. As a consequence, the leading contribution to the effective energy-stress tensor reads

$$T_{ab} = \frac{\Omega_{(2)}}{16\pi G}\,\mu\,(u_a u_b - \eta_{ab})\,. \tag{5.11}$$

Flat background quantities are obtained in the limit $\mu \to 0$, and in turn it means that T_{ab} is formally independent of a^2 with this parametrization. Therefore, we can write this

metric in the Camps-Emparan form, expressing it only in terms of conserved currents:

$$\begin{aligned} ds^2 = & \left(\eta_{ab} - 2K_{ab}{}^{\hat{i}} r\cos\theta + \frac{16\pi G}{\Omega_{(2)}}\left(T_{ab} - \frac{T}{3}\eta_{ab}\right)\frac{1}{r}\right) d\sigma^a d\sigma^b - \\ & - 2\frac{J_a}{r}\sin^2\theta d\sigma^a d\phi + \left(1 - \frac{16\pi G}{\Omega_{(2)}}\frac{T}{3r}\right) dr^2 + r^2\left(d\theta^2 + \sin^2\theta d\phi^2\right) + \\ & + \cos\theta\, \hat{h}_{\mu\nu}(r) dx^\mu dx^\nu + O\left(\frac{T_{ab}^2}{r^2}\right). \end{aligned} \tag{5.12}$$

As expected, the main difference with the analogous Schwarzschild black string metric is the presence of a new conserved current J_a related to the transverse spin of the solution initially considered, involving the off-diagonal $g_{a\phi}$ components.

Computing then the Einstein tensor components, one notices that the combination (3.49) is independent of $h_{\mu\nu}$ as well as before, and we have to leading order

$$G_{r\theta} - \frac{r}{2}\tan\theta\, G_{rr} = \frac{3}{2}\frac{\sin\theta}{r}\frac{8\pi G}{\Omega_{(2)}} T^{ab} K_{ab}{}^{\hat{i}} + O\left(\frac{a^2}{r^2}, \frac{\mu^2}{r^2}\right), \tag{5.13}$$

so that we recover the known expression for the blackfold extrinsic equations. Once more, it is noteworthy that the presence of an explicit dependence on the angular momentum density a is only at higher orders.

5.2 Doubly-spinning 6D MP black strings

We proved that it is possible to obtain the extrinsic equations for a 5D Kerr black string, which hints to the possibility of retrieving them in any case with transverse momenta. As we will see, increasing the number of transverse dimensions makes this issue less and less trivial.

We intend now to face the situation of two transverse momenta considering a $D = 6$ MP black string. We start from a 5-dimensional doubly-spinning MP black hole, whose metric, as we saw in Section 2.2, takes the form

$$ds^2 = -dt^2 + \frac{\mu r^2}{\Pi F}\left(dt + \sum_{i=1,2} a_i \mu_i^2 d\phi_i\right)^2 + \frac{\Pi F}{\Pi - \mu r^2} dr^2 + \sum_{i=1,2}\left(r^2 + a_i^2\right)\left(d\mu_i^2 + \mu_i^2 d\phi_i^2\right), \tag{5.14}$$

where we have now two planes for rotation, labelled by $i = 1, 2$. For each of them, we take the direction cosines to be

$$x_i = r\mu_i\cos\phi_i, \qquad y_i = r\mu_i\sin\phi_i, \qquad r^2 = \sum_{i=1,2}\left(x_i^2 + y_i^2\right). \tag{5.15}$$

We also defined

$$F = 1 - \sum_{i=1,2} \frac{a_i^2 \mu_i^2}{r^2 + a_i^2}, \qquad \Pi = \prod_{i=1,2} \left(r^2 + a_i^2\right). \tag{5.16}$$

We take now $\mu_1 = \sin\theta$ and $\mu_2 = \cos\theta$ as the direction cosines on the two planes and we name the angular momentum parameters $a_1 = a$ and $a_2 = b$. Adding then an extra direction l, the metric of a $D = 6$ MP doubly-spinning black string can be written as

$$\begin{aligned} ds^2 = &- \left(1 - \frac{\mu}{\Sigma}\right) dt^2 + 2a \sin^2\theta \, \frac{\mu}{\Sigma} \, dt d\phi_1 + 2b \cos^2\theta \, \frac{\mu}{\Sigma} \, dt d\phi_2 + \\ &+ \left(r^2 + a^2 + \frac{\mu}{\Sigma} \, a^2 \sin^2\theta\right) \sin^2\theta d\phi_1^2 + \left(r^2 + b^2 + \frac{\mu}{\Sigma} \, b^2 \cos^2\theta\right) \cos^2\theta d\phi_2^2 + \\ &+ 2ab \, \frac{\mu}{\Sigma} \sin^2\theta \cos^2\theta d\phi_1 d\phi_2 + \frac{r^2 \Sigma}{\Pi - \mu r^2} dr^2 + \Sigma d\theta^2 + dl^2, \end{aligned} \tag{5.17}$$

with

$$\Pi = (r^2 + a^2)(r^2 + b^2), \qquad \Sigma = r^2 + a^2 \cos^2\theta + b^2 \sin^2\theta. \tag{5.18}$$

By boosting this metric along the worldvolume directions $\sigma^a = (t, l)$, we obtain

$$\begin{aligned} ds^2 = &\left(\eta_{ab} + \frac{\mu}{\Sigma} \, u_a u_b\right) d\sigma^a d\sigma^b - 2 \frac{J_{1\,a}}{\Sigma} \sin^2\theta d\sigma^a d\phi_1 - 2 \frac{J_{2\,a}}{\Sigma} \cos^2\theta d\sigma^a d\phi_2 + \\ &+ \left(r^2 + a^2 + \frac{\mu}{\Sigma} \, a^2 \sin^2\theta\right) \sin^2\theta d\phi_1^2 + \left(r^2 + b^2 + \frac{\mu}{\Sigma} \, b^2 \cos^2\theta\right) \cos^2\theta d\phi_2^2 + \\ &+ 2ab \, \frac{\mu}{\Sigma} \sin^2\theta \cos^2\theta d\phi_1 d\phi_2 + \frac{r^2 \Sigma}{\Pi - \mu r^2} dr^2 + \Sigma d\theta^2. \end{aligned} \tag{5.19}$$

We notice that if we make a comparison with the Kerr black string, the main novelty is that the worldvolume boost brings about two angular momentum currents $J_{1\,a} = a\mu u_a$ and $J_{2\,a} = b\mu \, u_a$, with related off-diagonal terms in the metric. Also, from the original 5D MP metric, we find an additional mixing component $g_{\phi_1\phi_2}$.

Since we are starting from a 5-dimensional metric, it corresponds to taking $n = 2$ in the Schwarzschild discussion. It is consistent with $[\mu] \sim L^2$, and hence the first order asymptotic expansion must be up to $\frac{\mu}{r^2}$ contributions. In this way, the expanded metric reads

$$\begin{aligned} ds^2 = &\left(\eta_{ab} + \frac{\mu}{r^2} \, u_a u_b\right) d\sigma^a d\sigma^b - 2 \frac{J_{1\,a}}{r^2} \sin^2\theta d\sigma^a d\phi_1 - 2 \frac{J_{2\,a}}{r^2} \cos^2\theta d\sigma^a d\phi_2 + \\ &+ \left(r^2 + a^2\right) \sin^2\theta d\phi_1^2 + \left(r^2 + b^2\right) \cos^2\theta d\phi_2^2 + 2ab \, \frac{\mu}{r^2} \sin^2\theta \cos^2\theta d\phi_1 d\phi_2 + \\ &+ \left(1 + \frac{\mu}{r^2} - \frac{a^2 \sin^2\theta + b^2 \cos^2\theta}{r^2}\right) dr^2 + \left(r^2 + a^2 \cos^2\theta + b^2 \sin^2\theta\right) d\theta^2. \end{aligned} \tag{5.20}$$

It is now possible to perform the Brown-York computation of the effective energy-stress tensor, which results in

$$8\pi G \, T_{BY}^{ab} = \frac{\mu}{r^3} \left(u^a u^b - \frac{1}{2} \eta^{ab}\right). \tag{5.21}$$

After integrating over the transverse sphere S^3, we recover the same perfect fluid form

$$T^{ab} = \frac{\Omega_{(3)}}{16\pi G}\,\mu\left(2u^a u^b - \eta^{ab}\right) \tag{5.22}$$

as for the $n = 2$ Schwarzschild black string. After rescaling

$$\frac{16\pi G}{2\Omega_{(3)}}\,T^{ab} \longmapsto T^{ab}, \tag{5.23}$$

we can substitute

$$\mu = -\frac{T}{2}, \qquad \mu u^a u^b = T^{ab} - \frac{T}{4}\eta^{ab} \tag{5.24}$$

into (5.20), and get the Camps-Emparan form

$$\begin{aligned} ds^2 = &\left[\eta_{ab} + \frac{1}{r^2}\left(T_{ab} - \frac{T}{4}\eta_{ab}\right)\right] d\sigma^a d\sigma^b - 2\frac{J_{1\,a}}{r^2}\sin^2\theta d\sigma^a d\phi_1 - 2\frac{J_{2\,a}}{r^2}\cos^2\theta d\sigma^a d\phi_2 + \\ &+ \left(r^2 + a^2\right)\sin^2\theta d\phi_1^2 + \left(r^2 + b^2\right)\cos^2\theta d\phi_2^2 - 2ab\,\frac{T}{2r^2}\sin^2\theta\cos^2\theta d\phi_1 d\phi_2 + \\ &+ \left(1 - \frac{T}{2r^2} - \frac{a^2\sin^2\theta + b^2\cos^2\theta}{r^2}\right) dr^2 + \left(r^2 + a^2\cos^2\theta + b^2\sin^2\theta\right) d\theta^2. \end{aligned} \tag{5.25}$$

Our intention is to pull the extrinsic blackfold equations out of this metric. We see at first sight that a calculation based on the spherical symmetric framework that was used with Schwarzschild and Kerr black strings is doomed to fail, as here the angular sector is not symmetric under $SO(n+2)$ transformations.

Instead, we notice that corrections in $\frac{a^2}{r^2}$ and $\frac{b^2}{r^2}$ are present in the radial and angular diagonal components. Hence a promising guess is to perform a change of the coordinates (r, θ) of the form

$$\begin{aligned} \theta &= \chi + \frac{a^2}{\rho^2}\,h(\chi) + \frac{b^2}{\rho^2}\,m(\chi), \\ r &= \rho + \frac{a^2}{\rho}\,l(\chi) + \frac{b^2}{\rho}\,n(\chi). \end{aligned} \tag{5.26}$$

It is possible to find $h(\chi), m(\chi), l(\chi)$ and $n(\chi)$ by requiring that the following new contributions to the metric components do restore spherical symmetry in the angular sector. In principle, the change of coordinates (5.26) would require also an additional mixing term proportional to $\frac{ab}{r^2}$. As one can see from the explicit solution of the resulting system of PDEs, selecting the gauge in such a way that $g_{\phi_1\phi_2}$ vanishes actually makes this

additional term unnecessary. It turns out that, up to $O(1/r^4)$, the desired change of coordinates is

$$\begin{aligned} \theta &= \chi - \frac{a^2}{4\rho^2}\sin(2\chi) + \frac{b^2}{4\rho^2}\sin(2\chi), \\ r &= \rho + \frac{a^2}{2\rho}\sin^2\chi - \frac{b^2}{2\rho}\cos^2\chi. \end{aligned} \tag{5.27}$$

In these new coordinates, the expanded metric becomes

$$\begin{aligned} ds^2 = &\left[\eta_{ab} + \frac{1}{\rho^2}\left(T_{ab} - \frac{T}{4}\eta_{ab}\right)\right] d\sigma^a d\sigma^b - 2\frac{J_{1\,a}}{\rho^2}\sin^2\chi d\sigma^a d\phi_1 - 2\frac{J_{2\,a}}{\rho^2}\cos^2\chi d\sigma^a d\phi_2 + \\ &+ \left(1 - \frac{T}{2\rho^2}\right) d\rho^2 + \rho^2 d\chi^2 + \rho^2\sin^2\chi d\phi_1^2 - 2ab\frac{T}{8\rho^2}\sin^2(2\chi) d\phi_1 d\phi_2 + \rho^2\cos^2\chi d\phi_2^2. \end{aligned} \tag{5.28}$$

We observe that, besides the angular momentum components, (5.28) is precisely of the same form as the one from the Schwarzschild black brane computation, even in the transverse sector. We have here a non-vanishing component $g_{\phi_1\phi_2}$, but it is of first order in the mass scale T and, in particular, it consists in a $\frac{1}{\rho^4}$ contribution to the angular sector. Then, as it is easy to see with an explicit calculation, $g_{\phi_1\phi_2}$ does not influence the final result, as much as $g_{a\phi_i}$ does not. (5.28) behaves as if it were spherical symmetric. However, we observe that S^3 is parametrized in a different way from before. As a consequence, in this new set of coordinates the extrinsic equations are found in the same way as in the previous sections.

We will not delve further into the computation itself, since it is essentially equivalent to the ones already outlined. We just intend to remark that of course one can return to the more physical coordinates (r, θ) once performed the calculation. For instance, both the coefficient between the Einstein tensor components $G_{r\theta}$ and G_{rr} in the combination (3.49) and the factor in front of $K_{ab}{}^{\hat{i}}$ gets corrections in $\frac{a^2}{r^2}$ and $\frac{b^2}{r^2}$. In particular, the transverse coordinates $y^{\hat{i}}$ vary as well, and this fact follows again from the initial breaking of spherical symmetry due to the presence of angular momenta.

Finally, we notice that this change of coordinates is not necessary with the Kerr black string since there we have a lower number of transverse directions and consequently the expansion in r stops at $O\left(\frac{1}{r}\right)$. In $D \geq 5$, singly-spinning MP black strings do require a change of the transverse coordinates similar to (5.27) in order to recover a manifest spherical symmetry. As far as it concerns the discussion of more complicated situations, we consider the present section as an outline of the procedure to follow for any other higher-dimensional multi-spinning MP black strings. As a matter of fact, here we have dealt with and commented on the whole set of characteristics of a generic MP black string, namely the deformation of the transverse sphere in the expanded metric due to the angular momenta, the coupling of different angular momenta (as it happens for $g_{\phi_1\phi_2}$ in (5.20)) and the presence of extra off-diagonal components like $g_{a\phi_i}$.

5.3 Black ring strings

We intend now to obtain the extrinsic equations for a singly-spinning black ring string (BRS), and it is apparent that we have several different issues to deal with in this case. The first problem that we come across consists in the fact that the black ring solution (2.33) by Emparan and Reall does not include a global spherical symmetry of the spacetime in the angular part. In particular, we have rotational symmetry over S^2 and S^1 separately. Furthermore, the horizon itself has non-spherical topology.

However, intuitively we understand that if we expand the metric at spatial infinity and we place an observer there, he should simply see the effects of a point source, at first order in the mass scale. In turn, we must find first a set of coordinates where it is easier to see asymptotic flatness and to work with spatial infinity (which is described by $x, y \to -1$ in Emparan-Reall solution).

First of all [39], we impose the balancing condition (2.40) in the metric (2.33). In addition, we redefine the angular coordinates as

$$(\phi, \psi) \longmapsto \sqrt{1+\nu^2}(\phi, \psi), \tag{5.29}$$

in order to recover a periodicity of 2π and consequently a more standard behaviour of the angular coordinates. It is also convenient to redefine the ring radius as

$$R \longmapsto \sqrt{1+\nu^2}R. \tag{5.30}$$

Renaming then the parameter ν into λ, and adding an extra-direction l, the BRS metric can be written as

$$\begin{aligned} ds^2 = &-\frac{H(y)}{H(x)}\left(dt+\Omega_\psi d\psi\right)^2 + dl^2 + \\ &+\frac{R^2 H(x)}{(x-y)^2}\left[\frac{G(x)}{H(x)}d\phi^2 + \frac{dx^2}{G(x)} - \frac{G(y)}{H(y)}d\psi^2 - \frac{dy^2}{G(y)}\right], \end{aligned} \tag{5.31}$$

where we set

$$\begin{aligned} &H(x) = 1+2\lambda x+\lambda^2, \qquad G(x) = (1-x^2)(1+\lambda), \\ &\Omega_\psi = -CR\frac{1+y}{H(y)}, \qquad \text{with} \quad C = \lambda(1+\lambda)\sqrt{2\frac{1+\lambda}{1-\lambda}}. \end{aligned} \tag{5.32}$$

Performing then a generic boost along the worldvolume directions, the boosted metric has form

$$\begin{aligned} ds^2 = &\left[\eta_{ab} + \left(1-\frac{H(y)}{H(x)}\right)\right]d\sigma^a d\sigma^b - 2CR\frac{1+y}{H(x)}u_a d\sigma^a d\psi - \\ &-\frac{R^2}{H(x)H(y)}\left[C^2(1+y)^2 + \frac{H(x)^2 G(y)}{(x-y)^2}\right]d\psi^2 + \\ &+\frac{R^2 H(x)}{(x-y)^2}\left[\frac{G(x)}{H(x)}d\phi^2 + \frac{dx^2}{G(x)} - \frac{dy^2}{G(y)}\right]. \end{aligned} \tag{5.33}$$

We can now perform a change of coordinates in order to make the metric explicitly asymptotically flat. Following [39], we reparametrize (x, y) as

$$\begin{aligned} x &= -1 + \frac{2R^2}{\rho^2}(1-\lambda)\cos^2\theta, \\ y &= -1 - \frac{2R^2}{\rho^2}(1-\lambda)\sin^2\theta, \end{aligned} \tag{5.34}$$

with new domains $R\sqrt{1-\lambda} \leq \rho < \infty$ and $0 \leq \theta \leq \pi$. From this explicit transformation, it is easy to see that Minkowski in spherical coordinates

$$ds^2 \approx -dt^2 + d\rho^2 + \rho^2(d\theta^2 + \cos^2\theta d\phi^2 + \sin^2\theta d\psi^2, \tag{5.35}$$

is recovered at the leading order in $1/\rho$, as desired. Instead, if we expand up to order $\frac{1}{\rho^2}$, we find

$$\begin{aligned} ds^2 \approx & \left(\eta_{ab} + \frac{4R^2\lambda}{(1-\lambda)\rho^2}u_a u_b\right) d\sigma^a d\sigma^b + 2\frac{2\sqrt{2}R^3}{\rho^2}\lambda\left(\frac{1+\lambda}{1-\lambda}\right)^{\frac{3}{2}}\sin^2\theta\, u_a d\sigma^a d\psi + \\ & + \left(1 + \frac{R^2}{\rho^2}\frac{2\lambda + (1-2\lambda+3\lambda^2)\cos(2\theta)}{1-\lambda}\right) d\rho^2 + \\ & + 2\frac{R^2}{\rho}(1-3\lambda)\sin\theta\cos\theta d\rho d\theta + \rho^2\left(1 + \frac{4R^2\lambda}{(1-\lambda)\rho^2}\cos^2\theta\right) d\theta^2 \\ & + \rho^2\cos^2\theta\left(1 - \frac{R^2}{\rho^2}(1-3\lambda)\cos^2\theta\right) d\phi^2 + \\ & + \rho^2\sin^2\theta\left(1 + \frac{R^2}{\rho^2}\frac{4\lambda\cos^2\theta + (1+3\lambda^2)\sin^2\theta}{(1-\lambda)}\right) d\psi^2, \end{aligned} \tag{5.36}$$

which can be recast in the more compact form

$$\begin{aligned} ds^2 \approx & \left(\eta_{ab} + \frac{\mu}{\rho^2}u_a u_b\right) d\sigma^a d\sigma^b + 2\frac{J_a}{\rho^2}\sin^2\theta\, d\sigma^a d\psi + \\ & + \left(1 + \frac{\mu}{\rho^2}\cos^2\theta + \frac{R^2}{\rho^2}D(\mu)\cos(2\theta)\right) d\rho^2 + 2\frac{R^2}{\rho}D(\mu)\sin\theta\cos\theta d\rho d\theta + \\ & + \rho^2\left(1 + \frac{\mu}{\rho^2}\cos^2\theta\right) d\theta^2 + \rho^2\cos^2\theta\left(1 - \frac{R^2}{\rho^2}D(\mu)\cos^2\theta\right) d\phi^2 + \\ & + \rho^2\sin^2\theta\left(1 + \frac{\mu}{\rho^2} + \frac{R^2}{\rho^2}D(\mu)\sin^2\theta\right) d\psi^2, \end{aligned} \tag{5.37}$$

once we define the mass parameter μ, $D(\mu)$ and the angular momentum current as

$$\mu = \frac{8}{3\pi}M_{ADM} = \frac{4R^2\lambda}{1-\lambda} \quad \longleftrightarrow \quad \lambda = \frac{\mu}{4R^2+\mu},$$

$$D(\mu) = 1 - 3\lambda(\mu) = \frac{3\mu}{4R^2 + \mu}, \tag{5.38}$$

$$J^a = \frac{4}{\pi} J_{ADM} u^a = 2\sqrt{2} R^3 \lambda \left(\frac{1+\lambda}{1-\lambda}\right)^{\frac{3}{2}} u^a = \frac{\mu}{4R^2+\mu}(2R^2+\mu)^{3/2} u^a.$$

It is worth studying in more detail the weak-gravity limit of this metric. Introducing Φ as the asymptotic (Newtonian) potential, from the g_{00} component of (5.33) it follows that

$$\frac{H(y)}{H(x)} \approx 1 - 2\Phi, \tag{5.39}$$

and consequently

$$\Phi \approx -\frac{2R^2(1-\lambda)}{\rho^2(1-\lambda)^2 + 4\lambda R^2(1-\lambda)\cos^2\theta}. \tag{5.40}$$

But we are dealing with large ρ, and then we can neglect the second term in the denominator, obtaining a purely Newtonian behaviour of the effective gravitational potential[2]

$$\Phi \approx -\frac{\mu}{2\rho^2}, \tag{5.41}$$

where the remaining black ring physics is included in the effective Newtonian mass μ defined in (5.38). Therefore, we can be confident that an observer placed at spatial infinity would simply measure a spherically symmetric gravitational field. As discussed above, this hints at the possibility of finding the extrinsic equations in a way similar to the ones followed in the previous sections.

We can now perform the calculation of the Brown-York stress tensor; once integrated over the transverse sphere parametrized by (θ, ϕ, ψ), it can be recast in the usual perfect fluid form

$$T_{ab} = \int_{S^3} d\theta d\phi d\psi \, \sqrt{g_{\theta\theta} g_{\phi\phi} g_{\psi\psi}} \, T^{(BY)}_{ab} = \frac{\Omega_{(3)}}{16\pi G} \mu \, (2u_a u_b - \eta_{ab}), \tag{5.42}$$

which coincides with the known Schwarzschild result taking $n = 2$. Rescaling the stress tensor as in (5.24) for convenience, we get exactly the Camps-Emparan form in the worldvolume sector of the metric:

$$\begin{aligned} ds^2 = & \left[\eta_{ab} + \frac{1}{\rho^2}\left(T_{ab} - \frac{T}{4}\eta_{ab}\right)\right] d\sigma^a d\sigma^b + 2\frac{J_a}{\rho^2}\sin^2\theta \, d\sigma^a d\psi + \\ & + \left(1 - \frac{T}{2\rho^2}\cos^2\theta + \frac{R^2}{\rho^2} D(T)\cos(2\theta)\right) d\rho^2 + 2\frac{R^2}{\rho} D(T)\sin\theta\cos\theta d\rho d\theta + \\ & + \rho^2\left(1 - \frac{T}{2\rho^2}\cos^2\theta\right) d\theta^2 + \rho^2\cos^2\theta\left(1 - \frac{R^2}{\rho^2} D(T)\cos^2\theta\right) d\phi^2 + \\ & + \rho^2\sin^2\theta\left(1 - \frac{T}{2\rho^2} + \frac{R^2}{\rho^2} D(T)\sin^2\theta\right) d\psi^2, \end{aligned} \tag{5.43}$$

[2]We recall that with $D = 5$ transverse directions the Newtonian potential has power law $\sim \frac{1}{r^2}$.

where

$$D(T) = \frac{3T}{T - 8R^2}. \tag{5.44}$$

Now we want to investigate the possibility of recasting the whole angular part of this metric into a manifest spherically symmetric form, as done before. Here the starting metric did not show spherically symmetry at all, but, as we suggested above, the asymptotic expansion may have smoothed the S^1 dipolar contributions to the metric.

We consider an Ansatz for the new coordinates (r, χ) of the form

$$\theta = \chi + f(\chi)\frac{R^2}{r^2} + g(\chi)\frac{T}{r^2}, \tag{5.45}$$

$$\rho = r + h(\chi)\frac{R^2}{r} + l(\chi)\frac{T}{r}, \tag{5.46}$$

and we impose this change of coordinates to cancel out the deviations from sphericity due to both the mass and the transverse angular momentum scale R. By solving the related system of PDEs up to $\frac{1}{r^2}$, one obtains

$$\theta = \chi - \frac{\sin(2\chi)}{4r^2}\left(R^2 - \frac{T}{8}\right), \tag{5.47}$$

$$\rho = r + \frac{1}{2r}\left(R^2\cos(2\chi) + \frac{T}{8}\left(2\cos^2\chi + 1\right)\right). \tag{5.48}$$

Up to $\frac{1}{r^2}$ orders, the metric reads then

$$\begin{aligned} ds^2 = &\left[\eta_{ab} + \frac{1}{r^2}\left(T_{ab} - \frac{T}{4}\eta_{ab}\right)\right] d\sigma^a d\sigma^b + 2\frac{J_a}{r^2}\sin^2\chi d\sigma^a d\psi + \\ &+ \left(1 - \frac{T}{2r^2}\right) dr^2 + r^2 d\chi^2 + r^2\cos^2\chi d\phi^2 + r^2\sin^2\chi d\psi^2, \end{aligned} \tag{5.49}$$

which manifestly exhibits spherical symmetry.

Since we are analysing a singly-spinning transverse spacetime, we do not have a non-vanishing mixing component $g_{\phi\psi}$. As noticed in Section 5.2, it becomes now straightforward to obtain explicitly the corresponding blackfold extrinsic equations.

As shown in Appendix B, it is also possible to find the extrinsic equations explicitly for a BRBS by following a perturbative procedure. In fact, we know that the change of coordinates (2.25) and (2.26) lead to an asymptotically flat form of a singly-spinning black ring metric as well. In particular, we studied in Section 2.3 how to recover a black brane (with boost fixed by the balancing condition) by performing the ultra-spinning limit, which coincides with taking the angular momentum of the considered solution to be ideally infinite. We have already analysed how to obtain the extrinsic equations

for such a class of solutions, but one can inspect lower and lower angular momenta by expanding the black ring metric order by order in powers of $\frac{r_0}{R}$. This allows to find the extrinsic equations perturbatively up to some $O\left(\frac{r_0^j}{R^j}\right)$. Even if apparently this procedure is closer to the spirit of the original blackfold discussion, of course it gets quickly rather involved. The main issue resides in the assumption *a priori* of the explicit form of the contributions $h_{\mu\nu}$. The detailed procedure at first order in $\frac{r_0}{R}$ can be found in Appendix B, but we believe that further discussions concerning the matching with the generic angular momenta results of this section are required in order to eliminate the remaining ambiguities.

Chapter 6

New Solutions and Stability

Thanks to the results of Chapter 5, we are guaranteed that the blackfold approach can be generalized to configurations with transverse spins[1]. Since MP black holes are characterized by a spherical topology, we propose here to inspect more deeply *black ring blackfolds* instead, starting from black ring branes (BRBs) and using the results from Section 5.3.

In this chapter, we present the general setup for BRBs by considering the local thermodynamics associated to their effective theory, then we build new solutions. The configurations obtained in Section 6.2 do match with the corresponding solutions with same horizon topology previously found with the original Schwarzschild blackfold approach. On the other hand, the black ring p-balls of Section 6.3 are endowed with completely new features and horizon topology. After analysing their phase diagrams, we deal with the black ring branes stability.

Finally, we study the effective theory related to 5D singly-spinning MP black branes and their stability.

6.1 Black ring branes local thermodynamics

From the known black ring thermodynamics discussed in Section 2.3, we can obtain the leading order local thermodynamics for black ring p-branes. Parametrizing the black ring mass as in Section 5.3

$$M = \frac{3\pi}{8}\mu, \tag{6.1}$$

the local temperature reads

$$\mathcal{T} = \frac{R}{\sqrt{2}\pi\mu}. \tag{6.2}$$

[1] We will discuss elsewhere how to obtain the set of intrinsic equations for these configurations.

Following then [34] and accordingly to the discussion in Section B, we also define the horizon scale as

$$r_0 = \frac{1}{4\sqrt{2}\pi\mathcal{T}} = \frac{\mu}{4R}, \qquad \text{i.e} \qquad \mu = 4\, r_0 R. \tag{6.3}$$

We intend now to recast the parameters of our solutions R and μ in terms of the local independent thermodynamic variables $\mathcal{T}$ and ω, with

$$\omega = \frac{1}{\sqrt{2R^2+\mu}}. \tag{6.4}$$

From equations (6.2) and (6.4), we obtain

$$\mu(\omega,\mathcal{T}) = \frac{\sqrt{\omega^2+16\pi^2\mathcal{T}^2}-\omega}{8\pi^2\omega\mathcal{T}^2}, \tag{6.5}$$

$$R(\omega,\mathcal{T}) = \frac{\sqrt{\omega^2+16\pi^2\mathcal{T}^2}-\omega}{4\sqrt{2}\pi\omega\mathcal{T}}. \tag{6.6}$$

Defining then a global temperature $T = \mathrm{k}\,\mathcal{T}$ and a global transverse angular velocity $\Omega = \mathrm{k}\,\omega$, we can straightforwardly rewrite them as

$$\mu(\Omega,T) = \frac{\sqrt{\Omega^2+16\pi^2T^2}-\Omega}{8\pi^2\Omega T^2}\,\mathrm{k}^2, \tag{6.7}$$

$$R(\Omega,T) = \frac{\sqrt{\Omega^2+16\pi^2T^2}-\Omega}{4\sqrt{2}\pi\Omega T}\,\mathrm{k}^2. \tag{6.8}$$

It means in turn that the pressure can be expressed as

$$P = -\frac{\Omega_{(3)}}{16\pi G}\,\mu = -\frac{\sqrt{\Omega^2+16\pi^2T^2}-\Omega}{64\pi G\,\Omega\,T^2}\,\mathrm{k}^2. \tag{6.9}$$

Analogously, the transverse ADM angular momentum can be rewritten as

$$\mathcal{J} = \frac{\pi}{4}\frac{\mu(\omega,\mathcal{T})}{4R^2+\mu(\omega,\mathcal{T})}(2R^2+\mu(\omega,\mathcal{T}))^{3/2} = \frac{\pi}{4}\frac{\mathrm{k}^3}{\Omega^2\sqrt{\Omega^2+16\pi^2T^2}}. \tag{6.10}$$

Finally, we write the explicit form of the local entropy via the horizon area:

$$s = \frac{A_H}{4G} = \frac{\pi^2 R\mu^2}{\sqrt{2}G(4R^2+\mu)} = \frac{\Omega^2+8\pi^2T^2-\Omega\sqrt{\Omega^2+16\pi^2T^2}}{32\pi\Omega T^3\sqrt{\Omega^2+16\pi^2T^2}}\,\mathrm{k}^3. \tag{6.11}$$

For later convenience, we also define

$$\tilde{f}(\Omega,T) = \frac{\sqrt{16\pi^2T^2+\Omega^2}-\Omega}{64\pi GT^2\Omega}. \tag{6.12}$$

Finally, by integrating the related conserved currents as done for Schwarzschild black branes in Section 3.5, we can give a general expression for the mass and the worldvolume angular momenta of a configuration described by a Killing vector $\mathbf{k}$ with modulus

$$\mathrm{k} = R_0(\sigma)\sqrt{1 - V^2(\sigma)} \tag{6.13}$$

as

$$M = \tilde{f}(\Omega, T) \int_{\mathcal{B}_p} dV_{(p)} R_0(\sigma) \left[R_0(\sigma)^2(1 - V^2) + 2\right], \tag{6.14}$$

$$J_i = 2\Omega_i \tilde{f}(\Omega, T) \int_{\mathcal{B}_p} dV_{(p)} R_0(\sigma) R_i^2(\sigma), \tag{6.15}$$

while the transverse momentum and the entropy read

$$J = \frac{\pi}{4\Omega^2\sqrt{\Omega^2 + 16\pi^2 T^2}} \int_{\mathcal{B}_p} dV_{(p)} R_0^3(\sigma)(1 - V^2), \tag{6.16}$$

$$S = \frac{\Omega^2 + 8\pi^2 T^2 - \Omega\sqrt{\Omega^2 + 16\pi^2 T^2}}{32\pi\Omega T^3\sqrt{\Omega^2 + 16\pi^2 T^2}} \int_{\mathcal{B}_p} dV_{(p)} R_0^3(\sigma)(1 - V^2). \tag{6.17}$$

Ultraspinning regime

The reduced angular momentum squared for a black ring is

$$j^2 = \frac{(2R^2 + \mu)^3}{\mu(4R^2 + \mu)^2}, \tag{6.18}$$

and it is large if $\mu \ll R^2$, which effectively corresponds to the thin black ring limit, as well known from the phase diagram analysis in Figure 2.3.

We could also decide to write j^2 in terms of the global temperature and transverse angular velocity; for j^2 large, it can be shown that

$$j^2 \approx \frac{T}{\Omega}, \tag{6.19}$$

while the reduced horizon area has behaviour

$$a_H \approx \sqrt{\frac{\Omega}{T}}. \tag{6.20}$$

From the previous results, the asymptotic values of the thermodynamic observables in the sector where $\mu \ll R^2$ holds result in

$$\mathcal{J} \approx \frac{\pi}{\sqrt{2}} r_0 R^2, \tag{6.21}$$

$$\omega \approx \frac{1}{\sqrt{2}R}, \tag{6.22}$$

$$s \approx 2\sqrt{2}\pi^2 r_0^2 R. \tag{6.23}$$

We can now compare these quantities with the corresponding ones displayed in Section 3.7.1, in order to check again the claim that the blackfold approach reproduces the correct dynamics in the ultraspinning regime. A quick inspection shows that they match perfectly.

In general, we notice also that a very high angular momentum cannot translate into a high angular velocity simply because we are treating them as conjugated thermodynamic variables. Equations (6.21) and (6.22) explain this counterintuitive behaviour of the reduced angular momentum in (6.19) in the ultraspinning limit $R^2 \gg \mu$, since while $\mathcal{J}$ increases with R^2, the angular velocity is actually inversely proportional to R.

6.2 Black ring rings

We consider now a compact extra-dimension with topology S^1, that we think of as embedded in a generic worldvolume with constant redshift factor R_0. We endow it with an angular velocity by choosing a Killing vector $\mathbf{k}$ with modulus

$$\mathrm{k} = \sqrt{R_0^2 - R_W^2 \Omega_W^2}\,. \tag{6.24}$$

In Section 6.1 we obtained that

$$P \;=\; -\tilde{f}(\Omega, T)\left(R_0^2 - R_W^2 \Omega_W^2\right), \tag{6.25}$$

which means that in this case the effective action has form

$$I[X^\mu] = -\int_{\mathcal{B}_p} dV_{(p)}\; R_0 P = 2\pi R_0 R_W \left(R_0^2 - R_W^2 \Omega_W^2\right) \tilde{f}(\Omega, T), \tag{6.26}$$

after performing the integration over the spatial slices of the worldsheet. The equilibrium condition then follows from

$$\frac{\delta I}{\delta R_W} = 0 \qquad \Longleftrightarrow \qquad R_W = \frac{R_0}{\sqrt{3}\Omega_W}. \tag{6.27}$$

Imposing it, we find the on-shell effective action

$$I_{OS} = \frac{R_0^4}{48\sqrt{3} G \Omega_W} \frac{\sqrt{\Omega^2 + 16\pi^2 T^2} - \Omega}{\Omega T^2}. \tag{6.28}$$

Interpreting it as a free energy and considering also the ultraspinning regime, the global entropy is

$$\begin{aligned} S =& -\left.\frac{\partial F}{\partial T}\right|_{\Omega_W, \Omega} = \frac{R_0^4}{24\sqrt{3} G \Omega_W} \frac{\Omega^2 + 8\pi^2 T^2 - \Omega\sqrt{\Omega^2 + 16\pi^2 T^2}}{\Omega T^3 \sqrt{\Omega^2 + 16\pi^2 T^2}} \\ \approx& \frac{\pi R_0^4}{12\sqrt{3} G \Omega_W \Omega T^2}, \end{aligned} \tag{6.29}$$

while the worldvolume angular momentum reads

$$\begin{aligned} J_W = & -\left.\frac{\partial F}{\partial \Omega_W}\right|_{T,\Omega} = \frac{R_0^4}{48\sqrt{3}G\Omega_W^2}\frac{\sqrt{\Omega^2+16\pi^2T^2}-\Omega}{\Omega T^2} \\ & \approx \frac{\pi}{12\sqrt{3}G}\frac{R_0^4}{\Omega_W^2\Omega T}, \end{aligned} \tag{6.30}$$

and analogously the transverse momentum is

$$\begin{aligned} J = & -\left.\frac{\partial F}{\partial \Omega}\right|_{T,\Omega_W} = \frac{\pi^2}{3\sqrt{3}G}\frac{R_0^4}{\Omega_W\Omega^2\sqrt{\Omega^2+16\pi^2T^2}} \\ & \approx \frac{\pi}{12\sqrt{3}G}\frac{R_0^4}{\Omega_W\Omega^2 T}. \end{aligned} \tag{6.31}$$

Of course, the very same results are obtained by proceeding with the integration of the local conserved currents from equations (6.15), (6.16) and (6.17), while the mass results in

$$M = \frac{R_0^4}{4\sqrt{3}G}\frac{\sqrt{\Omega^2+16\pi^2T^2}-\Omega}{\Omega_W\Omega T^2} \approx \frac{\pi}{\sqrt{3}G}\frac{R_0^4}{\Omega_W\Omega T}. \tag{6.32}$$

It is interesting to notice that these quantities in the US limit match the corresponding ones of a Schwarzschild 2-Torus that one can compute with the usual blackfold formalism [34]. In fact, the horizon geometry of our solution consists in the transverse $s^2 \times s^1$ (coming from the black ring initial structure) fibered over S^1, where S^1 must be thought of as endowed with a very high spin. Instead, with the usual blackfold formalism we obtain a transverse s^2 fibered over $S^1 \times S^1 = \mathbb{T}^2$, in such a way that we have an overall topology $s^2 \times \mathbb{T}^2$ in both cases. Nonetheless, with our procedure we are inspecting a wider range of configurations with that same topology, since effectively we are extracting one S^1 from the worldvolume sector and hence we can access finite spins along that direction.

Let us now analyse the phase diagram of this class of solutions within Minkowski backgrounds, where $R_0 = 1$. Following the definitions (2.1), we start by defining the reduced horizon area a_H, the transverse angular momentum j and the worldvolume angular momentum j_W. Parametrizing these quantity in terms of the reduced temperature and of the angular momenta ratio

$$\tau = \frac{T}{\Omega}, \qquad \omega = \frac{\Omega}{\Omega_W}, \tag{6.33}$$

they can be written as

$$a_H^3 = \frac{\sqrt{2}}{3^4\,\pi}\frac{1+8\pi^2\tau^2-\sqrt{1+16\pi^2\tau^2}}{\tau\omega\left(1+16\pi^2\tau^2\right)^{3/2}}, \tag{6.34}$$

$$j^3 = \frac{2^{10}\pi^8}{3^4}\frac{\tau^8}{\omega\left(1+16\pi^2\tau^2\right)^{3/2}\left(\sqrt{1+16\pi^2\tau^2}\right)^4-1}, \tag{6.35}$$

$$j_W^3 = \frac{\omega^2}{2^6\,3^4}\left(1+\sqrt{1+16\pi^2\tau^2}\right). \tag{6.36}$$

The range of validity of the effective theory tells us the interval of the parameters τ and ω where we can trust our results. We know that any transverse scale is required to be much smaller than the typical worldvolume length scale, which is determined here by $R_W = \frac{1}{\sqrt{3}\Omega_W}$. We find then

$$r_0 \ll R_W \qquad \Longleftrightarrow \qquad \tau \gg \tau_0 = \frac{\sqrt{3}}{4\sqrt{2}\pi\omega}, \tag{6.37}$$

$$R \ll R_W \qquad \Longleftrightarrow \qquad \omega \gg 1, \tag{6.38}$$

meaning that we are describing configurations which are hot enough and rotating much faster along the transverse s^1, as expected[2].

It is interesting to compare this regime of validity with the one related to the observables from the original blackfold formalism in [34]. In this case, the reduced horizon area and angular momenta can be evaluated as

$$a_H^3 = \frac{1}{324\sqrt{2}\pi^2}\frac{1}{\widetilde{\tau}^2\,\widetilde{\omega}}, \tag{6.39}$$

$$j_1^3 = \frac{\pi\,\widetilde{\tau}}{1296\,\widetilde{\omega}}, \tag{6.40}$$

$$j_2^3 = \frac{\pi\,\widetilde{\tau}\,\widetilde{\omega}^2}{1296}, \tag{6.41}$$

where we defined

$$\widetilde{\tau} = \frac{T}{\Omega_1}, \qquad \widetilde{\omega} = \frac{\Omega_1}{\Omega_2}. \tag{6.42}$$

This time the interval of validity is determined by the conditions

$$r_0 \ll R_1 \qquad \Longleftrightarrow \qquad \widetilde{\tau} \gg \widetilde{\tau}_1 = \frac{\sqrt{3}}{4\pi}, \tag{6.43}$$

$$r_0 \ll R_2 \qquad \Longleftrightarrow \qquad \widetilde{\tau} \gg \widetilde{\tau}_2 = \frac{\sqrt{3}}{4\pi\omega}, \tag{6.44}$$

In Figures 6.1 and 6.2 in black we plot the reduced area as a function of the transverse and worldvolume angular momenta respectively for different values of ω. On the other hand, the solid blue lines correspond to the plots from the original blackfold approach.

[2]We recall that higher angular velocities correspond to lower angular momenta.

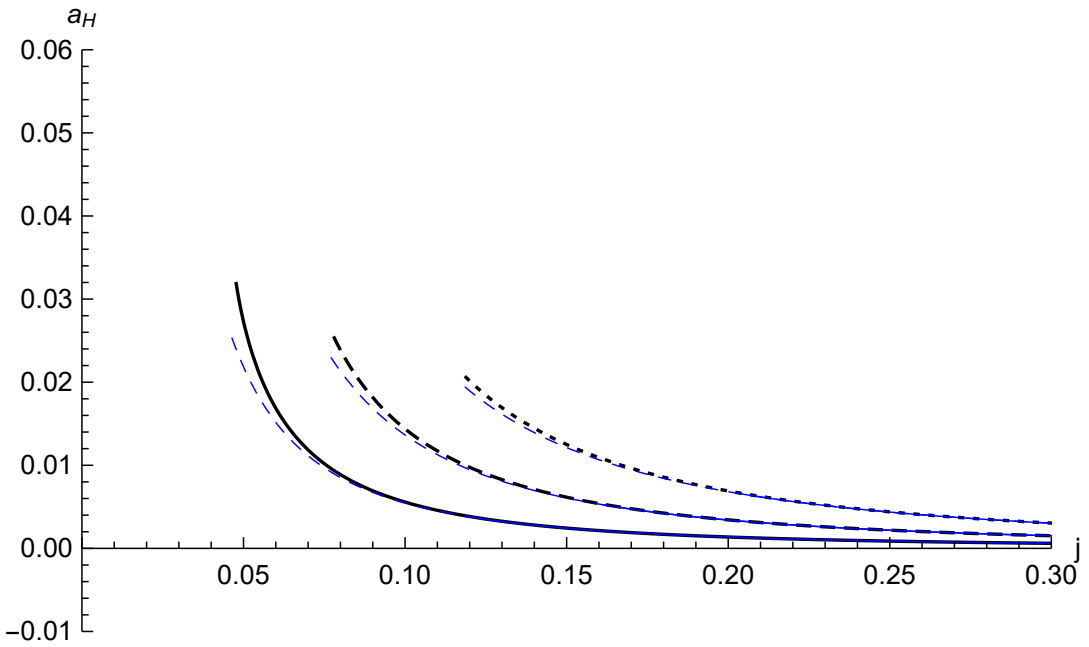

Figure 6.1: We display here the phase diagram $a_H(j)$ of black ring rings for $\omega = 4, 8, 20$ with the black dotted, dashed and solid line, respectively. As a comparison, in blue we depict the corresponding phase diagrams obtained from the original blackfold approach [34].We plot the phase curves in their regime of validity for values $\tau > 100\tau_0$ and $\widetilde{\tau} > 100\widetilde{\tau}_1$. The dashed blue lines represent the Schwarzschild blackfold phase diagrams outside their proper regime of validity, with $\widetilde{\tau} \gtrsim 10\widetilde{\tau}_1$.

From the considerations above, it follows that more accurate plots are found for higher ratios ω and $\widetilde{\omega}$. In order to implement the conditions $\tau \gg \tau_0$ and $\widetilde{\tau} \gg \widetilde{\tau}_0$, the quantities are plotted only for $\tau > 100\tau_0$, $\widetilde{\tau} > 100\widetilde{\tau}_1$ and $\widetilde{\tau} > 100\widetilde{\tau}_2$. We see that actually these conditions restrict the validity of our approach to configurations with high worldvolume angular momentum $j_W \gtrsim 1$, in the same fashion as for Schwarzschild blackfolds. On the other hand, we observe that we can access much lower transverse angular momenta with $j \gtrsim 0.05$ than before, thanks to our black ring effective theory.

In connection with this, the dashed blue curves show the behaviour of the phase diagrams from the original blackfold approach, once we consider them outside their proper regime of validity, that is for very low angular momenta j (we are plotting $\widetilde{\tau} \gtrsim 10\widetilde{\tau}_1$ and $\widetilde{\tau} \gtrsim 10\widetilde{\tau}_2$). We observe that there is no significant improvement as far as it concerns the phase diagrams of j_W. On the other hand, as one can see in Figure 6.1, the original blackfold approach appears to differ significantly from ours for lower reduced angular momenta j.

On more general grounds, one can also admit a dependence of R_0 on R_W, as it

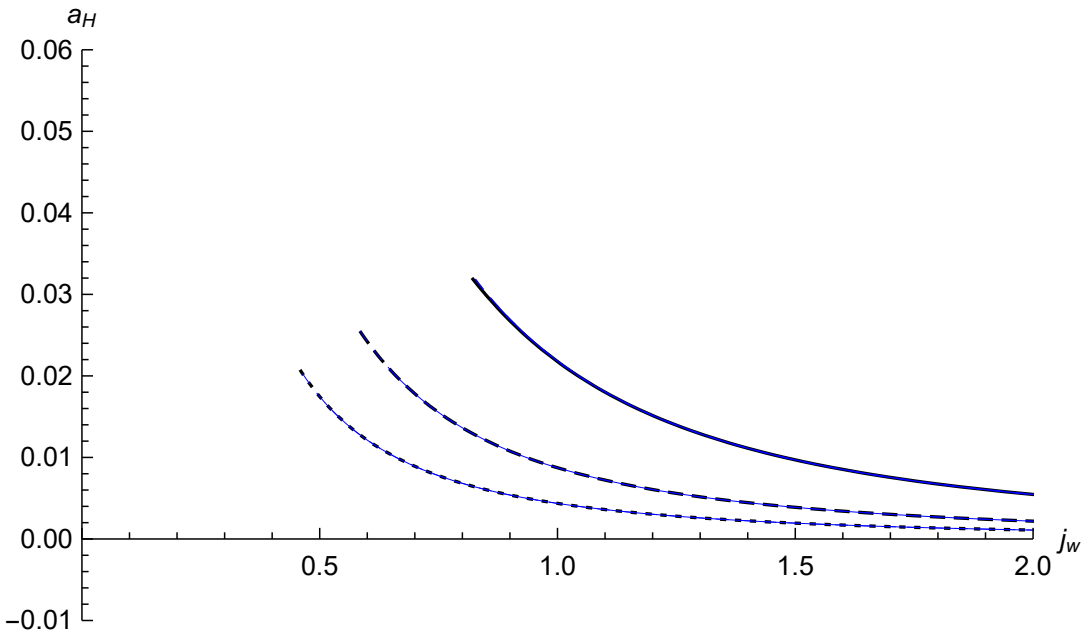

Figure 6.2: We present here the phase diagram $a_H(j_W)$ of black ring rings for $\omega = 4, 8, 20$ with the black dotted, dashed and solid line, respectively. As a comparison, in blue we depict the corresponding phase diagrams obtained from the original blackfold approach [34]. We plot the phase curves in their regime of validity for values $\tau > 100\tau_0$ and $\widetilde{\tau} > 100\widetilde{\tau}_2$. The dashed blue lines represent the Schwarzschild blackfold phase diagrams outside their proper regime of validity, with $\widetilde{\tau} \gtrsim 10\widetilde{\tau}_2$.

happens in the case of non trivial background spacetimes. Here

$$\mathrm{k} = \sqrt{R_0^2(R_W) - R_W^2\Omega_W^2}, \tag{6.45}$$

and hence the balancing condition reads

$$\frac{\delta I}{\delta R_W} + \frac{dR_0}{dR_W}\frac{\delta I}{\delta R_0} = 0. \tag{6.46}$$

In turn, it leads to

$$\Omega_W^2 = \frac{R_0^2}{R_W^2}\frac{3R_0'R_W + R_0}{R_0'R_W + 3R_0}, \tag{6.47}$$

which matches with (6.27). We notice that R_0 is in terms of R_W, in such a way that this equation gives Ω_W uniquely as a function of R_W, as before. For formal convenience, we consider R_W as the independent variable, leaving Ω_W implicit.

After imposing the balancing condition, the free energy (6.26) becomes

$$F = R_W R_0^3 \frac{R_0' R_W - R_0}{R_0' R_W + 3R_0} \frac{\Omega - \sqrt{16\pi^2 T^2 + \Omega^2}}{16 T^2 \Omega}, \tag{6.48}$$

from which we can obtain the entropy

$$S = -\left.\frac{\partial F}{\partial T}\right|_{R_W,\Omega} = R_W R_0^3 \frac{R_0 - R_0' R_W}{R_0' R_W + 3R_0} \frac{8\pi^2 T^2 + \Omega\left(\Omega - \sqrt{16\pi^2 T^2 + \Omega^2}\right)}{8 T^3 \Omega \sqrt{16\pi^2 T^2 + \Omega^2}}, \tag{6.49}$$

as well as the transverse angular momentum

$$J = -\left.\frac{\partial F}{\partial \Omega}\right|_{T,R_W} = R_W R_0^3 \frac{R_0 - R_0' R_W}{R_0' R_W + 3R_0} \frac{\pi^2}{\Omega \sqrt{16\pi^2 T^2 + \Omega^2}}. \tag{6.50}$$

We can finally turn to the worldvolume angular momentum

$$J_W = -\left.\frac{\partial F}{\partial \Omega_W}\right|_{T,\Omega} = -\left(\frac{d\Omega_W}{dR_W}\right)^{-1} \left.\frac{\partial F}{\partial R_W}\right|_{T,\Omega}. \tag{6.51}$$

Using the balancing condition, we find

$$J_W = R_W^2 R_0^2 \sqrt{\frac{3R_0' R_W + R_0}{R_0' R_W + 3R_0}} \frac{\sqrt{16\pi^2 T^2 + \Omega^2} - \Omega}{16 T^2 \Omega}. \tag{6.52}$$

One can check that these quantities all match with the previous ones, once $R_0(R_W)$ is set to a constant.

6.3 Black ring discs and p-balls

We intend now to build a $D = 7$ solution with discs as worldvolume spatial sections and discuss its thermodynamics. We start by choosing the following embedding into a flat background

$$\begin{gathered} X^0 = t, \\ X^1(\rho,\chi) = \rho\cos\chi, \qquad X^2(\rho,\chi) = \rho\sin\chi, \\ X^i = 0 \qquad \text{for each } i = 3\ldots 6, \end{gathered} \tag{6.53}$$

with $\rho \geq 0$ and $0 \leq \phi \leq 2\pi$, in a way analogous to (3.148). Consequently, the induced metric reads

$$ds^2 = -d\tau^2 + d\rho^2 + \rho^2 d\chi^2. \tag{6.54}$$

We introduce now a rotation on the worldvolume, by imposing the existence of a Killing vector

$$\mathbf{k} = \partial_t + \Omega_W \partial_\chi, \qquad \text{with} \quad \mathrm{k} = \sqrt{1 - \Omega_W^2 \rho^2}\,, \tag{6.55}$$

where we are considering only flat backgrounds. It means that we have a boundary surface on each worldvolume spatial section, determined by the maximum radius

$$\rho_+ = \frac{1}{\Omega_W}, \tag{6.56}$$

leading in turn to a spatial horizon geometry $S^2 \times S^1 \times \mathbb{D}^2$. From the local BRB thermodynamics discussed above, we find the horizon radius

$$r_0 = \frac{1}{4\sqrt{2\pi T}}\,\mathrm{k} = \frac{1}{4\sqrt{2\pi T}}\,\sqrt{1 - \Omega_W^2 \rho^2}\,, \tag{6.57}$$

which decreases down to zero at the boundary $\rho \to \rho_+$. As well as for Schwarzschild black discs, we must require

$$r_0 \;\ll\; \frac{1}{\Omega_W}\,\frac{1 - \Omega_W^2 \rho^2}{\sqrt{2 - \Omega_W^2 \rho^2}} \tag{6.58}$$

in order to ensure the validity of our procedure. This condition does not hold true for any temperature T near the limiting surface, and it means that we have to introduce again a small length parameter ϵ and to assume to be working within the radial interval $0 \leq \rho \leq \rho_+ - \epsilon$.

We propose to study the thermodynamics of this class of solutions. Rewriting the pressure (6.9) as

$$P = -\tilde{f}(\Omega, T)\left(1 - \Omega_W^2 \rho^2\right), \tag{6.59}$$

with

$$\tilde{f}(\Omega, T) \;=\; \frac{\sqrt{\omega^2 + 16\pi^2 \mathcal{T}^2} - \omega}{64\pi G\, \omega\, \mathcal{T}^2} = \frac{\sqrt{\Omega^2 + 16\pi^2 T^2} - \Omega}{64\pi G\, \Omega\, T^2}, \tag{6.60}$$

the free energy results in

$$\begin{aligned} F \;&=\; -\int_{\mathcal{B}_2} dV_2 P \;=\; 2\pi \tilde{f}(\Omega, T) \int_0^{\rho_+ - \epsilon} d\rho \rho \left(1 - \Omega_W^2 \rho^2\right) \;= \\ &= \frac{\pi}{2} \tilde{f}(\Omega, T) \left[\frac{1}{\Omega_W^2} - \frac{\epsilon^2}{4}\left(\epsilon \Omega_W - 2\right)^2\right] \;=\; \frac{\pi}{2} \tilde{f}(\Omega, T) \left[\frac{1}{\Omega_W^2} + O(\epsilon^2)\right], \end{aligned} \tag{6.61}$$

and it admit a finite limit for $\epsilon \to 0$. By deriving F in the suitable conjugated variables as usual, we obtain the thermodynamic observables

$$J = -\left.\frac{\partial F}{\partial \Omega}\right|_{T, \Omega_W} = \frac{\pi^2}{8G} \frac{1}{\Omega_W^2 \Omega^2 \sqrt{16\pi^2 T^2 + \Omega^2}}, \tag{6.62}$$

$$J_W = -\left.\frac{\partial F}{\partial \Omega_W}\right|_{T,\Omega} = \frac{\sqrt{16\pi^2 T^2+\Omega^2}-\Omega}{64 G \Omega_W^3 \Omega T^2}, \tag{6.63}$$

$$S = -\left.\frac{\partial F}{\partial T}\right|_{\Omega_W,\Omega} = \frac{8\pi^2 T^2+\Omega\left(\Omega-\sqrt{16\pi^2 T^2+\Omega^2}\right)}{64 G \Omega_W^2 \Omega T^3 \sqrt{16\pi^2 T^2+\Omega^2}}. \tag{6.64}$$

One can check these results by integrating the conserved currents as well. Following (6.14), we find also the global mass of this solution, with form

$$M \,=\, \int_{\mathcal{B}_2} dV_{(2)}\, T_{\mu\nu} n^\mu \xi^\nu \,=\, 2\pi \int_0^{\rho_+ - \epsilon} d\rho\, \rho\, T_{00} \,=\, \frac{5}{128 G}\frac{\sqrt{16\pi^2 T^2+\Omega^2}-\Omega}{\Omega_W^2 \Omega T^2}, \tag{6.65}$$

in the limit $\epsilon \to 0$.

In order to study the phase diagram of this class of solutions, we compute the reduced horizon area and the reduced angular momenta as usual and they result in

$$a_H^4 \,=\, \frac{2\,5^5}{3^4\pi^2}\,\frac{\left(1+8\pi^2\tau^2-\sqrt{1+16\pi^2\tau^2}\right)^4}{\tau^2\omega^2\left(1+16\pi^2\tau^2\right)^2\left(\sqrt{1+16\pi^2\tau^2}-1\right)^5}, \tag{6.66}$$

$$j^4 \,=\, \frac{2^{14}\,5^5\pi^{10}}{3^6}\,\frac{\tau^{10}}{\omega^2\left(\sqrt{1+16\pi^2\tau^2}-1\right)^5\left(1+16\pi^2\tau^2\right)^2}, \tag{6.67}$$

$$j_W^4 \,=\, \frac{5^5}{4\,3^6}\left(1+\sqrt{1+16\pi^2\tau^2}\right)\omega^2, \tag{6.68}$$

where we defined the reduced temperature τ and the angular velocities ratio ω as in (6.33).

Let us now turn to the validity analysis of our results. The condition (6.58) near the pole $\rho = 0$ allows to identify the characteristic worldvolume length scale to be $\frac{\rho_+}{\sqrt{2}}$. The requirement $r_0 \ll \frac{\rho_+}{\sqrt{2}}$ implies then

$$\tau \,\gg\, \tau_0 \,=\, \frac{1}{4\pi\omega}, \tag{6.69}$$

while demanding $R \ll \frac{\rho_+}{\sqrt{2}}$ leads to $\omega \gg 1$, similarly to the black ring ring case.

In Figures 6.3 and (6.4) we show the phase diagrams related to the transverse and worldvolume angular momenta. We plotted the curves for $\tau > 100\tau$ and for different values $\omega = 4, 8, 20$. Again, we must consider more accurate the curves with higher ω. We observe again that we can access only very high worldvolume angular momenta with $j_W \gtrsim 7$, while our procedure must be considered correct down to rather low transverse angular momenta $j \gtrsim 0.3$.

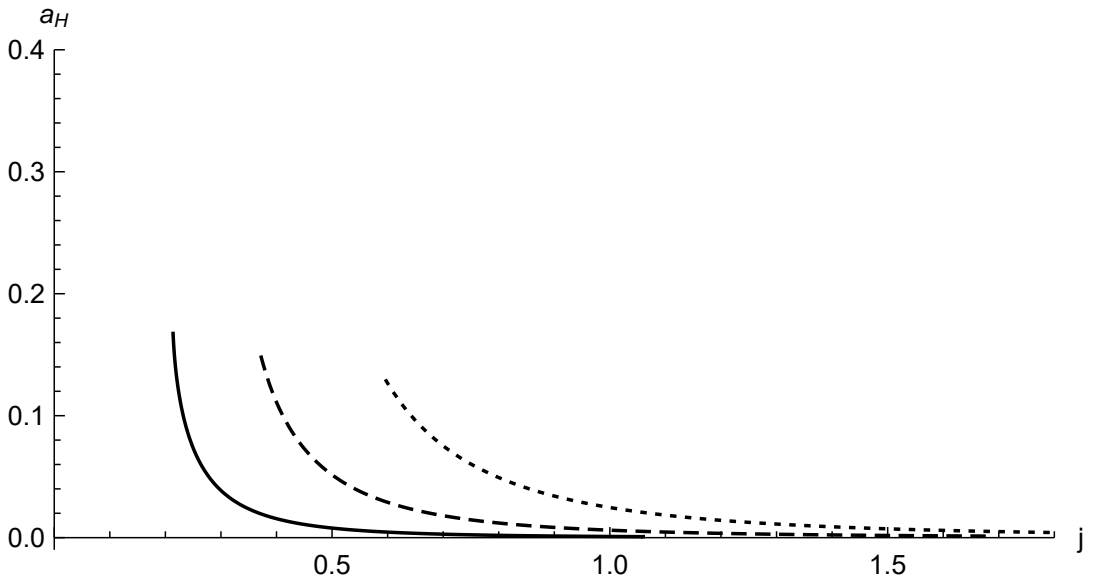

Figure 6.3: We display here the phase diagram $a_H(j)$ of black ring discs in Minkowski background for $\omega = 4, 8, 20$ with the dotted, dashed and solid line, respectively. We plot the phase curves for values $\tau > 100\tau_0$.

Let us now discuss the general case of p-balls embedded into Minkowski, with even $p = 2m$. In this case, we must consider the flat embedding

$$ds^2 = -d\tau^2 + \sum_{i=1}^{m} \left(d\rho_i^2 + \rho_i^2 d\chi_i^2 \right) . \tag{6.70}$$

We introduce m angular momenta Ω_i with the Killing vector

$$\mathbf{k} = \partial_t + \sum_{i=1}^{m} \Omega_i \partial_i, \qquad \text{with modulus} \quad \mathrm{k}^2 = 1 - \sum_{i=1}^{m} \Omega_i^2 \rho_i^2. \tag{6.71}$$

As a consequence, we have again compact worldvolume spatial slices, due to the constraint

$$\sum_{i=1}^{m} \Omega_i^2 \rho_i^2 < 1, \tag{6.72}$$

leading to an ellipsoidal configuration, as desired. The overall horizon geometry consists then in the fibration $s^2 \times s^1 \times \mathbb{B}^{2m}$. Defining again

$$P = -\tilde{f}(\Omega, T)\, \mathrm{k}^2, \tag{6.73}$$

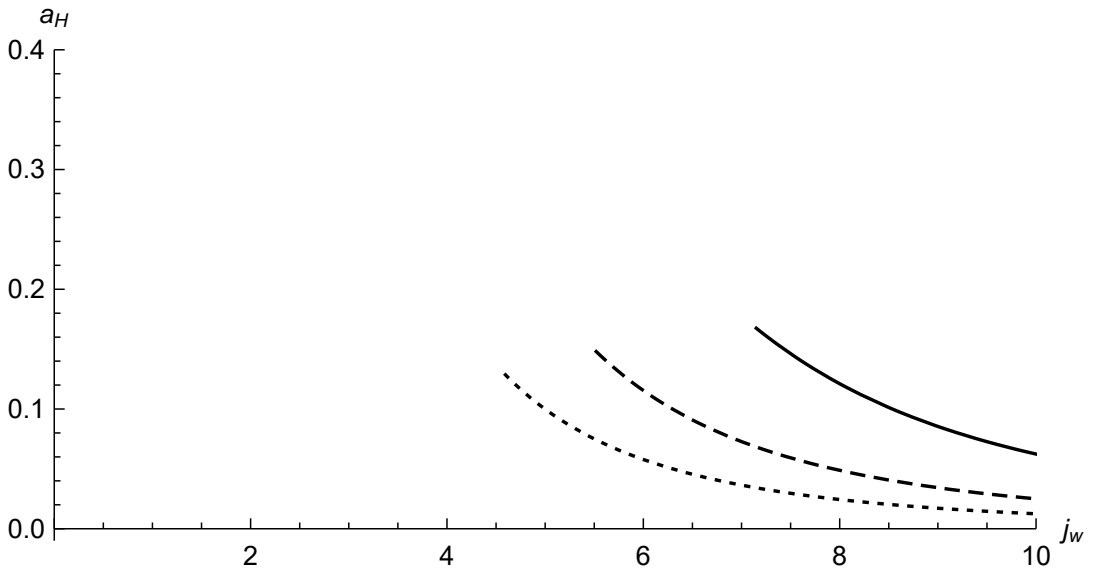

Figure 6.4: We present here the phase diagram $a_H(j_W)$ of black ring discs in Minkowski background for $\omega = 4, 8, 20$ with the dotted, dashed and solid line, respectively. We plot the phase curves for values $\tau > 100\tau_0$.

we can evaluate the free energy as

$$F = (2\pi)^m \tilde{f}(\Omega, T) \int_V \left(\prod_{i=1}^m \rho_i d\rho_i \right) \left[1 - \sum_{i=1}^m \Omega_i^2 \rho_i^2 \right], \tag{6.74}$$

where the integration is restricted to the region V identified by the constraint (6.72). As customary, we define $x_i = \Omega_i \rho_i$ where $0 \leq x_i < 1$, and hence

$$F = \tilde{f}(\Omega, T) \prod_{i=1}^m \left(\frac{2\pi}{\Omega_i^2} \right) \int_{V'} \left(\prod_{i=1}^m x_i dx_i \right) \left[1 - \sum_{i=1}^m x_i^2 \right]. \tag{6.75}$$

We can take advantage of the symmetry of this configuration and recast x_i in terms of the vector cosines μ_i of S^{m-1} as

$$x_i = r\mu_i, \tag{6.76}$$

with the constraint now reading $\mu_i \geq 0$. By doing this, it is possible to notice that

$$\int_{V'} \left(\prod_{i=1}^m x_i dx_i \right) \left[1 - \sum_{i=1}^m x_i^2 \right] = \frac{\Omega_{(2m-1)}}{(2\pi)^m} \int_0^1 dr \left(r^{2p-1} - r^{2p+1} \right), \tag{6.77}$$

in such a way that, on the whole, the free energy functional reads

$$F(\Omega_i, \Omega, T) = \frac{\Omega_{(2m-1)}}{2m(m+1)} \tilde{f}(\Omega, T) \prod_{i=1}^m \frac{1}{\Omega_i^2}, \tag{6.78}$$

and we recover correctly the black disc case (6.61) for $m = 1$.

Then, we can compute the entropy and the angular momenta by deriving F as usual, and they result

$$S = \frac{\Omega_{(2m-1)}}{2m(m+1)} \frac{\Omega\left(\Omega - \sqrt{16\pi^2T^2 + \Omega^2}\right) + 8\pi^2T^2}{32\pi GT^3\Omega\sqrt{16\pi^2T^2 + \Omega^2}} \prod_{i=1}^{m} \frac{1}{\Omega_i^2}, \tag{6.79}$$

$$J = \frac{\pi}{4G} \frac{\Omega_{(2m-1)}}{2m(m+1)} \frac{1}{\Omega^2\sqrt{16\pi^2T^2 + \Omega^2}} \prod_{i=1}^{m} \frac{1}{\Omega_i^2}, \tag{6.80}$$

$$J_i = \frac{\Omega_{(2m-1)}}{2m(m+1)} \frac{\sqrt{16\pi^2T^2 + \Omega^2} - \Omega}{32\pi GT^2\Omega} \frac{1}{\Omega_i^3} \prod_{j\neq i} \frac{1}{\Omega_j^2}. \tag{6.81}$$

On the other hand, we can calculate the mass M from (6.14), which leads to

$$M = (2\pi)^m \tilde{f}(\Omega, T) \int_V \left(\prod_{i=1}^{m} \rho_i d\rho_i\right) \left[3 - \sum_{i=1}^{m} \Omega_i^2\rho_i^2\right]. \tag{6.82}$$

If we define again $x_i = \Omega_i\rho_i$ and the direction cosines as in (6.76), we find

$$M = \tilde{f}(\Omega, T) \frac{\Omega_{(2m-1)}}{2} \frac{3+2m}{m^2+m} \prod_{i=1}^{m} \frac{1}{\Omega_i^2}, \tag{6.83}$$

which again returns correctly to (6.65) once we set $p = 1$.

6.4 Black ring branes stability

We start from a static fluid with velocity field $u^a = (1, \bar{0})$ and with homogeneous energy density ε and pressure P described by (5.42). The effective fluid is now characterized by a conserved local transverse charge $\mathcal{J}$, which we consider homogeneous on the worldvolume as well. We also choose a static gauge for the worldvolume embedding, that is

$$X^0 = t, \qquad X^i = z^i \quad \text{with } i = 1 \dots p, \tag{6.84}$$

keeping the transverse coordinates X^m, $m = p+1 \dots D$ fixed to a constant value. We refer to the worldvolume coordinates as $\sigma^a = (t, z^i)$ as usual. We intend to work at the leading order, which means that for our purposes the worldvolume intrinsic and extrinsic curvature vanish:

$$\Gamma^{(0)} \approx 0 \quad \text{and} \quad K_{ab}^{(0)\,i} \approx 0. \tag{6.85}$$

We assume plane wave perturbations of the independent thermodynamic variables

$$\begin{aligned} \mathcal{T} &\longrightarrow \mathcal{T} + \delta\mathcal{T}\, e^{i(wt+k_j z^j)}, \\ \omega &\longrightarrow \omega + \delta\omega\, e^{i(wt+k_j z^j)}, \\ u^a &\longrightarrow \left(1, \delta u^i\, e^{i(wt+k_j z^j)}\right). \end{aligned} \tag{6.86}$$

These variations will result in variations of the other thermodynamic quantities, as prescribed by the local thermodynamics in Section 6.1.

Longitudinal stability analysis

Our first aim is to study the linearized dynamics of longitudinal perturbations encoded into the intrinsic blackfold equation, with the transverse charge conservation equation acting as a constraint. Hence, the unperturbed equations that we have to deal with are

$$\partial_a T^{ab}_{(0)} = 0, \tag{6.87}$$

$$\partial_a \mathcal{J}^a_{(0)} = 0, \tag{6.88}$$

with $\mathcal{J}^a = \mathcal{J} u^a$, and they are trivially satisfied for the initial conditions chosen above.

In the perturbed case we have a dependence of the quantities on σ^a. We name for convenience $W = \varepsilon + P$ and $\theta = \partial_a u^a$ the expansion of the velocity field; we indicate also the derivative projected along u^a with a dot. Then, the stress tensor conservation leads to

$$(\dot{W} + W\theta)u^b + W\dot{u}^b + \partial^b P = 0 \tag{6.89}$$

for each b. Furthermore, we can use the orthogonal projector to the boost direction

$$\Delta_{ab} = \eta_{ab} + u_a u_b \tag{6.90}$$

in order to extract the dynamics on the surface orthogonal to u^a from (6.89). Recalling that the 4-acceleration $a^\mu = \frac{du^\mu}{d\tau} = \dot{u}^\mu$ is orthogonal to the 4-velocity, it is easy to see that by contracting (6.89) with Δ_{ab} we obtain

$$W\dot{u}_a + \partial_a P + u_a \dot{P} = 0. \tag{6.91}$$

Inserting it into (6.89), we recognize the projection of $\nabla_a T^{ab} = 0$ along u^a to be

$$\dot{\varepsilon} = -W\theta. \tag{6.92}$$

Analogously, the conservation law for the transverse angular momentum results in

$$\dot{\mathcal{J}} = -\mathcal{J}\theta. \tag{6.93}$$

Let us now translate these last three independent equations in terms of the phase of the perturbations. We recall that locally the First Law for such a charged fluid reads

$$d\varepsilon = \mathcal{T} ds + \omega d\mathcal{J} \tag{6.94}$$

and it involves differentials of extensive quantities. On the other hand, the Euler relation becomes

$$\varepsilon + P = \mathcal{T} s + \mathcal{J}\omega, \tag{6.95}$$

leading to the Gibbs-Duhem relation for the BRB effective fluid:

$$dP = s d\mathcal{T} + \mathcal{J} d\omega. \tag{6.96}$$

Since this expression only involves differentials of intensive quantities (which are the ones we are considering independent), we can use it to relate δP with $\delta\mathcal{T}$ and $\delta\omega$. Thus, with a straightforward computation we can recast eqs. (6.91), (6.92) and (6.93) as

$$wW\delta u_i + k_i \left(s\delta\mathcal{T} + \mathcal{J}\delta\omega\right) = 0, \tag{6.97}$$

$$w\left(\left.\frac{\partial\varepsilon}{\partial\mathcal{T}}\right|_{\omega}\delta\mathcal{T} + \left.\frac{\partial\varepsilon}{\partial\omega}\right|_{\mathcal{T}}\delta\omega\right) + Wk^i\delta u_i = 0, \tag{6.98}$$

$$w\left(\left.\frac{\partial\mathcal{J}}{\partial\mathcal{T}}\right|_{\omega}\delta\mathcal{T} + \left.\frac{\partial\mathcal{J}}{\partial\omega}\right|_{\mathcal{T}}\delta\omega\right) + \mathcal{J}k^i\delta u_i = 0. \tag{6.99}$$

As usual, it is possible to find the dispersion relation of the wave perturbations $w(|k|)$ by imposing the existence of a solution to this system, namely requiring its determinant to vanish. The result turns out to be independent of the dimension p of the considered brane, and it reads

$$w^2 \;=\; \frac{s\mathcal{J}\frac{\partial\varepsilon}{\partial\omega} + W\mathcal{J}\frac{\partial\mathcal{J}}{\partial\mathcal{T}} - sW\frac{\partial\mathcal{J}}{\partial\omega} - \mathcal{J}^2\frac{\partial\varepsilon}{\partial\mathcal{T}}}{\frac{\partial\varepsilon}{\partial\omega}\frac{\partial\mathcal{J}}{\partial\mathcal{T}} - \frac{\partial\mathcal{J}}{\partial\omega}\frac{\partial\varepsilon}{\partial\mathcal{T}}}\;\frac{|k|^2}{W} \;=\; c_s^2|k|^2. \tag{6.100}$$

Taking into account the known local thermodynamic relations from Section 6.1, we obtain a speed of sound

$$c_s^2 \;=\; -\frac{1}{3}, \tag{6.101}$$

which agrees with the corresponding result for Schwarzschild blackfolds if we take $n = 2$. However, it is different from the one that could be naively computed as $\frac{\partial P}{\partial\varepsilon} = -\frac{2}{3}$, as prescribed for neutral black branes. This fact must be considered related to the additional non-trivial transverse charge conservation constraint. Finally, we notice that this value of c_s leads to a dispersion relation $w(|k|)$ independent of $\mathcal{T}$ and ω at first order.

Transverse stability analysis

We now turn to the analysis of the extrinsic perturbations, following the previous dissertation for Schwarzschild blackfolds. We impose a variation of the transverse embedding with form

$$X^m \longrightarrow X^m + \xi^m. \tag{6.102}$$

We assume again that

- we work at first order in the mass scale, which means that the set of extrinsic equations read
$$T^{ab} K_{ab}{}^{i} = 0,$$
without additional spin-related terms in the r.h.s;
- we have a flat embedding at this order, that is
$$K_{ab}^{(0)\,i} \approx 0, \quad \Gamma^{(0)} \approx 0,$$
in such a way that the variation of the extrinsic curvature can be written once more as
$$\delta K_{ab}{}^{m} = \partial_a \partial_b \xi^m.$$

With this setup, we fully recover the calculation for Schwarzschild blackfolds, and therefore from the extrinsic equations we obtain straightforwardly

$$\left(\varepsilon \partial_t^2 + P \partial_i^2\right) \xi^m = 0, \tag{6.103}$$

so that

$$c_T^2 = -\frac{P}{\varepsilon} = \frac{1}{3}. \tag{6.104}$$

From these dispersion relations and after noticing that c_T and c_L are independent of $\mathcal{T}$ and ω, we conclude that a first order longitudinal Gregory-Laflamme instability occurs for each possible configuration[3] with $\mathcal{T}, \omega > 0$.

Thermodynamic stability analysis

It is possible to make a comparison with the thermodynamic instabilities of the BRB effective fluid. We know that a thermodynamic system endowed with a conserved charge like $\mathcal{J}$ is stable if and only if both the specific heat

$$c_v = \left.\frac{\partial \varepsilon}{\partial \mathcal{T}}\right|_{\omega} \tag{6.105}$$

[3] We exclude zero values of $\mathcal{T}$ and ω since we have no well-defined extremal limit for a black ring, and intuitively we can see the reason of this in having required a balancing condition for the angular velocity.

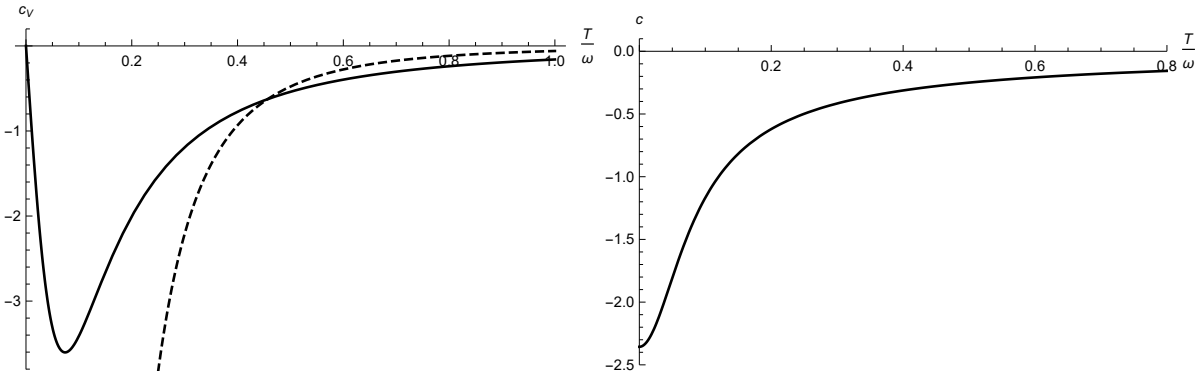

Figure 6.5: The left side shows the qualitative behaviour of the specific heat for a BRB as a function of the reduced temperature $\mathcal{T}/\omega$. As a comparison, the dashed line is the qualitative behaviour of the specific heat for a Schwarzschild black brane. On the right side, we display the permittivity of a BRB as a function of the reduced temperature.

and the acting-permittivity

$$c = \left.\frac{\partial \mathcal{J}}{\partial \omega}\right|_{\mathcal{T}} \tag{6.106}$$

are positive. An explicit calculation shows that

$$c_v = -3\,\frac{8\pi^2\mathcal{T}^2 + \omega\left(\omega - \sqrt{16\pi^2\mathcal{T}^2+\omega^2}\right)}{32\pi\omega\mathcal{T}^3\sqrt{16\pi^2\mathcal{T}^2+\omega^2}}, \tag{6.107}$$

while the permittivity results in

$$c = -\frac{\pi}{4\omega^3}\,\frac{32\pi^2\mathcal{T}^2+3\omega^2}{(16\pi^2\mathcal{T}^2+\omega^2)^{\frac{3}{2}}}. \tag{6.108}$$

Their qualitative behaviour is shown in Figure 6.4, where they are plotted as functions of the reduced temperature $\tau = \frac{\mathcal{T}}{\omega}$ for a fixed value of ω. We notice that both c_v and c are negative for all $\mathcal{T}, \omega > 0$, in perfect agreement with the previously found Gregory-Laflamme dynamic instability. This actually coincides with what happens for all the other known cases. For example, we analysed explicitly this matching of dynamic and thermodynamic instability for neutral Schwarzschild black branes in Section 4.1, but it can be also shown for black branes with other conserved transverse charges instead of $\mathcal{J}$ [40].

The dashed line in the l.h.s of Figure 6.4 represents the qualitative behaviour of the specific heat of a Schwarzschild black brane as a function of the local temperature $\mathcal{T}$. In fact, we have $r_0 \sim \mathcal{T}^{-1}$, and hence $\varepsilon_{Schw} \sim \mathcal{T}^{-2}$ for $n = 2$, which means that its specific heat goes as $c_v \sim \mathcal{T}^{-3}$. As a consequence, we see that the presence of a transverse

angular momentum makes the black brane less and less thermodynamically unstable as we approach a vanishing reduced temperature τ (which does not correspond to a physical configuration). We also recall that the US regime $j^2 \to \infty$ is accessed as $\tau \to \infty$.

6.5 5D MP black branes stability

Let us consider now the local thermodynamics of a 5-dimensional singly spinning MP black brane. Instead of defining the horizon scale r_0 from the local temperature as done for the black ring, here it is more viable to use the explicit solution of the event horizon equation (2.12). In $D = 5$, the outer solution is

$$r_0 = \sqrt{\mu - a^2}. \tag{6.109}$$

Consequently, we decide to consider r_0 and a as independent parameters of these solutions. From the study of the Killing vector field generating the horizon, we found that

$$\omega = \frac{a}{r_0^2 + a^2}. \tag{6.110}$$

On the other hand, by calculating the surface gravity, one obtains

$$\mathcal{T} = \frac{1}{2\pi} \frac{r_0}{r_0^2 + a^2}. \tag{6.111}$$

These two equalities are enough to recast r_0 and a in terms of the local temperature and angular velocity. They result in

$$r_0(\mathcal{T}, \omega) = \frac{2\pi\mathcal{T}}{4\pi^2\mathcal{T}^2 + \omega^2}, \tag{6.112}$$

$$a(\mathcal{T}, \omega) = \frac{\omega}{4\pi^2\mathcal{T}^2 + \omega^2}, \tag{6.113}$$

and they allow to write the mass parameter as

$$\mu(\mathcal{T}, \omega) = r_0^2 + a^2 = \frac{1}{4\pi^2\mathcal{T}^2 + \omega^2}. \tag{6.114}$$

It follows that

$$P(\mathcal{T}, \omega) = -\frac{\Omega_{(3)}}{16\pi G}\mu = -\frac{\pi}{8G} \frac{1}{4\pi^2\mathcal{T}^2 + \omega^2}, \tag{6.115}$$

$$\varepsilon(\mathcal{T}, \omega) = -3P = \frac{3\pi}{8G} \frac{1}{4\pi^2\mathcal{T}^2 + \omega^2}, \tag{6.116}$$

which we notice to coincide with the ADM mass of our solution. From an asymptotical analysis we find the transverse local angular momentum

$$\mathcal{J}(\mathcal{T},\omega) = \frac{\Omega_{(3)}}{8\pi G}\,\mu a = \frac{\pi}{4G}\frac{\omega}{\left(4\pi^2\mathcal{T}^2+\omega^2\right)^2}. \tag{6.117}$$

Finally, from the horizon area one gets the local entropy density

$$s(\mathcal{T},\omega) = \frac{a_H}{4G} = \frac{\Omega_{(3)}}{4G}r_0(r_0^2+a^2) = \frac{\pi^3}{G}\frac{\mathcal{T}}{\left(4\pi^2\mathcal{T}^2+\omega^2\right)^2}. \tag{6.118}$$

Dynamic and thermodynamic stability

We are now able to study the dynamic and thermodynamic stability of a MPBB. We could follow the same procedure as for BRBs, and we would obtain again the dispersion relation (6.100). By using the local thermodynamics just found, it is easy to see that also in this case the sound speed is

$$c_s^2 \;=\; -\frac{1}{3}, \tag{6.119}$$

and, analogously, following the previous discussion, we obtain

$$c_T^2 \;=\; -\frac{P}{\varepsilon} \;=\; \frac{1}{3}, \tag{6.120}$$

as well as before.

From these values, we can state that also for MPBBs a Gregory-Laflamme instability is present. Then, there are strong hints that the presence of a transverse spin does not stabilize enough the dynamics, even if an extremal configuration is accessible to the system, as in this case.

It is interesting to compare this dynamic analysis with the thermodynamic stability of the system, which is dictated by the positivity of the specific heat and of the permittivity. The specific heat is

$$c_v \;=\; \left.\frac{\partial\varepsilon}{\partial\mathcal{T}}\right|_{\omega} \;=\; -\frac{3\pi^2}{G}\frac{\mathcal{T}}{\left(4\pi^2\mathcal{T}^2+\omega^2\right)^2}, \tag{6.121}$$

while the acting-permittivity results

$$c \;=\; \left.\frac{\partial\mathcal{J}}{\partial\omega}\right|_{\mathcal{T}} \;=\; \frac{\pi}{4G}\frac{4\pi^2\mathcal{T}^2-3\omega^2}{\left(4\pi^2\mathcal{T}^2+\omega^2\right)^3}. \tag{6.122}$$

The specific heat is manifestly negative for each $\mathcal{T},\omega>0$, and it vanishes at extremality $\mathcal{T}=0$. On the other hand, the permittivity is positive if $\mathcal{T} > \frac{\sqrt{3}}{2\pi}\,\omega \simeq 0.276\,\omega$. Their precise behaviour is plotted in Figure 6.5.

We recall that we need both c_v and c to be positive in order to have thermodynamic stability. Thus, we conclude that a MPBB is dynamically and thermodynamically unstable in each of its accessible configurations.

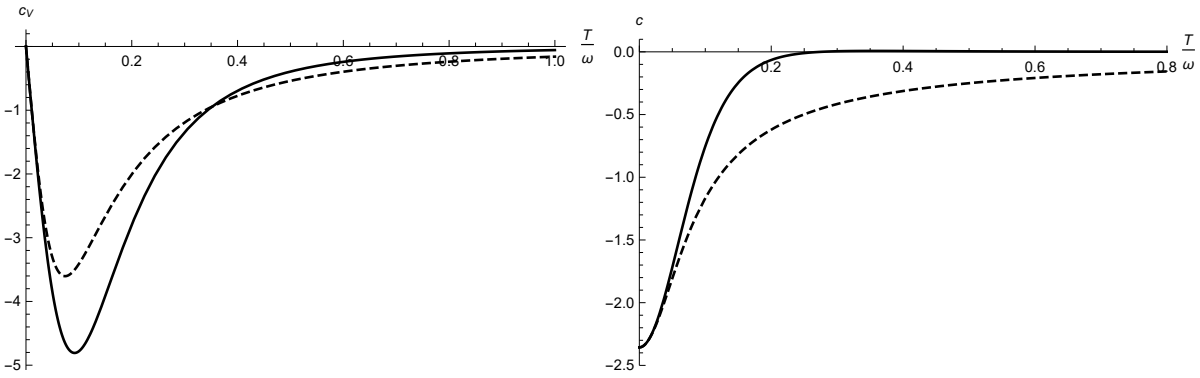

Figure 6.6: The left side shows the qualitative behaviour of the specific heat for a MPBB as a function of the reduced temperature $\mathcal{T}/\omega$. As a comparison, the dashed line is the qualitative behaviour of the specific heat for a BRB. We stress out that for a MPBB the configuration $\mathcal{T} = 0$ is accessible. On the right side, we display the permittivity of a BRB as a function of the reduced temperature; remarkably, it is (slightly) positive for $\frac{\mathcal{T}}{\omega} > \frac{\sqrt{3}}{2\pi}$. We compare it with the (dashed) permittivity of a BRB, and we notice that c approaches the value of $-\frac{3\pi}{4G\omega^4}$ in the limit $\mathcal{T} \to 0$ for both of these black branes.

Conclusions

We introduced the main features of $D = 4$ neutral black holes discussing Schwarzschild and Kerr solutions, then we turned briefly to the reasons that allow to endow stationary black holes with a well-defined thermodynamics.

In Chapter 2, we showed the different behaviour that neutral higher dimensional black holes can exhibit in comparison with their $D = 4$ relatives, by focussing on the most important families of known exact solutions. We analysed the generalization of Schwarzschild black holes and black branes, which result from adding flat extra-directions to the former. We discussed Myers-Perry solutions, which can be thought of as a generalization to Kerr black holes in $D > 4$, since they have spherical horizon topology and they admit the presence of at most $\lfloor (D-1)/2 \rfloor$ angular momenta. We also described how a singly-spinning MP black hole in $D \geq 6$ can access the ultra-spinning limit and how it can be seen as a black 2-brane in this regime.

Another important class of higher dimensional black holes is represented by $D = 5$ black rings. As we saw in Section 2.3, their horizon topology is $S^2 \times S^1$, and actually they were the first solutions with non-spherical horizon topology to be discovered. If we ask for a stable configuration (or equivalently no conical singularity in the centre of the ring), it is necessary to require a rotation along S^1. It has the effect of balancing the ring from its gravitational self-attraction. After analysing the phase diagram related to this class of solutions, we also concluded that in $D > 4$ no black hole uniqueness principle holds. Remarkably, a black ring with a very high angular momentum can be thought of as a black brane (in particular, as a boosted black string), similarly to what happens to ultra-spinning MP black holes.

In Chapter 3, we showed the main aspects of the blackfold approach, following [31, 35]. It was developed arguing that any neutral higher dimensional black hole in the ultra-spinning limit must indeed follow a black brane behaviour, but it results to be a formalism valid for dealing with any higher dimensional black hole solution with a well-separated hierarchy of length scales along different directions on the horizon. This assumption allows a splitting between the long wavelength gravitational degrees of freedom and the ones localized near the horizon. As a consequence, the long wavelength ones can be associated to an asymptotic background geometry acting as the embedding of the worldvolume, which is formed by the extended directions. On the other hand, as we saw

in Section 3.1, the short wavelength degrees of freedom can be encoded into an effective fluid living on the worldvolume, with energy-stress tensor defined by the Brown-York quasilocal prescription. In this approximation, the black hole dynamics is specified by a set of D constraints (that we referred to as blackfold equations) that one can extract from Einstein's Field Equations.

After that, we inspected how to generate approximated stationary solutions by fixing a background spacetime and the symmetries of the considered black holes, as it was done in [34]. It was showed how to solve the blackfold equations explicitly and we discussed what are the consequent observables and horizon geometries. Finally, we presented an alternative procedure relying on an effective action that leads to the blackfold equations, and from which one can obtain (often more straightforwardly) the same observables and thermodynamics.

We concluded the part of this thesis devoted to previous work with Section 3.7, where we discussed extensively some simple examples of approximated solutions that one can build. We presented the general theory of $p = 1$ blackfolds, specializing then to the case of Minkowski background in general dimensions. In these conditions, a complete classification of stationary 1-folds was found, and it was noticed that ultra-spinning $D = 5$ black rings are correctly recovered as a particular case. Black discs were discussed as well, and they were found to reproduce perfectly the thermodynamics of ultra-spinning $D = 6$ MP black holes.

In Chapter 4, we first generalized the previous quasinormal modes analysis restricted to static black strings from [31], by considering the effective theory of a boosted black string in Minkowski background at the perfect fluid level. We found a longitudinal Gregory-Laflamme instability for any boost β, as expected.

Then we turned to ultraspinning black rings. After choosing a suitable worldvolume embedding and after imposing rotation, we finally added a finite extrinsic curvature radius R. Intrinsic and extrinsic perturbations here couple, and, as a result, we found corrections in $\left(\frac{1}{R^2}\right)^j$ to the boosted black string frequencies, with a perfect match with the corresponding large-D expansions at the $O(1/\sqrt{n})$ order. We also discussed the range of validity of our results with regards to the mode numbers m.

After that, we inspected the effects of viscous contributions brought about by the first order effective theory. The boosted black string modes get further corrections in $\frac{r_0}{R}$, and again they perfectly agree with the known results in the limit of a large number of dimensions D. New imaginary terms suppressed in $\frac{r_0}{R}$ arise, in such a way that the longitudinal unstable behaviour gets corrections as well.

It would be interesting to analyse the effect of viscous corrections to the perfect fluid black ring frequencies in Section 4.3. Due to the coupling between intrinsic and extrinsic equations, we expect to capture, at least partially, also the thin ring transverse instability that was detected numerically in [3]. Furthermore, one can consider second-order dissipative corrections to the fluid behaviour, as well as the so-called *bending* contribu-

tions to the ring, leading to modifications of the blackfold equations form, as explained in [33, 6].

The aim of Chapters 5 and 6 was to build a new effective theory based on the blackfold formalism and describing higher dimensional solutions with non-zero angular momenta along the transverse directions. Then, instead of a Schwarzschild spacetime, in Chapter 5 we considered transverse spaces consisting in rotating black holes. We computed the Brown-York effective energy-stress tensor and showed explicitly how to extract the extrinsic blackfold equations from Einstein's Equations in case of Kerr black strings, doubly-spinning Myers-Perry black strings and black ring strings. We also discussed how to generalize these calculations to $p > 1$ and to a higher number of transverse angular momenta.

In Chapter 6, thanks to these achievements, we studied *black ring blackfolds* and their local thermodynamics, in view of using them as starting point to generate new solutions. First, we built black holes with $S^2 \times \mathbb{T}^2$ horizon topology. These configurations have two angular momenta, one of which is very high, while the other can span a wider range of values in comparison with the analogous horizon configuration found in [34], which was endowed with two very high angular momenta instead.

In addition, we inspected a new class of higher dimensional black hole solutions with horizon geometry $S^2 \times S^1 \times \mathbb{B}^{2m}$, where $\mathbb{B}^{2m}$ identifies a $2m$-dimensional ball. We found a well-posed thermodynamics, and, after analysing the corresponding phase diagrams, we observe again that the new effective theory here developed is accurate down to rather low transverse spins, allowing to describe higher dimensional black holes with not all the angular momenta in ultra-spinning regime.

Finally, we studied the leading order stability of two representative classes of solutions that one can build with this new effective theory, namely the ones following from black ring branes and from $D = 5$ Myers-Perry black branes. In comparison with the Schwarzschild black brane case, here the additional transverse angular momentum conservation law had to be taken into account. The results confirmed the presence of a Gregory-Laflamme-like instability under perturbations along the worldvolume directions. We also found a thermodynamic instability of these classes of black branes, and thus we concluded that they are both dynamically and thermodynamically unstable in each of their accessible configurations, similarly to what happens for Schwarzschild black branes.

In principle, it is possible to develop further the effective theory involving rotating blackfolds here depicted in the same ways followed for standard blackfolds. A future development in this direction consists of finding explicitly the intrinsic equations from EFE for some specific classes of black branes, as done in Chapter 5 for the extrinsic equations. In addiction to this, it would be interesting to generate other solutions with non-trivial horizon topology, with the possibility of exploring in particular new Supergravity solutions.

Acknowledgements

In first place, I am very grateful to my supervisor, Prof. Roberto Balbinot, for his valuable advice, especially during the initial phases of this project. Then I want to thank all the staff at the University of Amsterdam and in particular Jay for this opportunity. I also thank Jay for his continuous guidance and for his firm enthusiasm, which is often the most useful attitude to get things done.

Moreover, I would like to show my gratitude to all the people that I have known during these last years of studies. I want to thank my office mates Alex, Ariane, Julien, Kayed and Mart for interesting discussions during lunch-time in Amsterdam. I must thank many of my colleagues in Bologna, who entered my academic life and quickly became part of what I am, and among whom I will only mention Pedro, Serena and Teo.

Finally, I would like to thank my closest friends in Bologna and my family for limitless patience and support. The kindest words are to be addressed to my girlfriend Nicole, for staying so close even from a distance.

Appendix A

Submanifolds and Embeddings

In this appendix we present several results that are useful for dealing with submanifold calculus, following Refs. [31, 38].

Consider a D-dimensional spacetime $\mathcal{M}$ with coordinates x^α and metric $g_{\mu\nu}(x^\alpha)$, and a surface $\mathcal{W}$ with dimension $p < D$ and boundary ∂W with coordinates σ^a, where $a = 1 \dots p$.

We say that $\mathcal{W}$ is embedded into $\mathcal{M}$ if there exists an injective map $X^\mu : \mathbb{R}^p \to \mathbb{R}^D$ between the target space of the charts σ^a and x^α, with the property of preserving the differential structures.

We see that $x^{-1} \circ X \circ \sigma$ defines a diffeomorphism from $\mathcal{W}$ to a subset of $\mathcal{M}$, and it allows us to perform the push-forward of vectors via $e^\mu{}_a = \partial_a X^\mu$ as

$$V^\mu = \frac{dX^\mu}{dt} = e^\mu{}_a V^a \tag{A.1}$$

from $\mathcal{W}$ to $\mathcal{M}$. Analogously, we can build the pull-back of $g_{\mu\nu}$ from $\mathcal{M}$ to $\mathcal{W}$, resulting in the induced metric on $\mathcal{W}$

$$\gamma_{ab} = e^\mu{}_a e^\nu{}_b g_{\mu\nu}. \tag{A.2}$$

If we think of $e^\mu{}_a = (e_a)^\mu$ as a set of p tangent vectors to the subset of $\mathcal{M}$ corresponding to $\mathcal{W}$, we can simply identify the $n = D - p$ normal vectors $n^\mu{}_i = (n_{\,i})^\mu$ by demanding

$$e^\mu{}_a n_\mu{}^i = 0, \qquad n^\mu{}_i n^\nu{}_j g_{\mu\nu} = 0. \tag{A.3}$$

Of course, we notice that these requirements only fix the orthonormal vectors $n^\mu{}_i$ up to $O(n)$ transformations acting on the orthogonal subspace.

Furthermore, these definitions allow us to recover a manifest covariance on the embedding spacetime, by considering the subset of $\mathcal{M}$ corresponding to $\mathcal{W}$ and forgetting about the manifold $\mathcal{W}$ itself (and the indices a, b). We define the first fundamental form of this submanifold as

$$\gamma^{\mu\nu} = e^\mu{}_a e^\nu{}_b \gamma^{ab} = e^\mu{}_a e^{\nu\,a}, \tag{A.4}$$

while we can build the transverse metric $\perp^{\mu\nu} = n^{\mu}{}_{i} n^{\nu\, j}$ in such a way that we can separate the initial metric on $\mathcal{M}$ as

$$g_{\mu\nu} = \gamma_{\mu\nu} + \perp_{\mu\nu} . \tag{A.5}$$

From the conditions (A.3) it also follows that

$$\gamma^{\mu\nu} \perp_{\mu}{}^{\lambda} = 0, \tag{A.6}$$

and we can state that $\gamma_{\mu\nu}$ projects over the submanifold, while $\perp^{\mu\nu}$ acts as a projector over the transverse space. On the whole, we must expect to lose the global symmetries which initially endowed $g_{\mu\nu}$, while we will maintain the diffeomorphism invariance of the submanifold and the $O(n)$ invariance of the transverse space mentioned above.

From (A.4) it also follows that

$$\gamma^{\mu}{}_{\nu} \partial_a X^{\nu} = \partial_a X^{\mu}, \qquad \text{i.e.} \quad \gamma^{\mu}{}_{\nu} e^{\nu}{}_{a} = e^{\mu}{}_{a}, \tag{A.7}$$

as well as

$$\gamma^{\mu}{}_{\nu} \gamma^{\nu}{}_{\rho} = \gamma^{\mu}{}_{\rho}. \tag{A.8}$$

Analogously, by using (A.5), these relations consistently imply

$$\perp^{\mu}{}_{\nu} e^{\nu}{}_{a} = 0, \qquad \perp^{\mu}{}_{\nu} \perp^{\nu}{}_{\rho} = \perp^{\mu}{}_{\rho} . \tag{A.9}$$

Now that we have build a sensible metric structure for the submanifold, we can think of a suitable connection related to the metric connection of the target space. We define the tangential covariant derivative

$$\overline{\nabla}_{\lambda} = \gamma^{\mu}{}_{\lambda} \nabla_{\mu} \tag{A.10}$$

acting on tensors living on the submanifold; on such tensors both the projection $\perp^{\mu}{}_{\lambda} \nabla_{\mu}$ and the entire ∇_{μ} are not well defined. We also notice that obviously $\left[\overline{\nabla}_{\lambda}, g_{\mu\nu}\right] = 0$.

It allows us to define the extrinsic curvature tensor as

$$K_{\mu\nu}{}^{\rho} = \gamma^{\sigma}{}_{\nu} \overline{\nabla}_{\mu} \gamma^{\rho}{}_{\sigma} = -\gamma^{\sigma}{}_{\nu} \overline{\nabla}_{\mu} \perp^{\rho}{}_{\sigma}, \tag{A.11}$$

thanks to (A.5). From (A.11) we see that the two lower indices correspond to tangential directions to the submanifold, while the upper index must be an orthogonal one, that is

$$\perp^{\mu}{}_{\alpha} K_{\mu\nu}{}^{\rho} = \perp^{\nu}{}_{\alpha} K_{\mu\nu}{}^{\rho} = 0, \qquad \gamma^{\alpha}{}_{\rho} K_{\mu\nu}{}^{\rho} = 0. \tag{A.12}$$

Let us inspect the geometrical meaning of $K_{\mu\nu}{}^{\rho}$. First of all, it is possible to show that the two lower indices are symmetric under exchange:

$$K_{\mu\nu}{}^{\rho} = K_{(\mu\nu)}{}^{\rho}. \tag{A.13}$$

Furthermore, it holds that

$$2K_{\mu(\nu\rho)} = \overline{\nabla}_\mu \gamma_{\nu\rho}, \tag{A.14}$$

that is, we can interpret the extrinsic curvature tensor as a measure of the variations of the tangential and orthogonal metric tensors $\gamma_{\nu\rho}$ and $\perp_{\nu\rho}$ along the surface direction X^μ. On the other hand, given v^α tangent vector to the submanifold, it is easy to show with the definitions above that

$$v^\mu v^\nu K_{\mu\nu}{}^\rho = \perp^\rho{}_\sigma \; v^\mu \nabla_\mu v^\sigma, \tag{A.15}$$

and hence $K_{\mu\nu}{}^\rho$ is also related to the variation of tangent vectors along the direction X^ρ orthogonal to the surface. We will see later on that the extrinsic curvature is actually related to second derivatives of the embedding coordinates X^μ. In turn, it justifies its name *curvature*, while this is not apparent from results (A.14) and (A.15).

Finally, in the previous sections we also made use of the contraction

$$K^\rho = \gamma^{\mu\nu} K_{\mu\nu}{}^\rho, \tag{A.16}$$

which effectively consists in the mean extrinsic curvature of the submanifold, extracting the orthogonal information contained in $K_{\mu\nu}{}^\rho$.

However, it is often convenient to work explicitly with the construction over $\mathcal{W}$. We showed above the push-forward of vectors by using the tangent vectors $e^\mu{}_a$. Of course, this can be generalized to the whole associated tensorial algebra, while the connection transforms according to

$$e^\mu{}_a e^\nu{}_b \gamma^\sigma{}_\rho \, \Gamma^\rho_{\mu\nu} = e^\sigma{}_c \Gamma^c_{ab} - \gamma^\sigma{}_\rho \partial_a e^\rho{}_b \tag{A.17}$$

due to its non-tensorial nature. This relation also allows us to obtain a more compact and manageable expression for the pull-back of $K_{\mu\nu}{}^\rho$ on $\mathcal{W}$, and it reads

$$K_{ab}{}^\rho \;=\; e^\mu{}_a e^\nu{}_b K_{\mu\nu}{}^\rho \;=\; D_a \partial_b X^\rho + \Gamma^\rho_{\mu\nu} \partial_a X^\mu \partial_b X^\nu, \tag{A.18}$$

where of course we understand

$$D_a \partial_b X^\rho = \partial_a \partial_b X^\rho - \Gamma^c_{ab} \partial_c X^\rho. \tag{A.19}$$

Variational calculus on submanifolds

Let us consider a congruence of curves with tangent vector field N^μ, intersecting $\mathcal{W}$ orthogonally and smooth in a neighbourhood of $\mathcal{W}$. From (A.5) it follows that

$$N^\mu \gamma_{\mu\nu} = 0, \qquad N^\mu \perp_{\mu\nu} = N_\nu. \tag{A.20}$$

We can Lie-drag the points of $\mathcal{W}$ with the local map $X^\mu \mapsto X^\mu + \lambda N^\mu$, and it results interesting to study the consequent variation of the tangential metric $\gamma_{\mu\nu}$. We have

$$\pounds_N \gamma_{\mu\nu} = N^\rho \nabla_\rho \gamma_{\mu\nu} + \gamma_{\rho\nu} \nabla_\mu N^\rho + \gamma_{\mu\rho} + \nabla_\nu N^\rho, \tag{A.21}$$

leading to

$$\gamma^\lambda{}_\mu \gamma^\sigma{}_\nu \pounds_N \gamma_{\lambda\sigma} = \gamma^\lambda{}_\mu \gamma^\sigma{}_\nu N^\rho \nabla_\rho \gamma_{\lambda\sigma} + \gamma^\lambda{}_\mu \gamma^\sigma{}_\nu \gamma_{\rho\sigma} \nabla_\lambda N^\rho + \gamma^\lambda{}_\mu \gamma^\sigma{}_\nu \gamma_{\lambda\rho} \nabla_\sigma N^\rho. \tag{A.22}$$

We observe that the first term in the r.h.s. is zero, while

$$\gamma^\sigma{}_\nu \gamma_{\rho\sigma} \overline{\nabla}_\mu N^\rho + \gamma^\lambda_\mu \gamma_{\lambda\rho} \overline{\nabla}_\nu N^\rho = -2 N_\rho K_{\mu\nu}{}^\rho. \tag{A.23}$$

Then, on the whole, (A.22) means that

$$N_\rho K^\rho = N_\rho \gamma^{\mu\nu} K_{\mu\nu}{}^\rho = -\frac{1}{2} \gamma^{\mu\nu} \pounds_N \gamma_{\mu\nu}, \tag{A.24}$$

which means that the mean extrinsic curvature tells how much the induced metric varies after orthogonal Lie-dragging. By simply making use of the well-known matrix identity

$$\mathcal{D} \det(A) = \det(A) \operatorname{Tr}\left[A^{-1} \mathcal{D} A\right], \tag{A.25}$$

with $\mathcal{D}$ a derivative operator, it follows that

$$N_\rho K^\rho = -\frac{1}{\sqrt{\gamma}} \pounds_N \sqrt{\gamma}, \tag{A.26}$$

where we defined $\gamma = |\det(\gamma)|$.

This relation is particularly useful for dealing with several variational principles. For instance, let us take a generic Polyakov-like volume action

$$S[\mathcal{W}] = \int_{\mathcal{W}} \sqrt{\gamma}. \tag{A.27}$$

Thanks to (A.26), we can write the variation of the volume under Lie-dragging along N^ρ as

$$\delta_N S \;=\; \pounds_N \sqrt{\gamma} = -\sqrt{h} N_\rho K^\rho. \tag{A.28}$$

Then, the related variational principle simply reads $K^\rho = 0$ for any orthogonal vector N^ρ, and actually it is the usual condition associated with NG worldvolumes.

Starting instead from an action of the form

$$S[\mathcal{W}] = \int_{\mathcal{W}} \sqrt{\gamma} \Phi(\sigma) \tag{A.29}$$

with $Phi(\sigma)$ function over $\mathcal{W}$, we find that its variation reads

$$\delta_N S \;=\; \pounds_N \left(\sqrt{\gamma}\Phi\right) = -\sqrt{\gamma}\left(N_\rho K^\rho \Phi - N^\rho \partial_\rho \Phi\right). \tag{A.30}$$

Such a generic worldvolume functional is minimal $\delta_N S = 0$ if

$$N_\rho K^\rho \Phi \;=\; N^\rho \partial_\rho \Phi, \tag{A.31}$$

that is

$$K^\rho \;= \perp^{\rho\sigma} \partial_\sigma (\ln \Phi), \tag{A.32}$$

where we explicitly keep track of the orthogonality of the mean extrinsic curvature.

Appendix B

Emparan-Reall US limit of a BRS

Starting from the known metric by Emparan and Reall, we can impose the balancing condition, add an extra direction l and perform a boost along it. Then, if we expand in the US limit $r, r_0 \ll R$ to the leading order in r_0/R, we obtain the metric

$$\begin{aligned} ds^2 = &\left(\eta_{ab} + \frac{2r_0}{r}\, u_a u_b\right) d\sigma^a d\sigma^b + \sqrt{2}\frac{r_0}{r} u_a d\sigma^a dz + \left(1 + \frac{r_0}{r}\right) dz^2 \\ &+ \left(1 + \frac{r_0}{r}\right) dr^2 + r^2 \left(d\theta^2 + \sin^2\theta d\phi^2\right), \end{aligned} \tag{B.1}$$

with $\sigma^a = (t, l)$. It is easy to see that we have recovered the asymptotic metric of a boosted Schwarzschild black membrane, with a specific boost along z (fixed by the balancing condition) and a generic one along l. Redefining the worldvolume coordinates as $\sigma^a = (t, l, z)$ and setting $u^a = \left(u^0, u^1, \frac{1}{\sqrt{2}}\right)$, it is possible to rewrite (B.1) in the usual and more compact form

$$ds^2 = \left(\eta_{ab} + \frac{2r_0}{r}\, u_a u_b\right) d\sigma^a d\sigma^b + \left(1 + \frac{r_0}{r}\right) dr^2 + r^2 \left(d\theta^2 + \sin^2\theta d\phi^2\right). \tag{B.2}$$

The subsequent effective energy-stress tensor can be computed straightforwardly, and it results to be of the usual perfect fluid form, even if we are in presence of a compactified dimension, namely

$$T_{ab} \;=\; \frac{2\pi^2}{16\pi G}(4r_0 R)\,(2u_a u_b - \eta_{ab}). \tag{B.3}$$

From the explicit calculation, one can observe that the right dimensionality of $[L]^2$ is restored thanks to the integration over the compact direction z, which provides a global $2\pi R$ factor. We also notice that (B.3) is in exact agreement with the stress tensor (5.42), since the translation from Durkee's parametrization to this one reads in the US limit

$$\mu \;=\; \frac{4r_0 R^2}{R - r_0} \;\approx\; 4r_0 R. \tag{B.4}$$

As a consequence, we do not need to verify directly how to obtain the blackfold extrinsic equations for a BRS in the thin ring limit, that is in case of a very high transverse angular momentum. The whole calculation simply reduces to the one related to Schwarzschild black p-branes, here with $p = 2$.

Our aim is to study if it is possible to recover the blackfold extrinsic equations for *any* angular momentum, and not only for very high ones. Then, we intend to decrease $\mathcal{J}$ a little, which is a requirement that effectively reduces to considering the next-to-leading order corrections in r_0/R to the membrane limit (B.1). Of course, this will prevent us from dealing with z as an additional worldvolume direction, as it was done in (B.2).

In this way, if we neglect the terms proportional to $(r_0)^m$ with $m > 1$ from the start (since they will not enter our later analysis), the expanded metric becomes

$$\begin{aligned} ds^2 = & \left(\eta_{ab} + \frac{2r_0}{r}\left(1 + \frac{r}{R}\cos\theta\right) u_a u_b\right) d\sigma^a d\sigma^b + \sqrt{2}\frac{r_0}{r}\left(1 + \frac{r}{R}\right) u_a d\sigma^a dz \\ & + \left(1 + \frac{r_0}{r} - 2\frac{r}{R}\cos\theta\right)\left(dz^2 + dr^2\right) \\ & + r^2\left[1 - 2\frac{r}{R}\cos\theta\left(1 + \frac{r_0}{2r}\right)\right]\left(d\theta^2 + \sin^2\theta d\phi^2\right). \end{aligned} \tag{B.5}$$

Except for g_{az}, we see that all the other corrections have a dipolar nature, as expected. It is important to recall the length scale hierarchy $r_0 \ll r \ll R$ that is present in this case.

Instead of going through the Brown-York computation of the effective stress tensor, which is rather cumbersome to perform, we simply expand $\mu(r_0)$ from (B.4) to first order in $1/R$ and substitute it into (5.42). It turns out that $\mu \approx 4r_0 R + O(r_0^2)$, which means that (B.3) remains unchanged at any order in $(r_0/R)^j$, as far as it concerns our Camps-Emparan analysis. We find then

$$r_0 \;=\; -\frac{T}{16R} + O\left(\frac{1}{R^3}\right), \tag{B.6}$$

$$r_0 u_a u_b \;=\; \frac{1}{8R}\left(T_{ab} - \frac{T}{4}\eta_{ab}\right) + O\left(\frac{1}{R^3}\right). \tag{B.7}$$

Before plugging these reparametrizations into (B.5), it is relevant to think of the perturbative orders that we are considering, and we can make an explicit comparison with the analogue Schwarzschild discussion for $n = 2$. In the limit $r_0 \ll r$, we are allowing the presence of $O\left(\frac{r_0^{2n}}{r^{2n}}\right) = O\left(\frac{r_0^4}{r^4}\right)$, but by construction we are also neglecting terms of order equal to or higher than $O\left(\frac{r_0^2}{R^2}\right)$. This fact means that our US expansion effectively leads the metric to satisfy automatically the requirement of slow, long wavelength intrinsic perturbations. Then, working at r_0/R order implies that we have still a rather simple metric to deal with.

From the relations found above, the Camps-Emparan form for a BRS in these limits reads

$$\begin{aligned} ds^2 = &\left[\eta_{ab} + \frac{1}{4Rr}\left(T_{ab} - \frac{T}{4}\eta_{ab}\right)\left(1 + \frac{r}{R}\cos\theta\right)u_a u_b\right] d\sigma^a d\sigma^b \\ &+ 2\left(1 + \frac{r}{R}\right) J_a d\sigma^a dz + \left(1 - \frac{T}{16Rr} - \frac{2r}{R}\cos\theta\right)\left(dz^2 + dr^2\right) \\ &+ r^2\left[1 - \frac{2r}{R}\cos\theta\left(1 - \frac{T}{32Rr}\right)\right]\left(d\theta^2 + \sin^2\theta d\phi^2\right), \end{aligned} \tag{B.8}$$

where as usual we define the angular momentum current

$$J_a = \frac{r_0}{\sqrt{2}r}u_a = -\frac{T}{16\sqrt{2}Rr}u_a. \tag{B.9}$$

We see that the main difference from the Camps-Emparan form of a Schwarzschild black brane is the presence of a dipolar deviation in r/R in the worldvolume sector. In fact, we are not dealing anymore with a solution endowed with spherical topology, but with a $S^1 \times S^2$ topology, and hence we must expect corrections to the spherical setup with a new dependence on the characteristic scale[1] R of S^1.

In the original procedure to extract the extrinsic equations from a Schwarzschild black brane, spherical symmetry is present from the start, and subsequently one breaks it by adding the dipolar perturbations $h_{\mu\nu}$, linear in the inverse of the extrinsic curvature scale. In this case, instead, $SO(n+1)$ is broken by similar dipolar corrections, now linear in the inverse of the transverse rotation scale R.

A good guess may be to perform a change of the coordinates (r, θ) in order to recover explicitly the spherical symmetry in the angular sector of the metric (B.21). Naming the new coordinates $(\tilde{\theta}, \tilde{r})$, we set

$$\theta = \tilde{\theta} + \frac{g(\tilde{\theta}, \tilde{r})}{R}, \tag{B.10}$$

$$r = \tilde{r} + \frac{l(\tilde{\theta}, \tilde{r})}{R}. \tag{B.11}$$

Imposing the diagonality of the new metric and to recover spherical symmetry in the angular part up to $O(1/R^2)$, we obtain the three conditions

$$g_{\tilde{r}\tilde{\theta}} = 0, \tag{B.12}$$

$$g_{\tilde{\theta}\tilde{\theta}} = \tilde{r}^2, \tag{B.13}$$

$$g_{\tilde{\phi}\tilde{\phi}} = \tilde{r}^2 \sin^2\theta. \tag{B.14}$$

[1] Remarkably, this scale is also the one associated with the angular velocity, due to the balance condition for black rings.

From these, one finds the explicit form of the change of coordinates

$$\theta = \tilde{\theta} + \frac{\sin\tilde{\theta}}{R} G(\tilde{r}), \tag{B.15}$$

$$r = \tilde{r} + \frac{\tilde{r}}{R}\cos\tilde{\theta}\left(\tilde{r} + \frac{T}{32R} - G(\tilde{r})\right). \tag{B.16}$$

where

$$G(\tilde{r}) \;=\; \frac{r}{2} - \frac{e^{-\frac{T}{16Rr}}}{2r}\frac{T^2}{256R^2}\int_{-\frac{T}{16Rr}}^{+\infty}\frac{e^{-t}}{t}dt \;=\; \frac{r}{2} + O(T^2). \tag{B.17}$$

Hence, as far as it concerns our analysis, we can write the new coordinates as

$$\theta = \tilde{\theta} + \frac{\tilde{r}}{2R}\sin\tilde{\theta}, \tag{B.18}$$

$$r = \tilde{r}\left[1 - \frac{\tilde{r}}{2R}\left(1 + \frac{T}{16R\tilde{r}}\right)\cos\tilde{\theta}\right], \tag{B.19}$$

up to higher order contributions. In particular, we notice that $\tilde{r}(r)$ is a monotonic function, and does not show any singularity. Here we have chosen the gauge of $\tilde{r}$ in such a way that it is zero when $r = 0$. Dropping now all the tildes, we can rewrite the metric as

$$\begin{aligned} ds^2 = &\left[\eta_{ab} + \frac{1}{4Rr}\left(T_{ab} - \frac{T}{4}\eta_{ab}\right)\left(1 + \frac{r}{2R}\left(1 - \frac{T}{16Rr}\right)\cos\theta\right)u_a u_b\right]d\sigma^a d\sigma^b \\ &+ 2\left[1 - \frac{r}{R}\left(1 + \frac{1}{2}\left(1 + \frac{T}{16Rr}\right)\cos\theta\right)\right]J_a d\sigma^a dz \\ &+ \left[1 - \frac{T}{16Rr} - \frac{2r}{R}\left(1 - \frac{T}{64rR}\right)\cos\theta\right]dz^2 \\ &+ \left[1 - \frac{T}{16Rr}\left(1 + \frac{\cos\theta}{2}\right)\right]dr^2 + r^2\left(d\theta^2 + \sin^2\theta d\phi^2\right). \end{aligned} \tag{B.20}$$

We keep in mind that, due to the form of $\mu(r_0)$, $\frac{T}{R^2}$ terms are allowed in our expansion, since they are of the same order of $\frac{r_0}{R}$. Interestingly enough, we notice the dipolar deviations related to the extrinsic perturbations and the dipolar corrections due to the transverse rotation do not seem to decouple from each other, but they appear to factorize their amplitudes. In short, this is connected with the fact that their two characteristic length scales are independent and not related.

At this point, we can add the extrinsic perturbations and the corrections $h_{\mu\nu}$, in such a way that the perturbed expanded metric reads

$$\begin{aligned} ds^2 = &\left[\eta_{ab} - 2K_{ab}{}^{\hat{i}} y_{\hat{i}} + \frac{1}{4Rr}\left(T_{ab} - \frac{T}{4}\eta_{ab}\right)\left(1 + \frac{r}{2R}\cos\theta\right) u_a u_b\right] d\sigma^a d\sigma^b \\ &+ 2\left[1 - \frac{r}{R}\left(1 + \frac{1}{2}\left(1 + \frac{T}{16Rr}\right)\cos\theta\right)\right] J_a d\sigma^a dz \\ &+ \left[1 - \frac{T}{16Rr} - \frac{2r}{R}\left(1 - \frac{T}{64rR}\right)\cos\theta\right] dz^2 \\ &+ \left[1 - \frac{T}{16Rr}\left(1 + \frac{\cos\theta}{2}\right)\right] dr^2 + r^2\left(d\theta^2 + \sin^2\theta d\phi^2\right) + h_{\mu\nu}(r,\theta) dx^\mu dx^\nu. \end{aligned} \tag{B.21}$$

At this point, a safe procedure to find the extrinsic equations consists in

1. imposing a variation of the transverse coordinate in r/R in such a way that the final combination of Einstein components is proportional to the mass scale and inversely proportional to the extrinsic curvature radius at each order in R, as it should be;

2. once turned off $h_{\mu\nu}$ and naming $G_{r\theta} - \alpha G_{rr}$, imposing a variation of the known coefficient α for Schwarzschild of the form

   $$\alpha = \frac{r}{2}\tan\theta\left(1 + f(\theta)\frac{r}{R}\right),$$

   and it is possible to find a unique $f(\theta)$ just by requesting $G_{r\theta} - \alpha G_{rr}$ to be proportional to $K_{ab}{}^{\hat{i}} T^{ab}$ also at first order in r_0/R (at the leading order we are guaranteed that it is);

3. turning on $h_{\mu\nu}$ and using the coefficient α found above, we impose θ-dependent corrections in r/R in each of its component. It is then possible to make $G_{r\theta} - \alpha G_{rr}$ independent of $h_{\mu\nu}$ and find consequently the corrections of the latter.

Following this procedure, two solutions were found. They coincide as far as it concerns both the transverse coordinates and the coefficient α, but they are different in the dipolar corrections that one finds for $h_{\mu\nu}$. Even though we simply restrict to presenting these solutions now, we believe that future discussions concerning the matching with the results of Section 5.3 should be able to solve this ambiguity.

First solution Assuming the transverse coordinates and all the other (non-tensorial) quantities to have corrections in $1/R$ independently of the mass scale r_0, it is possible to recover the blackfold extrinsic equations by taking the transverse coordinate to be

$$y^{\hat{i}} = r\cos\theta\left(1 + \frac{r}{4R\cos\theta}\right) + O\left(\frac{1}{R^2}\right), \tag{B.22}$$

and a perturbation tensor consisting of both a spherical dipole (due to the bending of S^2) and of a dipolar correction related to the expansion in $1/R$, only along the transverse directions:

$$\begin{aligned} h_{\mu\nu}(r,\theta)dx^\mu dx^\nu = \cos\theta \Big[\hat{h}_{ab} d\sigma^a d\sigma^b + \Big(1 - \frac{r}{R}\cos\theta\Big) \Big(\hat{h}_{rr} dr^2 + \hat{h}_{zz} dz^2 + \\ + \; r^2 \hat{h}_{\theta\theta} (d\theta^2 + \sin^2\theta d\phi^2) \Big) \Big] , \end{aligned} \tag{B.23}$$

together with the constraint $\hat{h}_{zz} = 2\hat{h}_{\theta\theta} - \hat{h}_{rr}$. This all leads to a combination

$$\begin{aligned} G_{r\theta} \; - \frac{r}{2}\tan\theta \Big(1 + \frac{r}{2R}\sin\theta\tan\theta\Big) G_{rr} = \\ = \; \frac{3G}{2\pi r}\sin\theta \left(1 + \frac{r}{2R\cos\theta}(1 - \frac{1}{3}\cos 2\theta)\right) \; K_{ab}{}^{\hat{i}} T^{ab} \end{aligned} \tag{B.24}$$

independent of $h_{\mu\nu}$, where we left implicit higher orders in r_0/R. We find that there is no physical reason justifying such a strong constraint on $\hat{h}_{zz}$.

Second solution Instead, maintaining the same transverse components (B.22) and final solution (B.24), we can think of having components $h_{\mu\nu}$ all independent of each other, imposing now corrections also along the worldvolume. Nonetheless, we consider the same dipolar variation for the spherical sector of the perturbations $h_{\mu\nu}$, and analogously we assume that the worlvolume part of the metric gets corrected by a single global function.

It can be shown by direct calculation that these assumptions are satisfied uniquely by the tensor

$$\begin{aligned} h_{\mu\nu}(r,\theta)dx^\mu dx^\nu = \; \cos\theta \Big[\Big(1 - m(\theta)\frac{r}{R}\Big) \hat{h}_{ab} d\sigma^a d\sigma^b + \Big(1 - l(\theta)\frac{r}{R}\Big) \hat{h}_{rr} dr^2 + \\ + \Big(1 - f(\theta)\frac{r}{R}\Big) \hat{h}_{zz} dz^2 + r^2 \Big(1 - g(\theta)\frac{r}{R}\Big) \hat{h}_{\theta\theta} (d\theta^2 + \sin^2\theta d\phi^2) \Big] , \end{aligned} \tag{B.25}$$

with

$$\begin{aligned} m(\theta) &= -\frac{1}{2}(\cos\theta + \sec\theta) , & g(\theta) &= \frac{1}{3}(2\cos\theta - \sec\theta) , \\ l(\theta) &= \frac{1}{2}(3\cos\theta + \sec\theta) , & f(\theta) &= \frac{1}{4}(3\cos\theta - \sec\theta) . \end{aligned}$$

Bibliography

[1] T. Andrade, R. Emparan, and D. Licht, "Rotating black holes and black bars at large D," 2018.

[2] J. E. Santos and B. Way, "Neutral Black Rings in Five Dimensions are Unstable," *Phys. Rev. Lett.*, vol. 114, p. 221101, 2015.

[3] P. Figueras, M. Kunesch, and S. Tunyasuvunakool, "End Point of Black Ring Instabilities and the Weak Cosmic Censorship Conjecture," *Phys. Rev. Lett.*, vol. 116, no. 7, p. 071102, 2016.

[4] K. Tanabe, "Black rings at large D," *JHEP*, vol. 02, p. 151, 2016.

[5] K. Tanabe, "Elastic instability of black rings at large D," 2016.

[6] J. Armas and T. Harmark, "Black Holes and Biophysical (Mem)-branes," *Phys. Rev.*, vol. D90, no. 12, p. 124022, 2014.

[7] S. Carlip, "Black hole thermodynamics and statistical mechanics," *Lect.Notes Phys.769:89-123*, 2009.

[8] H. Reall, "Black holes lectures," 2014.

[9] T. Padmanabhan, *Gravitation: Foundations and frontiers.* Cambridge University Press, 2014.

[10] M. Visser, "The Kerr spacetime: A Brief introduction," in *Kerr Fest: Black Holes in Astrophysics, General Relativity and Quantum Gravity Christchurch, New Zealand, August 26-28, 2004*, 2007.

[11] R. M. Wald, *General Relativity.* University of Chicago Press, 1984.

[12] P. O. Mazur, "Black hole uniqueness theorems," 2000.

[13] M. Alcubierre, *Introduction to 3+1 Numerical Relativity.* Oxford University Press, 2008.

[14] J. M. Bardeen, B. Carter, and S. W. Hawking, "The four laws of black hole mechanics," *Comm. Math. Phys.*, vol. 31, no. 2, pp. 161–170, 1973.

[15] J. D. Bekenstein, "Black holes and entropy," *Phys. Rev. D*, vol. 7, pp. 2333–2346, Apr 1973.

[16] M. Visser, "Essential and inessential features of hawking radiation," *Int.J. Mod. Phys. D12:649-661*, 2003.

[17] M. Visser, "Thermality of the hawking flux," 2015.

[18] A. Strominger and C. Vafa, "Microscopic origin of the Bekenstein-Hawking entropy," *Phys. Lett.*, vol. B379, pp. 99–104, 1996.

[19] R. Emparan and H. S. Reall, "Black Holes in Higher Dimensions," *Living Rev. Rel.*, vol. 11, p. 6, 2008.

[20] F. R. Tangherlini, "Schwarzschild field inn dimensions and the dimensionality of space problem," *Il Nuovo Cimento*, vol. 27, pp. 636–651, Feb. 1963.

[21] R. C. Myers, "Myers-Perry black holes," *ArXiv e-prints*, Nov. 2011.

[22] R. C. Myers and M. J. Perry, "Black Holes in Higher Dimensional Space-Times," *Annals Phys.*, vol. 172, p. 304, 1986.

[23] R. Emparan and R. C. Myers, "Instability of ultra-spinning black holes," *JHEP*, vol. 09, p. 025, 2003.

[24] R. Emparan and H. S. Reall, "A Rotating black ring solution in five-dimensions," *Phys. Rev. Lett.*, vol. 88, p. 101101, 2002.

[25] R. Emparan and H. S. Reall, "Black Rings," *Class. Quant. Grav.*, vol. 23, p. R169, 2006.

[26] R. Emparan, "Rotating circular strings, and infinite nonuniqueness of black rings," *JHEP*, vol. 03, p. 064, 2004.

[27] J. Camps, R. Emparan, and N. Haddad, "Black Brane Viscosity and the Gregory-Laflamme Instability," *JHEP*, vol. 05, p. 042, 2010.

[28] J. D. Brown and J. W. York, Jr., "Quasilocal energy and conserved charges derived from the gravitational action," *Phys. Rev.*, vol. D47, pp. 1407–1419, 1993.

[29] J. Camps and R. Emparan, "Derivation of the blackfold effective theory," *JHEP*, vol. 03, p. 038, 2012. [Erratum: JHEP06,155(2012)].

[30] D. Gorbonos and B. Kol, "Matched asymptotic expansion for caged black holes: Regularization of the post-Newtonian order," *Class. Quant. Grav.*, vol. 22, pp. 3935–3960, 2005.

[31] R. Emparan, T. Harmark, V. Niarchos, and N. A. Obers, "Essentials of Blackfold Dynamics," *JHEP*, vol. 03, p. 063, 2010.

[32] J. Armas and M. Blau, "Blackfolds, Plane Waves and Minimal Surfaces," *JHEP*, vol. 07, p. 156, 2015.

[33] J. Armas, "How Fluids Bend: the Elastic Expansion for Higher-Dimensional Black Holes," *JHEP*, vol. 09, p. 073, 2013.

[34] R. Emparan, T. Harmark, V. Niarchos, and N. A. Obers, "New Horizons for Black Holes and Branes," *JHEP*, vol. 04, p. 046, 2010.

[35] R. Emparan, "Blackfolds," 2011.

[36] R. Gregory and R. Laflamme, "Black strings and p-branes are unstable," *Phys. Rev. Lett.*, vol. 70, pp. 2837–2840, 1993.

[37] T. Harmark, V. Niarchos, and N. A. Obers, "Instabilities of black strings and branes," *Class. Quant. Grav.*, vol. 24, pp. R1–R90, 2007.

[38] J. Armas and J. Tarrio, "On actions for (entangling) surfaces and DCFTs," 2017.

[39] M. Durkee, "Geodesics and Symmetries of Doubly-Spinning Black Rings," *Class. Quant. Grav.*, vol. 26, p. 085016, 2009.

[40] J. Gath and A. V. Pedersen, "Viscous asymptotically flat Reissner-Nordstrom black branes," *JHEP*, vol. 03, p. 059, 2014.